

AD-A071 783

ROSENBLATT (M) AND SON INC NEW YORK

F/G 13/10

DEVELOPMENT OF A TECHNICAL PRACTICE FOR RUDDERS AND DIVING PLAN--ETC(U)

AUG 74 R SHEFFIELD

N00024-73-C-5189

UNCLASSIFIED

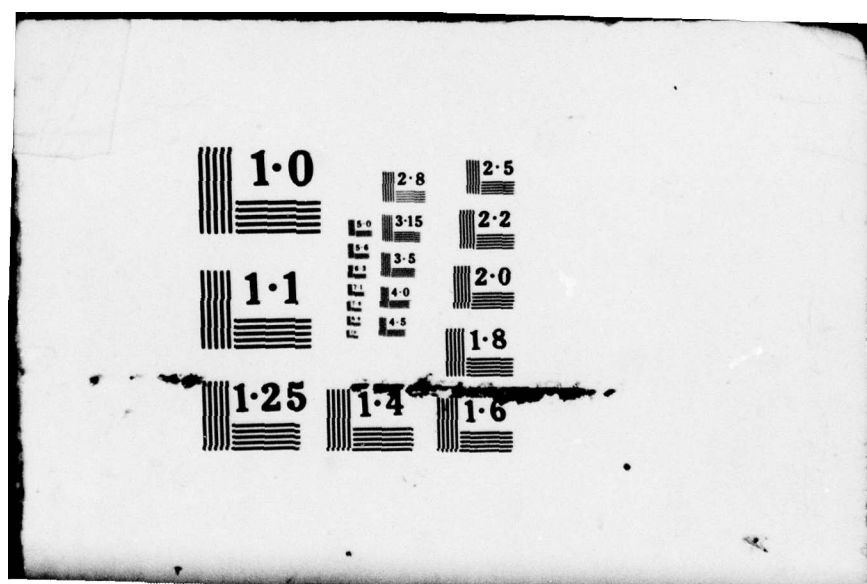
MR/S-2566-3

NAVSEC-6136-74-271

NL

1 OF 2  
AD  
A071783





1·0

2·8

2·5

3·15

2·2

1·1

3·5

2·0

4·0

4·5

1·8

1·25

1·4

1·6

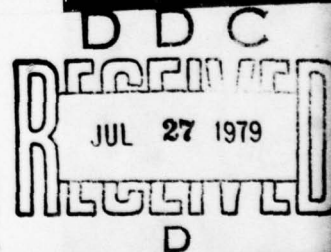


DEVELOPMENT OF A TECHNICAL PRACTICE FOR  
RUDDERS AND DIVING PLANES

PART I  
DESIGN CONSIDERATIONS

2

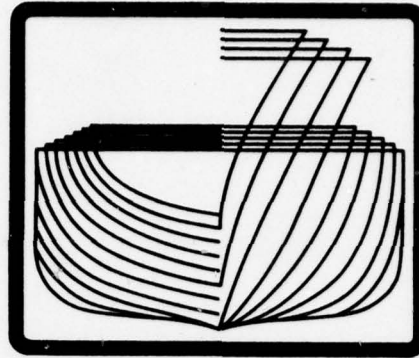
NAVSEC Report 6136-74-271  
August 30, 1974



## **DISCLAIMER NOTICE**

**THIS DOCUMENT IS BEST QUALITY  
PRACTICABLE. THE COPY FURNISHED  
TO DDC CONTAINED A SIGNIFICANT  
NUMBER OF PAGES WHICH DO NOT  
REPRODUCE LEGIBLY.**

Accession For	
NTIS GRA&I	<input checked="" type="checkbox"/>
DDC TAB	<input type="checkbox"/>
Unannounced	<input type="checkbox"/>
Justification	
By	
Distribution/	
Availability Codes	
Just	Avail and/or Special
A	23



6 DEVELOPMENT OF A TECHNICAL PRACTICE FOR RUDDERS AND DIVING PLANES.

PART I-  
DESIGN CONSIDERATIONS,

18 NAVSEC Report 6136-74-271  
11 30 August 1974

Prepared for  
Hull Form and Fluid Dynamics Branch (SEC 6136)  
Naval Ship Engineering Center  
Hyattsville, Maryland 20782

10 By  
Richard Sheffield  
M. Rosenblatt and Son, Inc.  
350 Broadway  
New York, New York 10013  
14 (MR/S Report-2566-3)

15 Under  
Contract N00024-73-C-5189  
Task 6120-173  
(NAVSEC TPOC: W. L. Louis & H. Lo)

APPROVED FOR PUBLIC RELEASE. DISTRIBUTION UNLIMITED.

DDC  
RECEIVED  
JUL 27 1979  
RECEIVED  
D

404192  
79 07 24 067

## TABLE OF CONTENTS

	<u>Page</u>
1. INTRODUCTION	1-1
2. DOCUMENTATION OF CURRENT PROCEDURES	2-1
2.1 Size, Shape and Location of Rudders and Diving Planes	2-1
2.2 Computer Programs for Control Surface Design	2-7
2.3 Stress Analysis of Surface Ship Rudders	2-9
2.4 Optimization of Surface Ship Rudder Weight and Cost	2-17
3. STATE OF THE ART FOR CONTROL SURFACE DESIGN	3-1
3.1 Introduction	3-1
3.2 Handling Quality Criteria for Surface Ships	3-1
3.3 Prediction of Ship Maneuverability for Surface Ships	3-4
3.4 Handling Quality Criteria for Submarines	3-9
3.5 Prediction of Submarine Maneuverability	3-10
3.6 References	3-15
4. RECOMMENDATIONS	
4.1 Future Research and Development	4-1
4.2 Revisions to the Current NAVSEC Design Procedure	4-6
4.3 Revised Technical Practices Manual	4-7
Appendix A Derivation of Minimum Cost and Minimum Weight Equations	
Appendix B Report Titled Experimental Stress Analysis of a Socketed Connection in Bending	

Appendix C Report Titled Method of Calculating Stress  
in a Gudgeon - Envelope 010809

~~\*Appendix D Computer Program Documentation for Rudder  
and Fairwater Plane Design~~

~~\*Appendix E Computer Program Documentation for Stern  
Plane Design~~

\*Appendixes D & E are contained in Part II of this Technical  
Practice (NAVSEC Report 6136-74-272) as appendixes G & H.

## 1. INTRODUCTION

The purpose of the subject report is to present a technical practice for the design of rudders and diving planes. This report precedes NAVSEC Report 6136-74-272, titled "Development of a Technical Practice for Rudders and Diving Planes, Part II, Torque Predictions" which assumes a given control surface configuration and provides a procedure for calculating the forces and moments acting on the rudder. This report addresses those design considerations not involved in the actual control surface torque calculation. In the course of this development the current NAVSEC procedure for certain aspects of control surface design was updated and documented, the current state of the art for control surface design was defined and recommendations were made for future research and development to fill gaps in the current technology.

Section 2 of this report contains the documentation of the following current procedures.

- (1) Size, Shape and Location of Rudders and Diving Planes
- (2) Computer Programs for Control Surfaces Design
- (3) Stress Analysis of Surface Ship Rudders
- (4) Minimum Cost and Minimum Weight of Surface Ship Rudders

In addition to documenting the procedure for estimating the minimum cost and weight of rudders a correction was made to the equation for rudder cost which yields answers different from those obtained with the original equation from Mr. Hewitt Lo in Code 6136.

In Section 3 the current state of the art is defined. Emphasis is placed on describing the handling quality criteria and the methods of prediction of ship motion as these are the areas of greatest interest relative to NAVSEC's design procedure.

Section 4 presents our recommendations for future research and development based on the survey and interpretation of literature reviewed. The Technical Practices Manual has been revised to properly represent current rudder design practice.

## 2. DOCUMENTATION OF CURRENT DESIGN PROCEDURES

### 2.1 Size, Shape and Location of Rudders and Diving Planes

#### 2.1.1 Surface Ship Rudders

In general the number of rudders, their size and location are determined on the basis of previous experience as well as the particular requirements on the design itself.

##### 2.1.1.1 Number of Rudders

The number of rudders nearly always matches the number of propellers. Even on a single screw ship with stringent maneuverability requirements, one rudder would generally be preferred over two since two rudders are costlier, heavier, and require more area for the same lift produced. For a twin screw ship two rudders are usually called for in order to obtain better maneuverability at low speed by placing each rudder in the wake of the propeller.

##### 2.1.1.2 Rudder Location

Rudders are generally located away from the position directly in line with the propeller shafting in order to avoid the propeller cone vortex. This is even done, wherever possible, for high power single screw ships. However, the rudder is always placed partially in the propeller race.

Adequate clearance should be provided to minimize the risk of vibration and allow the removal of the propeller without unshipping the rudder. In some cases unshipping the tail shaft may require turning the rudder and removing portable rudder plates, although this is avoided whenever possible.

To avoid vibration the minimum distance allowed between the leading edge of the rudder and a point on the line of maximum thickness of the propeller blade and 0.7 radius from the shaft centerline should equal one-half the propeller diameter.

The rudder - rudder stock combination should be designed so as to permit unshipping the rudder without special high blocking. Where the rudder cannot be dropped enough directly downward, provision should be made for first lifting the stock within the ship. Tilting the rudder on the rudder stock is possible but should be avoided except as a last resort.

The rudder should be well submerged even with the ship lightly loaded aft and heeling in a turn. In some cases it may be necessary to use a rudder stool to obtain proper rudder immersion and to place more of the rudder into the propeller race. The rudder should extend below the baseline as little as possible to minimize grounding damage. However, some rudders extend as much as six feet below the baseline to obtain adequate submergence and the desired aspect ratio.

#### 2.1.1.3 Rudder Shape

Rudder section shape is defined by the NACA symmetrical four-digit series. The maximum thickness/chord ratio normally permitted is 0.23.

Spade rudders are generally preferred over the horn rudders since they develop more lift for the same area, are easier to unship and the design data is less empirical than

that for horn rudders.

The after edge has a definite half-breath and is left sharp since this slightly improves lift. The sharp edges do not add to the cost and provide the required strength. Sections are specified at the root and tip chord with straight lines connecting like numbered stations.

The rudder profile should be tapered to save weight and reduce the bending moment.

#### 2.1.1.4 Rudder Size

Rudder areas are generally proportioned upon length and draft from similar previous ships. An approximation for the required rudder size to provide adequate directional stability and the required turning radius can be obtained from statistical data. DTMB translation #321 provides a graph for minimum rudder sizes for directional stability and for rudder size and turning ability at a 35 degree rudder angle. For destroyer-type ships the tactical diameter can be checked to see if it meets the requirements in the ship specification by running NSRDC program Code 1524 for several rudder areas. The output from this program is turning diameter in shiplengths and yards versus rudder angle and speed-length ratio.

#### 2.1.1.5 Verification of Preliminary Design Estimate

In the final contract design free running model tests are run to verify the computer results. These model tests when compared to full scale results are accurate to  $\pm 5\%$ . However, to ensure meeting the required turning radius in sea

trials a minimum of a 10% margin over model test predictions should be provided since full scale trial data may be erratic. In addition, to tactical diameter model tests, zig-zags (Kempf or Z maneuver) and spiral maneuver (Dieudonné) tests are run.

#### 2.1.2 Submarine Control Surfaces

The basic function of submarine control surfaces is to give positive directional stability, good depth and course keeping ability and good ability to initiate and check trajectory changes. The preliminary design estimate of required control surfaces is generally model tested by NSRDC and adjustments made as necessary.

##### 2.1.2.1 Submarine Rudders and Rudder Stools

The design of submarine rudders is generally similar to that of surface ships. One special problem associated with the topside rudder of a submarine is the flow disturbance caused by the sail and the superstructure. Because of this wake disturbance the topside rudder is not very effective for directional stability where small angles are involved even though quite effective for turning. In some designs the topside rudder is mounted on a rudder stool to decrease the wake disturbance and improve the directional stability. Directional stability may be improved with the use of vertical stabilizers which may also house the sonar units.

For an initial estimate, rudder area is considered proportional to displacement and ratios of these are obtained from similar previous submarines. The rudder may extend below the baseline if necessary.

#### 2.1.2.2 Fairwater Planes

Fairwater planes are more commonly called for in design than bow planes. Bow planes have to be stowed by folding or rotating when surfaced. Even when folded they protrude from the hull so pounding in a seaway is increased and docking is made more difficult. The use of fairwater planes also releases space forward for sonar and torpedo tubes, removes forward plane noise from the sonar dome area, and fairwater planes may be used as a gangway for access.

Fairwater plane outreach is usually kept within maximum hull dimensions to allow for rolling alongside a dock. The height of the planes is of importance in relation to avoiding difficulties in periscope - depth control. Positioning the planes too high may cause loss of plane effectiveness at periscope depth.

The leading edge is usually raked to deflect mine cables. Tips should be rounded to reduce noise levels.

As with the submarine rudders, the fairwater plane areas are proportional with displacement and ratios of these are obtained from similar previous submarines.

#### 2.1.2.3 Stern Planes and Stabilizers

Stern plane area is directly proportional to displacement and inversely proportional to length. The area required is usually too large to be all moveable to accommodate the necessary steering gear so part of it is installed as a fixed stabilizer.

The planform and location of stern plane and stabilizer are selected with the following considerations in addition to conventional hydrodynamic efficiency.

a) The leading edge rake should be such as to deflect mine cables; for no rake or very small rake, cable guards should be provided.

b) A minimum distance equal to one propeller radius should be maintained between a point located on the line of maximum blade thickness 0.7 radius from the shaft centerline to the nearest edge of the stern plane.

c) The span which usually exceeds the beam should be limited so as to facilitate nesting, coming alongside a dock, and for larger subs to increase the availability of the number of drydocks and building ways that may be employed.

#### 2.1.2.4 X-Stern

The X-stern is another arrangement of the control surfaces in the stern of a submarine. The X-stern of the Albacore (AG 596) has been tested and results are available in formal DTMB classified reports.

The X-Stern:

a) Solves the problem of getting adequate rudder effectiveness without exceeding hull block dimensions.

b) Adds some complexity to the controls.

c) Provides even more diving plane effectiveness than the cruciform stern than is desirable at high speeds.

#### 2.1.2.5 Verification of Preliminary Design Estimate

Once the initial control surface configurations are established a computer program is run to determine the linear coefficients and these can be inserted into a linear equation of motion to check for directional stability. The accuracy of these calculated coefficients are checked later by captive model tank tests. The size of the control surface may be altered depending on the results obtained from the model tests. Free running model tests serve as a final check on the control surface design.

### 2.2 Computer Programs for Control Surface Design

#### 2.2.1 Computer Program Documentation for Rudder and Fairwater Plane Design

This program performs torque calculations for rudder and fairwater planes and permits the use of an iterative procedure to determine optimum stock locations and diameters.

The general method employed in this program is the minimization of the difference between the most positive (upsetting) and most negative (restoring) torques. These torques are calculated at different deflection angles of the control surface and the largest positive torque is compared with the most negative torque. The stock location which gives this minimum difference within some small interval is the answer. The output consists of the final rudder configuration, stock location and stock diameter and the hydrodynamic characteristics of the rudder.

The final rudder configuration includes a small change of rudder root chord to ensure the stock location is set at an even measurement (i.e. to the nearest 1/8").

The program documentation in the report titled "Control Surfaces Calculations & Programs" found in file Code 6136 is complete. Sections of that report are reproduced in Appendix G of Part II (NAVSEC Report 6136-74-272).

For a complete description of the aerodynamic method used in developing this program refer to NAVSEC Report 6136-74-272 titled "Development of a Technical Practice for Rudders and Diving Planes, Part II." This report also contains a detailed hand calculation procedure as used in this program. As discussed in the above report, this program does not provide the proper balance ratio for surface ship rudders or fairwater planes. At the present time this correction must be performed by hand with the aid of the computer.

#### 2.2.2 Computer Program Documentation for Stern Plane Design

This program performs torque calculations for stern planes with stabilizers and permits the use of an iterative procedure to determine optimum stock location and balance. The output is the geometric location of the balanced stock; at the corresponding torque results for intermediate calculations are given. The program documentation in the report titled "Control Surfaces Calculations and Programs" found in file Code 6136 is complete. Sections of that report are reproduced in Appendix H of Part II (NAVSEC Report 6136-74-272).

For a complete description of the semi-empirical method used in developing this program and a complete example

hand calculation, refer to NAVSEC Report 6136-74-272, titled "Development of a Technical Practice for Rudders and Diving Planes, Part II". This program does not properly balance the negative and positive torque curves so this must be corrected by a hand calculation, with the aid of the computer.

### 2.3 Stress Analysis of Surface Ship Rudders

A rough stress analysis is made during preliminary design and the shipbuilder is usually required to make one to determine actual scantlings. Stresses are limited so as to provide a minimum factor of safety of 2.0 on yield point for spade rudders, where loads are calculated using aerodynamic or hydrodynamic data and a factor of safety of 2.5 on yield point for horn rudders, where loads are calculated using DTMB Report 915.

#### 2.3.1 Spade Rudder

The following steps outline the procedure for the stress analysis of a spade rudder. A rudder and stock stress diagram for the DD931 Class found in Code 6136, meets the specifications set by the Navy.

##### Steps in Spade Rudder Stress Analysis

(1) Determine forces acting on the rudder:

a) Hydrodynamic force - See Section 2.2.1 of this report for the calculation of the total resultant force and center of pressure. This method supersedes the rudder torque calculation shown on the stress diagram for the DD931 class.

b) Sea Slap - The practice is to assume a maximum static load of 1000 pounds per square foot. Over the rudder span a triangular load is assumed with the maximum load

at the root chord. Over the rudder chord a uniform distribution is used. Using this loading the structure may be stressed up to the yield point.

c) Hydrostatic force - This pressure in head of water is simply equal to the depth of water of the point on the rudder for which the pressure is calculated.

d) For rudder plate panel design all three forces (a), (b) and (c) are considered, but in calculating the bending stress, only (a) is considered.

(2) Determine the reactions for the two bearing supports

$F_u$  = Reaction at upper bearing

$F_L$  = Reaction at lower bearing

$Z$  = Distance of center of pressure from the root chord.

$L_1$  = Distance between bearings

$L_2$  = Distance from lower bearing to root chord

$F_R$  = Resultant force at center of pressure

Equations for Bearing Reactions

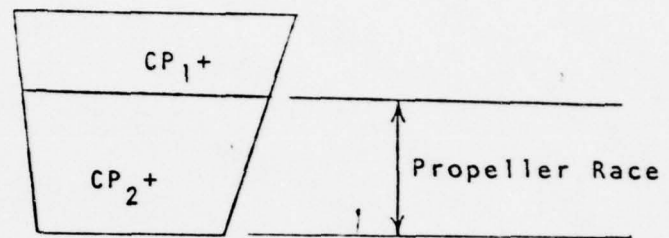
$$F_u = F_R \left( \frac{Z + L_2}{L_1} \right)$$

$$F_L = F_R + F_u$$

Solve the two equations for the two unknowns  $F_u$  and  $F_L$ .

(3) Develop the spanwise load curve over the span of the rudder and the chordwise load curve over the chord of the rudder. The load distribution is trapezoidal in form and is derived so the centroid of the trapezoid coincides with the spanwise

or chordwise center of pressure. Note that if the rudder is not located completely within the propeller race, two separate chordwise and spanwise center of pressures must be calculated. The basic procedure described below remains the same.



SKETCH OF RUDDER PARTIALLY IN A PROPELLER RACE

Calculation of load distribution over chord.

$a$  = load at aft end of chord

$b$  = load at forward end of chord

$x$  = distance of center of pressure from forward edge of chord

$L$  = chord

$\frac{F_R}{L}$  = Load per foot of chord

Force = Area of trapezoid

$$\frac{F_R}{L} = \frac{a + b}{2}$$

$$a + b = \frac{(2) F_R}{L} \quad (1)$$

Equation for Centroid of trapezoid

$$x = \frac{L(2a + b)}{3(a + b)}$$

$$2a + b = \frac{(x)(3)(a + b)}{L} \quad (2)$$

Solve equation (1) and (2) for the unknowns  $a$  and  $b$ . Follow the same procedure for calculating the spanwise load distribution.

(4) Integrate the load curves over the span and chord of the rudder to obtain the shear curves.

$$V = \int w dx$$

$V$  = Shear force

$w$  = Load/Ft.

$X$  = Distance along span or chord

(5) Integrate the shear curves to obtain bending moment curves.

$$M = \int V dx$$

$M$  = Bending Moment

(6) Integrate the bending moment curves twice to obtain the deflection curves.

$$y' = \int \frac{M}{EI} dx$$

$$y = \int y' dx$$

$y'$  = Angular deflection

$y$  = Vertical deflection

(7) Determine the spanwise and chordwise moment of inertia.

(8) Calculate the stress in various sections along the span and chord.

(9) The stress in the rudder key, tiller key and rudder hub will be calculated separately.

(10) Determine the thickness for the rudder hub and yoke. DTMB Report 1592 gives values for K which equals experimental stress for a socketed connection. This report may theoretical stress be used to determine the stress for the hub and yoke casting. See Appendix B for the report titled "Experimental Stress Analysis of a Socketed Connection in Bending." Page 15 of this report presents graph of K versus stock penetration.

(11) Determine the stress in the rudder stock using the equations below.

$\ell$  = distance from the center of pressure  
to the stock centerline

$M_t$  = torsional moment

$$= F_R \times \ell$$

$d$  = shaft diameter

Maximum Normal Stress

$$(S_n)_{\max.} = \frac{16}{\pi d^3} (M + \sqrt{M^2 + M_t^2})$$

Maximum Shear Stress

$$(S_s)_{\max.} = \frac{16}{\pi d^3} \sqrt{M^2 + M_t^2}$$

Note that the yield stress divided by the factor of safety may be substituted above and the diameter solved for directly.

An example calculation for stress analysis of spade rudders can be found in Code 6136 file.

This was performed for the DD931 Class. Note that the stress calculations should be tabulated in the same manner as done for the DD931.

### 2.3.2 Horn Rudder

The following steps outline the procedure for the stress analysis of a horn rudder. A horn rudder and stock stress diagram for the BB 61 that meets the specifications set by the Navy may be found in Code 6136 files.

#### Steps in Horn Rudder Stress Analysis

##### (1) Determine forces acting on the rudder

a) Hydrodynamic force - See NAVSEC Report 6136-74-272, titled "Development of a Technical Practice for Rudders and Diving Plane Part II" for the calculation method for total resultant force and center of pressure. The method provides an analytical approach instead of relying on model test data as shown on the stress diagram for the BB-61 class. Note that in this calculation procedure for the hydrodynamic force, the force normal to the chord of the rudder is calculated and this is assumed to be equal to the resultant force.

b) Sea Slap - Follow the same practice as used for spade rudders (See Section 2.3.1).

c) Hydrostatic force - Follow the same practice as used for spade rudders (See Section 2.3.1).

d) For rudder plate panel design all three forces (a), (b) and (c) are considered, but in calculating the bending stress.

and rudder torque, only (a) is considered.

(2) Determine the pressure distribution on each bearing and the resultant force acting on the bearing. See the "Bearing Pressure Diagram" on the stress diagram for the BB 61. The following steps are followed in determining the pressure distribution.

a) Establish a baseline for pressures due to direct load and to eccentricity.

b) Find the center of gravity of the projected bearing areas.

c) Determine the eccentricity which is the distance from the eccentric load (resultant force) to the center of gravity of the projected bearing areas.

d) Find the resultant bearing pressure by establishing unknown pressure  $f$  due to eccentricity is established at the top to the upper bearing. The bearing pressure is assumed to vary linearly so a line may be drawn through the center of gravity to indicate in terms of  $f$ , the resultant pressures due to eccentricity for the other bearings. A moment equation about the center of gravity is written to solve for  $f$ .

e) Divide the eccentric load by the total bearing area to obtain the pressure due to direct load.

f) Establish a baseline for resultant pressures  $P/A$  from the baseline for direct load.

g) Summary of pressure due to eccentricity and direct load.

h) Calculate the magnitude and location of the resultant force on each bearing. The pressure distribution for each bearing is trapezoidal in form so the magnitude and location of the resultant force on each bearing can be calculated using equations for the area and center of gravity of a trapezoid.

(3) Construct a load distribution along the rudder stock using the forces determined in step 2 - h.

(4) Integrate the load curve over the rudder stock to obtain a shear curve. See step (4) of spade rudder calculation for the equation for shear.

(5) Integrate the shear curves to obtain bending moment curves. See step (5) for the spade rudder.

(6) Determine the moment of inertia over the rudder stock for various sections along the stock.

(7) Calculate the stress for the sections used in step (6). See step (11) for the spade rudder.

(8) Determine the stress for sections along the span and chord of the rudder by following steps (3) through (8) for the spade rudder.

#### Steps in Skeg Stress Analysis:

(1) The hydrodynamic force acting on the skeg is calculated by assuming the skeg is a spade rudder. A calculation is performed for the normal force on the skeg alone and this is added to the normal force of the rudder at the lower bearing to obtain the total force on the skeg.

(2) The bending, torsion and combined stress is calculated

for a section taken at the root chord. See the calculation for section "A-A" on the rudder stress diagram for the BB-61.

(3) The stresses in step 2 are also calculated for the skeg just above the gudgeon. See the calculation for section "B-B" on rudder stress diagram for the BB-61.

(4) The stress calculation for a non-tapered rudder gudgeon is calculated using NAVSEC envelope 010809 titled "Method of Calculating Stress in a Gudgeon." Refer to the stress curve on page 17 of the above report to obtain the stress per square unit. This report is reproduced in Appendix C. The total load per inch of length of the gudgeon is calculated. A ratio of this load to the load per inch calculated with the chart is used to correct the stress.

The stress calculation for a tapered gudgeon can be performed using DTMB Report 1592. This report is reproduced in Appendix B. The calculation procedure followed is the same as that for the spade rudder (see section 2.3.1 step 10).

#### 2.4 Optimization of Surface Ship Rudder Weight and Cost

This procedure establishes the minimum weight and minimum cost for rudders. In this process the stress is assumed to be adequate.

The cost of the rudder is determined by the cost of material, iron worker (including installation, testing and painting) and welding. The cost of the material and iron worker can be measured by the weight of the material and the cost of the welder is judged by the linear foot of welding. The following pages describe the calculation procedure for minimum rudder thickness using equations

for minimum weight and minimum cost. Using these values for minimum thickness, the weight and cost of the rudder may be determined. Appendix A provides the derivation of the equations for minimum thickness based on minimum cost and weight and a detailed example calculation using the procedure outlined in this section.

### 2.4.1 Calculation of Rudder Plate Thickness for Minimum Weight

W = Wt. of Rudder, Lbs.

A = Rudder area = Ft.<sup>2</sup>

t = Min. Rudder Plate Thickness or Adjusted Thickness, inches.

t' = Stiffeners and Flat Bars Thickness, inches

b = Rudder Span = Ft.

c = Mean Chord = Ft.

D = Average Rudder Thickness = 0.684 x Mean Thickness = Ft.

m = Stiffener Panel Constant = 50 (For the Example  
in Appendix A)

Mean Thickness = Maximum Thickness at Mean Chord c., Ft.

a<sub>1</sub> = b x c x D =

a<sub>2</sub> = A ÷ 12 =

a<sub>3</sub> = (b + c) ÷ 48 =

$$t = \left[ \frac{a_1 \times t'}{m(a_2 + a_3 \times t')} \right]^{\frac{1}{2}}$$

①	②	③	④	⑤	t
t'	a <sub>3</sub> x t'	② + a <sub>2</sub>	t' ÷ ③	$\frac{a_1}{m} \times ④$	⑤ <sup>½</sup> For Min Wt

#### 2.4.2 Calculation of Minimum Thickness

To determine minimum thickness based on cost the equation below must be iterated using an assumed thickness  $t$  until the result equals zero. It will be useful to plot the result of each iteration versus  $t$  to speed convergence to the value of zero. Since the equation is a cubical equation, at least three points should be plotted. Note that one of these points should have an opposite sign compared with the other points.

$$a_4 = 81.7 (A) =$$

$$a_5 = 20.42 (b + c) =$$

$$a_6 = a_1 \left( \frac{980}{m} \right) =$$

$$N = \frac{KP_w}{P_s + P_L} = 6 \text{ (or an actual number derived from a cost study)}$$

$$a_7 = N (a_1) \left( \frac{576}{m^2} \right) =$$

$$a_8 = \frac{N (48) (cD + bc)}{m} =$$

①	②	③	④	⑤	⑥	ITERATION CHECK
Assumed $t$	$a_5 \times t$	$\frac{a_6 \times t^2}{t^2}$	$\frac{a_7}{t^3}$	$\frac{a_8}{t^2}$	$\textcircled{2} - \textcircled{3} - \textcircled{4} - \textcircled{5} + a_4$	1) If $\textcircled{6} = 0$ then assumed $t = t$ for minimum cost 2) If $\textcircled{6} \neq 0$ assume a new $t$ and iterate again

### 2.4.3 Calculation of Rudder Weight

$$a_{10} = A \div 6 = \quad \div 6 =$$

$$a_{11} = (b + c) \div 24 = 2 \times a_3 = 2 \times \quad =$$

$$a_{12} = 2bcD \div m = 2a_1 \div m = 2 \times \quad \div =$$

$$a_{13} = (b + c) \times D \div 12 =$$

$$a_{14} = b \times c \div m = \quad = \underline{\hspace{2cm}}$$

$$a_{15} = (a_{13} + a_{14}) = \quad + = \quad =$$

$$W = 490 \left[ (a_{10} + a_{11} t')t + a_{12} \left( \frac{t'}{t} \right) + (a_{13} + a_{14}) t' \right]$$

①	②	③	④	⑤	⑥	⑦	W
t	$a_{11}xt'$	② + $a_{10}$	③ $\times$ t	$a_{12}xt'/t$	$a_{15} \times t'$	④ + ⑤ + ⑥	490 $\times$

#### 2.4.4 Calculation of Rudder Cost

$$a_{16} = \frac{288 (a_1)}{m^2}$$

$$a_{17} = b + c + D$$

$$\text{Cost} = W + N \left[ \frac{a_{16}}{t^2} + \frac{a_8}{Nxt} + 2 \times a_{17} \right]$$

①	②	③	④	⑤	Cost \$
t	$\frac{a_{16}}{t^2}$	$\frac{a_8}{Nxt}$	② $\times a_{17}$	$N \times [② + ③ + ④]$	$W + ⑤$

### 3. CURRENT STATE OF THE ART FOR CONTROL SURFACE DESIGN

#### 3.1 Introduction

In describing the current state of the art for control surface design, emphasis will be placed on those aspects of design which contribute directly to the NAVSEC design procedure. Generally when the control surface design is conducted, the hull shape, ship powering and speed have already been determined. Therefore, the control surface design problem is a problem of selecting a control surface which will enable the ship to satisfy all of its maneuverability requirements as outlined in a directive from Project Manager Ships (PMS). To test a ship to see if its requirements are met necessitates some criteria which can quantitatively measure ship maneuverability. Using this criteria, predictions must be made for control surface characteristics which will satisfy the ship requirements.

This section on the state of the art is directed to the most up-to-date maneuvering criteria for surface ships and submarines and the available techniques used to predict the ship motions resulting from a given control surface configuration. Prediction techniques from commercial practice as well as NAVSEC's practice are discussed here.

#### 3.2 Handling Quality Criteria for Surface Ships

##### 3.2.1 Standard Maneuvers

There are three maneuvers now in common use by the U.S. Navy as well as in commercial practice and are referred to as the Standard Maneuvers. The Standard Maneuvers is a set of trials consisting of a turning circle, a zig-zag and a spiral maneuver.

The ITTC maneuverability committee has made up a standard procedure for these tests and published it in its 12th ITTC meeting (14)\*. Since these tests are in common use their procedure will not be explained here.

### 3.2.2 New Definitive Maneuvers

New maneuvers have been established over the last few years to deal in particular with unstable ships and to provide a more thorough definition of ship control for all ships.

One new method introduced by Bech in 1966 is the reversed spiral test which has now received wide support (14). Like the spiral test this is a way of examining a ships course keeping ability. In this test the rudder angle  $\delta$  which will give a specified turning rate  $r$  is measured. This is just the opposite of the usual spiral test where the turning rate is measured as a function of specified rudder angles. Advantages of the reversed spiral test are that it produces an  $r$ - $\delta$  relationship for the complete range of rudder angles while the curve from the spiral test forms a hysteresis loop. This method works particularly well for directionally unstable ships. The reversed spiral test also has the advantage that the test takes less time and sea room than the spiral test.

Another new test suggested by Thieme and Motora is the modified zig-zag test where instead of running the tests at equal rudder angles and switching heading angles  $10^\circ$ - $10^\circ$ ,  $15^\circ$ - $15^\circ$ , etc., the switching angle is made less than the rudder angle (1). This avoids the problem encountered with unstable ships at small rudder angles where the results tend to diverge.

\*Number in parenthesis refers to reference listed in Section 3.5.

Two other maneuvers called the pull out and weave maneuvers more accurately define the Dieudonné spiral loop. The pull out maneuver is a test where the ship is first kept turning at a specified rudder angle and then the rudder is set to zero and the successive heading angle is recorded until the ship's motion becomes steady. The steady turning rate obtained will be equal to the height of the hysteresis loop of the  $r-\delta$  curve. The weave maneuver is basically a modified zig-zag maneuver conducted with a variety of rudder angles and yaw angles of small magnitude. By trial and error the lower limiting value of the rudder execute angle as a function of yaw angle can be determined. Extrapolation of these values to zero gives the width of the Dieudonné spiral loop.

One important aspect of ship maneuverability, which is not directly measured by any of the tests mentioned, is the ability of a ship to run alongside in close proximity to another ship. Newton performed some tests which indicated that the most important factors governing the ability of a ship to pass closely to another is the speed of the ships and the magnitude of the transverse distance between them, assuming that both ships are directionally stable. In view of this study it is not important to establish a special criteria for this situation but the designer should make sure the ships are directionally stable according to the criteria outlined above.

### 3.3 Prediction of Ship Maneuverability for Surface Ships

It is desirable to predict for surface ships and submarines the handling characteristics before the ship is built. All of the methods described attempt to predict ship maneuverability in terms of the standard maneuvers.

#### 3.3.1 Use of Statistical Data

It is still part of the present NAVSEC design procedure to rely on statistical data based on parent ships. This gives an approximation for the required rudder size to provide adequate directional stability and the required turning radius. For a first rough cut of determining rudder size, the report "Design of Ship Rudders" by H. Thieme (12) could be used. In this reference Thieme provides a graph for minimum rudder sizes for directional stability and for rudder size and turning ability at a 35 degree rudder angle. The accuracy of this data is based on a small number of ship parameters and over a limited range of ship characteristics. Another problem is that this method does not provide an accurate prediction of the ship meeting the handling criteria requirements. As a quick estimating tool this method is still useful, but the following methods for the prediction of ship maneuverability hold greater promise for accuracy and versatility.

#### 3.3.2 Free Running Model Tests

Free running model tests offer the most direct method of predicting ship motions, however, there are drawbacks to this method of prediction. The biggest problem is that the

scaling laws cannot be completely satisfied. Because of the friction correction due to Reynolds number scale effect, the loading of the model propeller is larger than that of a full scale propeller. The model slip stream is increased and this increases the effectiveness of the rudder. This could account for the fact that at low rudder angles model ships tend to have greater directional stability than the full size ship. Another problem is that the difference in Reynolds number between the model and ship must be considered since the thickness of the boundary layer which varies with Reynolds number determines the point of flow separation on the rudder. Rakamarie has performed tests where the rudder is heated to provide an apparent increase in Reynolds number. For the very limited range of temperature and Reynolds number tested, this appears to yield good results.

### 3.3.3 Approximate NSRDC Prediction Method for Tactical Diameter

This method developed by NSRDC is very useful for preliminary design of control surfaces. A pilot study was performed for predicting the tactical diameter for twin screw destroyers. This method utilizes historical data gathered from previous tank tests for a large number of twin screw destroyers. Ship and rudder parameters were selected. To determine the relationships of these parameters with tactical diameter, a multiple regression analysis was used. The tactical diameter can then be expressed in terms of an equation derived from these curves. This method produces results which may be accurate to  $\pm 5\%$  for a certain range of rudder angles although an error of 15% may occur if the ship falls near the

ends of the data curves. The greatest accuracy occurs if the ship in question falls in the region of greatest data concentration.

Eda performed a study for the Coast Guard which was similar to that of NSRDC in that he used a large amount of data from previous free-running model tests to establish equations for ship trajectories (4). His method permits a greater range of parameters to be varied and gives good correlation with model tests as indicated by sample test runs in his report.

#### 3.3.4 Semi-Empirical Method

In commercial practice a semi-empirical approach utilizing both the non-linear equations of motion and tank test results, provides the most accurate means of predicting ship maneuvering. The biggest problem with this method is predicting the dynamic derivative of force and moment for the higher order non-linear equations. Captive model tests may be used to determine these coefficients. In this test the model is forced to perform definite motions, and dynamometers are used to measure the corresponding hydrodynamic force responses. The derivatives of these responses yield the coefficients of the motion parameters. The most commonly used test mechanisms are the rotating arm and the Planar Motion Mechanism (PMM).

The rotating arm is well suited for the generation of yaw velocity and the combination of drift angle and yaw velocity. Due to the limited radius of the rotating arm it is difficult to measure the linear coefficients so these are commonly measured by drift angle (oblique flow) tests in a conventional towing tank.

Acceleration derivatives cannot be obtained with the rotating arm. The PMM technique is more versatile than the rotating arm in that it enables all of the coefficients to be measured but in practice it may be difficult to measure the non-linear coefficients in the derivative of the yaw velocity accurately. Large yaw velocity may be obtained only at high frequency of oscillation which may cause frequency problems. These problems arise from the fact that some of the acceleration and sway damping derivatives are frequency dependent. The new high amplitude HyA-PMM recently constructed in the Hydro-09-Laboratorium in Denmark may solve this problem.

Once the hydrodynamic derivatives are obtained from tank tests, the digital computer is used to solve the non-linear equations of motion. Strom-Tejsen has produced a computer program for surface ships which accurately predicts the Standard Maneuvers (8). The basic input data for the program consists of: 1. principal ship data, 2. effective horsepower data and open water propeller characteristics and 3. nondimensional coefficients from PMM or rotating arm tests. From the limited results studied, this program appears to give very accurate results for the prediction of turning circle parameters, turning circles, zig-zag maneuvers and spiral maneuvers. More recent programs include subroutines for the effect of wind and bow thrusters.

The main advantages of the semi-empirical method is that scaling laws to correct for Reynolds number, propeller RPM and ship speed can be taken into account. This provides more accuracy and once the coefficients are obtained, individual parameters such

as rudder rate can be measured. Simulations can be performed for auto-pilot design or for training purposes. Many more operating conditions can be studied than would be practical for free - running models.

### 3.3.5 Analytical Method

In commercial practice tank testing techniques have been developed to the point where they now yield accurate results but are costly and time consuming. In an effort to reduce this cost many researchers have been trying different approaches to obtain a completely analytical method for determining the derivatives for the equation of motion.

Jacobs has developed equations based on simplified potential flow theory and low aspect ratio wing theory with empirical modifications for a real viscous fluid to determine first order hydrodynamic force and moment derivatives (16), (17). In this approach the bound vortex and direction of the free vortex sheet are properly assumed to give reasonable results. However, since the hydrodynamic relation between the vortex distribution and the ships form has not been clarified, the modifications made for viscosity are in need of verification.

Inoue (22) and Fedyaevsky (23) have derived semi-empirical formulas for the hydrodynamic force and moment velocity derivatives by introducing coefficients which are chosen to fit each ship's form.

Acceleration derivatives can be obtained with the use of Lewis form sections and the strip method. Agreement is good for the force derivatives but only fair for the moment derivatives according to graphs in reference (1).

By the combination of the above theories, fairly accurate linear coefficients may be determined. Although theoretical velocity derivatives contain a non-linear term due to cross-flow, the theory has not been developed to the point to be able to give higher order derivatives containing non-linear parts (1). For immediate application these theories would have to be supplemented by tank tests.

### 3.4 Handling Quality Criteria for Submarines

Unlike surface ships there is no fixed criteria for defining the maneuverability characteristics of a submarine (29). Standard maneuvers exist but preliminary specifications specify only in general terms, levels of performance required for submarine directional control. Although few definite requirements are established, the designer is interested in predicting the motion of the submarine before the ship construction commences, and if in his opinion performance is unsatisfactory, adjustments will be made to the size and location of the control surfaces. The maneuvers which are initially studied are the definitive maneuvers which play an important role in sizing the control surfaces and the emergency maneuvers. The normal maneuvers are studied later in the design sequence in order to predict the capability of the submarine to perform specific operational or tactical maneuvers. Many of these operational maneuvers are closed loop, that is, involve the action of a helmsman or autopilot. Listed below are those maneuvers of interest to the designer (26):

1. Definitive maneuvers (open loop) to evaluate inherent handling qualities

- a. Meanders (vertical plane)
- b. Vertical overshoots
- c. Horizontal steady turns
- d. Horizontal overshoots
- e. Horizontal spirals
- f. Acceleration and deceleration in straightline motion

2. Normal maneuvers (operational or tactical)

- a. Depthkeeping and coursekeeping at various speeds including hovering, using manual or automatic control
  - 1. Near-surface under various sea states
  - 2. Near-bottom including large-scale bottom irregularities
- b. Transient horizontal turns using manual, semi-automatic, or automatic control
- c. Mission profiles of various types including target tracking, weapons delivery, and a variety of evasive maneuvers
- d. Limit dives using manual, semi-automatic, or automatic control.

3. Emergency Maneuvers

- a. Recovery from sternplane jam casualties using various combinations of recovery measures
- b. Recovery from flooding casualties using various combinations of recovery measures
- c. Buoyant ascents to develop safe procedures for exercising emergency ballast blow systems

3.5 Prediction of Submarine Maneuverability

It is desirable for the designer to predict how the submarine will perform the maneuvers listed above as early as possible in the design sequence. The designer will make use of analytic estimating methods, captive model testing and free running model testing to aid in the prediction of submarine maneuvers. The advantages and limitations of each of the three prediction methods are described below.

### 3.5.1 Analytical Technique

In recent years greater use has been made of an analytic approach to the prediction of submarine maneuvers. Now it is possible to estimate all of the coefficients required for the Standard Equations of motion. One computer program called DERIVS can estimate the linear hydrodynamic stability and control derivatives. The program is based on various hydrodynamic theories such as potential flow, slender body, lifting line and boundary layer theory as well as experimental data from Planar Motion Mechanism studies. A detailed explanation of how these various techniques were incorporated in the program has not yet been documented. The program DERIVS is applicable to submarine hulls which are streamlined bodies of revolution with parallel middlebodies. The fineness ratio of the hull should be greater than seven. The appendages of the submarine may include: a deck similar to that on the Fleet Ballistic Missile submarines, a fairwater forward of the center of gravity, a single propeller, a cruciform tail configuration with diving planes, rudders, and vertical stabilizers and sailplanes. The input data for a given submarine configuration includes geometric characteristics of the hull and the appendages. Output includes the non-dimensional stability and control derivatives, mass, estimated moments of inertia and the vertical and horizontal plane indices for dynamic stability. This program will provide the coefficients required for limited maneuvers and can be used to test initial submarine configurations for directional stability which require only the linear equations of motion.

For more complex maneuvers (particularly closed loop), non-linear and cross-coupling coefficients are required and these are obtained from a second program. This program determines certain cross-coupling coefficients which cannot be determined easily from submerged, straightline captive model experiments using the PMM system. The program utilizes both semi-empirical and theoretical equations. The input data consists of ship geometric data and coefficients for the Standard Equation which can be determined with the program DERIVS.

By combining these two programs it is possible to solve the Standard Equations and predict the trajectories for the definitive maneuvers. In order to solve the equations of motion for many normal and emergency maneuvers, special subroutines are required to provide a complete simulation of the motion of the submarine. For example one subroutine for sternplane jams provides a time history for the control surface movements, propeller RPM change from full ahead to back emergency and for the weight of ballast water discharged or taken on. Another subroutine called the sea-state analog provides a representation for the effects of ahead random seas for near surface operation. Typical data required for these subroutines are coefficients or forcing functions for the particular phenomenon being simulated. The data is obtained by special model experiments, by theory or a combination of both.

The analytic approach described above is always checked by captive model testing to verify the estimated coefficients. The Planar Motion Mechanism is used to obtain these coefficients but some crosscoupling terms and those non-linearities

associated with high values of non-dimensional velocity components, such as those associated with tight turns, can be more accurately determined by theoretical methods.

### 3.5.2 Free Running Tests

Free running model tests are generally run to test the final submarine configuration. This enables the designer to verify the results obtained from the analytical study and captive model testing. These tests are particularly important for those motions such as snap roll which cannot be accurately determined with these two techniques.

### 3.5.3 Validity of Prediction Techniques

When using the Standard Equations of Motion for prediction, it is very important to check the results obtained with full scale trial results, particularly if the coefficients were analytically derived. It is difficult to provide a full account of the correlation between computer predictions and full scale trial results. Although a great deal of correlation work has been performed, very little of this work has been published. In May 1970 some data was published for the SSBN 610 and 617 which indicated that vertical plane maneuver computer data correlated very closely with full scale results. For the horizontal plane, data was available only for the SSBN 617. For this vessel, correlations of computer results with full scale are only fair and predictions of snap roll are poor. Fortunately, correlation between full scale and free-running model results for turning diameter and snap roll are quite good. Linear theory is weak for these maneuvers, so free running tests are well justified. Correlation work is being

performed in the area of near surface depth keeping, vertical plane behavior in turns, and emergency maneuvers. Although the work is not complete, the general indications are that computer predictions show better depth keeping performance and that stern-plane jam recovery predictions yield greater depth and pitch excursions than experienced in full scale. The cross-coupling effects which occur in emergency recovery operations are not completely understandable or predictable.

Discussions with some of the designers at NAVSEC have indicated that with some of the more recent projects such as the SSN 688 and the Trident, the analytical estimation of the definitive and emergency maneuvers seem to correlate well with the model tests. The analysis included the new cross-coupling terms calculated in the computer program described above. Documentation of these correlation studies would be helpful in determining whether the Standard Equations of Motion should be extended to include additional cross-coupling terms.

### 3.6 References

1. Matora, Dr. S., "Maneuverability, State of the Art." Department of Naval Architecture, University of Tokyo, August, 1972
2. Newman J. N. "Some Theories for Ship Maneuvering." Massachusetts Institute of Technology. January 11, 1972
3. Bech, Mogens and Smith, Wagner L., "Analogue Simulation of Ship Maneuvers." Hydrodynamics Dept. Hynby-Denmark Report No. Hy - 14. September 1969.
4. Eda, Haruzo, "Ship Maneuvering Motion Prediction for a Safety Model". Stevens Institute. Report No. 723461. August 1972.
5. Clarke, D. "A New Non-Linear Equation for Ship Maneuvering." International Shipbuilding Progress. Volume 18. No. 201 May 1971
6. Paulling, J. R. and Wood, Lloyd W., "The Dynamic Problem of Two Ships Operating on Parallel Courses in Close Proximity." University of California. Series 189 Issue 1. July 18, 1962.
7. Gertler, Morton and Gover, S.C., "Handling Quality Criteria for Surface Ships" NSRDC Report 1514. May 1959.
8. Strom - Tejsen, J. "A Digital Computer Technique for Prediction of Standard Maneuvers of Surface Ships." NSRDC Report 2130. December 1965.

9. Newton, R. N. "Some Notes on interaction Effects Between Ships Close Aboard in Deep Water." DTMB Report 1961 October 1960.
10. Norrbin, Nils H. "A Study of Course Keeping and Maneuvering Performance DTMB Report 1461. October 1960.
11. Chen, Hsao - Hsin "Some Aspects of Ship Maneuverability" Journal of Ship Research volume 13 no. 2. June 1969
12. Thieme, H., "Design of Ship Rudders" DTMB Translation 321. 1965
13. Smith, Leif Wagner, "Steering and Maneuvering of Ships - Full Scale and Model Tests." European Shipbuilding No. 6. 1970
14. Mandel, Philip. "International Towing Tank Conference (12th), Rome Italy," September 1969. NTIS AD 700 305 January 13, 1970.
15. Eda, Haruzo and Crane, C. Lincoln. "Research on Ship Controllability Part 1 Survey and Long Range Program." Davidson Laboratory Report No. 922. October 1962
16. Jacobs, Winnifred R. "Method of Predicting Course Stability and Turning Qualities of Ships" Davidson Laboratory Report 945. March 1963.
17. Jacobs, W. R. "Estimation of Stability Derivatives and Indices of Various Ship Forms and Comparison With Experimental Results". Journal of Ship Research. September 1966.

18. Schoenherr, Karl E. "A Program for an Investigation of the Rudder - Torque Problem". Marine Technology. July 1965
19. Eda, Haruzo. "Directional Stability and Control of Ships Research". volume 16 number 3. September 1972.
20. Chen, Hsao - Hsin. "The Experimental Determination of the Rudder Forces and Rudder Torque of a Mariner Class Ship Model." University of California. Report No. NA-63-5.
21. Crane, C. Lincoln. "Studies of Ship Maneuvering" "Response to Propeller and Rudder Actions."
22. Inoue S. "On the Turning of Ships, Memoirs of the Faculty of Engineering." Kyushu University. 1956
23. Fedyaevsky K.K., and Sobolev, G.V. "Application of the Results of Low Aspect Ratio Wing Theory to the Solution of Some Steering Problems." Wageningen. 1957.
24. Tuck, E. O. "A New Approach to the Strip Theory of Forced Ship Motion. NSRDC Tech. Note. September 1966.
25. Submarine Control Study Group. "Development Plan for Improved Design of Submarine Control Systems." Phase 1, Confidential NAVSEC Report. May 1, 1970.
26. Gertler, Morton and Hagen, Grant, "Standard Equations of Motion for Submarine Simulation." NSRDC Report 2510. June 1967.
27. Landweber, L. and Johnson J. L., "Prediction of Dynamic Stability Derivatives of an Elongated Body of Revolution." Confidential DTMB Report C - 359. May 1951

28. General Dynamics. "ULMS Baseline Design Report"  
Confidential, EB DIV Report No. 409/RWB - 1531 (701).  
April 17, 1972.
29. Office of Submarine Control System Manager "Submarine  
Control Improvement Plan" Confidential NAVSEC Report.  
June 1, 1972
30. Day W. G. and Lin W. C., "Tactical Diameter Prediction  
for Twin Screw Destroyers." NSRDC Report C-455-H-01  
April 1972
31. Saunders, Captain H. E., USN. "Notes on Casualties to  
the Twin Rudders of United States Destroyers" DTMB  
Report R-354. November 1947
32. Code #6136 NAVSEC. "Sea Control Ship - Maneuvering  
and Rudder" Confidential. November 25, 1972

#### 4. RECOMMENDATIONS

The recommendations discussed below are based on the study of the state of the art and the current NAVSEC design procedure for control surfaces. Emphasis has been placed on the development of an analytical approach to control surface design since this development could provide good results at substantially lower cost when compared with model testing.

This section on recommendations is divided into three groups as follows:

1. Proposed future research and development is presented using as a basis, the state of the art as discussed in section 3 of this report.
2. Revisions are recommended for those specific design procedures discussed in section 2 of this report.
3. The technical practices manual is updated to reflect the current NAVSEC design procedure. The section concerning rudder torque calculation is not included since it may be found in NAVSEC's report titled "Establishment of Design Practice for Rudders and Diving Planes" (MR&S Report 2499-2).

##### 4.1 Future Research and Development

###### 4.1.1 Surface Ships

No change to the surface ship handling criteria is recommended at this time. The three Standard Maneuvers provide an adequate quantitative measure of the ship's maneuverability characteristics. There may be some cases where special maneuvers may be required to define particular tactical or operational maneuvers

of the ship. Most of the analytical methods have been developed to handle only the Standard Maneuvers. In order to measure a special tactical requirement, special test procedures will be necessary both in full scale trials and model tests. As the analytical and empirical methods of predicting ship maneuverability improve in accuracy, further development of the handling criteria would be practical.

The approximate NSRDC computer program for tactical diameter is very useful for preliminary design, and is relatively inexpensive compared with other methods of prediction. Where sufficient model test data exists this method should be extended to include spiral and zig-zag maneuvers. The current method is restricted to twin screw destroyers so other ship types should be included. This technique would be extremely valuable in quickly estimating a good rudder and skeg configuration before the expensive model testing commences.

It would be desirable to limit the amount of model testing required for a new design to reduce cost. Ideally then a complete analytical procedure could enable the designer to predict the ship maneuverability characteristics for the Standard Maneuvers without any tank testing. The first step toward this goal would be to utilize the equations which now exist to determine the linear coefficients for the equations of motion. Unfortunately higher order non-linear coefficients cannot be obtained accurately using theory as developed up to this time. Further work should proceed

with refining potential flow, low aspect wing, slender body and boundary layer theory to obtain suitable equations for these coefficients. In the meantime, a semi-empirical analytical method could be developed which utilizes both theory and experimental data. Past captive model tests could provide data for non-linear coefficients and equations for these coefficients could be developed using a regression analysis. Since the Navy has not used captive model experiments extensively for surface ship design, the use of data from tests of similar commercial ships may be necessary.

More extensive use should be made of captive model tests for the reasons cited in section 3.3.4. In addition to providing a more accurate analysis of the maneuverability of a given ship, the results of these tests could also be utilized in the analytic method described above. Free running model tests would only be preferable if a very limited study of the ship was required.

Finally, a complete correlation with full scale trial results should be undertaken to verify the accuracy of the method of prediction employed. This is particularly important for the analytical method since it is necessary to know the sensitivity of the various coefficients in the equation of motion and the adequacy of the equation used.

The following task statements summarize the recommendations made above for surface ship rudder design:

1. Utilize the Standard Maneuvers as the handling quality criteria.

2. Develop further the NSRDC programs for the prediction of the tactical diameter for surface ships so it includes more ship types. Where sufficient data exists from sea trials or free running model tests, the spiral and zig-zag maneuvers could also be included.
3. Develop further the present hydrodynamic theories in an effort to predict the non-linear coefficients for the equations of motion.
4. Develop an analytic procedure for predicting all of the coefficients for the equations of motion. This method should be calculated using a computer.
5. Make greater use of captive model tests in lieu of or in addition to free running model tests.
6. Conduct a continuing study to correlate full scale trial results with the results obtained with the prediction method used.

#### 4.1.2 Submarines

No handling criteria exists for submarines in the current procedure. In the past this was unavoidable since little information existed for the maneuvering capability for modern submarine designs. Now a substantial amount of test data exists for the most modern submarines and it should be possible to specify requirements for the maneuverability and control of the submarine. The maneuvers that are recommended for use as a criteria are the definitive and emergency maneuvers which would apply to all submarines as listed in Section 3.4. The normal maneuvers would have

to be selected for the particular submarine under study.

Methods for determining the coefficients for the equations of motion should be improved using potential, slender body and boundary layer theories. Particular emphasis should be placed on those coefficients which must now be estimated with the use of empirical data. A completely analytical procedure for predicting submarine maneuvers would be a powerful design tool. With the present procedure, by the time the final results are obtained from tank tests, it is too often late to initiate major changes to the control surface configuration. Even an approximate analytic prediction method would be useful since it would eliminate the need for major design changes in the detail design stage of the submarine.

Experimental techniques should be developed for determining the cross coupling terms for the equations of motion which are now determined only analytically. This would enable the designer to directly check the accuracy of the analytic method he is now using to calculate these terms. Good experimental data would facilitate corrections to the analytic method should this be required.

The theory and rational used in developing the current computer programs for estimating the coefficients should be documented to facilitate additional research in this area.

A complete correlation study should continuously be employed to compare full scale trial results with results obtained from captive model tests, free running tests and particularly with the new analytic method of prediction available. One of the biggest

questions facing the designer which only a correlation study could answer, is the adequacy of the equations of motion used to predict submarine maneuvers. Recently, new terms have been added to the standard equations and results obtained for the Trident and SSN 688 should be correlated with the free running model test results.

The following task statements summarize the recommendations made above for submarine control surface design:

1. Utilize the normal and emergency maneuvers listed in Section 3.4.1 as the standard handling criteria.
2. Develop further the existing hydrodynamic theory to more accurately estimate the coefficients required for the equations of motion.
3. New experimental techniques should be developed to determine derivatives for the equations of motion which cannot be measured now in the test tank.
4. The current computer programs for estimation of hydrodynamic coefficients should be completely documented including the rationale used in their development.
5. A complete correlation study should be employed to compare results of prediction methods with full scale results.

#### 4.2 Revisions to the Current NAVSEC Design Procedure

The following revisions are recommended to the design

procedures discussed in Section 2 of this report:

1. The computer programs for control surface torque estimation should be modified so that any desired balance of steering gear torque may be obtained.
2. Use the updated hydrodynamic torque calculation as discussed in Section 2.2 of this report in lieu of the method shown on the stress diagrams for the DD-921 (spade rudder) and BB-61 (horn rudder).
3. Modify the equations for minimum cost of rudders as indicated by Section 2.4 and Appendix A of this report.

#### 4.3 Revised Technical Practices Manual

The following pages contain the original Technical Practices Manual and the changes made for each page. For changes made to Section 3 of Part A and Sections 3.4, 4.2, 5.1 and 7.1 of Part B of the Manual, refer to NAVSEC Report 6136-74-272, titled "Development of a Technical Practice for Rudders and Diving Planes, Part II, Torque Predictions".

## Hydrodynamic Design

### Practice:

#### Preliminary Design of Ships Appendages

A completed preliminary ship design frequently has an appendage plan as part of the drawings describing the ship. The appendage design has an effect on the maneuverability, speed, endurance, seakindliness, weight, and space of the ship. These important aspects must be considered and when possible predicted by the preliminary designer. For this reason considerable attention is often given to the design of appendages as well as to assist in the construction of models to be tested.

The following appendages are included on almost every naval ship. A brief description of the designer's practice for determining size, shape, and location is given.

(a) Rudders - Number of rudders, their size and location, are determined on the basis of previous experience as well as the particular requirements of the design itself. Rudder section shape is defined by the NACA-OO section offsets with thickness to cord ratios dependent on stock size and selected rudder profile. Forty degrees rudder swing is considered maximum. Reference material to assist the designer can be found in Code 420 File 2.100 and a 1953 SNAME paper titled "Some Hydrodynamic Aspects of Appendage Design" by Mr. Mandel.

(b) Bilge Keels - Preliminary appendage plans generally show the bilge keels at the midships section with reference to their extent along the hull. Final location is left for further development depending on model tests and detailed structural considerations. Size is governed by previous designs of similar ships types. Guides are again given by Mr. Mandel's 1953 paper.

(c) Shafts and struts - It is only necessary to approximate shaft diameter on the preliminary plan. Inboard location of the shaft can be determined with the assistance of the Marine Engineer (Code 430) doing the preliminary machinery arrangement. However, shaft location at the propeller is dependent on the entire stern arrangement. Such aspects as propeller diameter, tip clearance, and rudder location, all must be considered by the designer. Guidance for determining strut and shaft size is given in section DD94301-1 and 2, of the "Design Data Book for Ships of The United States Navy."

Two additional appendages are often required by the characteristics of recent ship designs.

(a) Sonar Domes - The sizes of Sonar Transducers have grown in recent years to such an extent that considerable emphasis is now placed on the integration of the sonar dome within the hull lines. Two fundamental aspects of sonar dome design must be considered by the designer:

- (1) The effect of size, shape, and location on performance of the sonar transducer.
- (2) The effect of size, shape, and location on the ship's speed, endurance, structure, and anchoring.

To assist the designer in determining the effect on sonar performance of his design he should call on Code 688 (Sonar branch). To estimate the effect on ship speed and endurance Code 420 File 1.708 records the results of model tests with methods for predicting dome resistance. Future ship trials will aid considerably in determining good sonar appendage design practice.

(b) Fin Stabilizers - Code 420 File 3.230 outlines the present method of determining stabilizer capacity and resulting size of Fins. Again

CHANGES

COMMENT

Insert Page 45

Change #1 Delete remainder of  
paragraph after "and  
selected rudder profile".  
Insert: Thirty-five + two  
degrees rudder swing Ts  
considered maximum. Refer-  
ence material can be found  
in Code 6136.

future ship trials will aid considerably in determining good in design practice.

## Hydrodynamic Design

### Practice:

Prediction of Surface Ship Motion; Status of

The state of the art of predicting surface ship motion rests upon the following areas of endeavor:

- Assumptions of small non-linearities such that a linear mathematical model will suffice.
- The nature of the cross-coupling between the degrees of freedom.
- Accuracy in obtaining the stability derivatives used in the differential equations of motion
- Characterization of the actual input.

Present day practices depend a lot on the use of a simple mathematical model in which items a and b are then relegated toward future investigation. Non-linear solutions are quite difficult to handle without special computing machines and a proper analogue of the actual physical situation. For "ball park" approximations, the experiences of the aerodynamic field show that the answers obtained from such simplifications are tenable without getting involved in complicated mathematics. For example, the investigation of turning can be idealized as:

$$(m'_1 - Y' r') r' - m'_2 \beta' s - Y'_\beta \beta' = U'_1 (r')$$

$$U'_1 r'_s - N'_1 r' r' - N'_\beta \beta' = U'_2 (r')$$

The success in solving the equations of motion, assuming the hypothesized mathematical model is reasonable, lies in the success of obtaining the information listed under items c and d.

The Taylor Model Basin should be able to furnish experimental information with the advent of the new facilities - Rotating Arm and Maneuvering Basin. The measured derivatives are used to furnish analogue computer studies. The results can be compared to similar class ships for qualitative evaluation to some "datum" ship if not for quantitative prediction. The latter is much more difficult because of the obvious problem of predicting and delineating the input. The extension of the response to an actual seaway is presently undergoing investigation by application of the principle of linear superposition and advanced concepts of spectral analysis.

## Hydrodynamic Design

### Practice:

#### Control Surface Design

Maneuverability and directional stability are important aspects of a surface ship's and submarine's operational value. Control surface design (rudders, stern planes and bow planes) is vital in this consideration.

Some guides are given on other sheets (Prediction of Directional Stability and Predictions of Tactical Diameter).

As a first step, areas are generally proportioned upon length x beam, from similar previous ships, modifications and variations are made to suit the ship under consideration. Further guiding information may be found in file #2.160 (General Control Surface Data), file #2.140 (Active Rudders), file #2.150 (Flapped Control Surfaces). Mandel's 1953 SNAME paper and the model and full-scale results of particular submarines in file #2.601 through 2.614 and for surface ships in file #2.201 through 2.349, and Table 10 of the Manual for Prediction of Submerged Speeds of Submarines.

## Hydrodynamic Design

### Practice:

#### Submarine Directional Stability Prediction

Positive directional stability in the horizontal and vertical planes is an important built-in feature of submarines that has a strong effect on the handling qualities.

Current practice is to follow the procedure in file 2.520 (Prediction Methods - Directional Stability). Stabilizing area and shape are determined by trial-and-error until a value of about  $\nabla = -0.3$  is achieved.

The intent is to keep the control surfaces within the block dimensions (beam and draft) if possible. This guide, however, has been violated in a few of our latest submarines.

The directional stability should be checked by a model test program at the earliest opportunity.

## Hydrodynamic Design

### Practice:

#### Surface Ship Tactical Diameter Prediction

The tactical diameter that a ship should make is specified in the characteristics. This is an important operational maneuver.

The current practice of prediction can be found in file No. 2.202 (Predictions of Tactical Diameter). This includes, in an empirical system,

## CHANGES

## COMMENT

Insert Page 46

Change #2 Replace words...length  
x beam... with...length  
x draft...

Rudder area is proportional to profile area.

Change #3 Delete words after ...  
ship under consideration...and replace with:  
Further guiding information  
may be found in file #6136,  
DTMB translation #321, and  
NSRDC program Code 1524 for  
tactical diameter.

Much of the material  
listed is now out of  
date.

Change #4 Delete paragraph  
current...is achieved.  
Insert: Control surface  
areas are initially estimated  
with the aid of proportional  
relationships based on data  
from similar submarines.  
Rudder and fairwater plane  
areas are proportional to  
displacement and stern plane  
area is directly proportional  
to displacement and inversely  
proportional to length.

all the pertinent parameters in our present knowledge. An important part of this is the rudder design. This is a highly individualistic procedure (one closely adapted to the particular ship) but this would follow loosely the concepts outline in SNAME, 1953 Transactions, "Some Hydrodynamic Aspects of Appendage Design" by P. Mandel.

These maneuvers include turns (pertinent parameter are tactical diameter, advance, transfer, time to change heading  $90^\circ$  and  $180^\circ$  rate of change of heading and speed loss), zig-zags and Dieudonne spirals. These tests are generally requested by Code 421 or 442, either at the end of the preliminary design or the beginning of the contract design. (5)

#### Hydrodynamic Design

##### Practice:

###### Submarine Maneuverability Estimate

Maneuverability of submarines in the vertical and horizontal planes is an important feature of the submarine's behavior.

Current practice is to compare DTMB results of certain standard maneuvers to a similar ship for differences. These maneuvers include in the vertical plane overshoots in pitch and depth, and time to reach, execute, in the horizontal plane, overshoots and Dieudonne Spirals. At this time, the results require model tests and analogue computer studies, it is anticipated that in the future these can be determined at the drawing board.

#### Hydrodynamic Design

##### Practice:

###### Submarine Angle of Heel in Turns, Prediction of

At this time, the snap inboard heel, experienced by our modern submarines when entering a turn, is a limiting factor on the speed and tightness of turn that may safely be accomplished.

The method of prediction of steady angle of heel in a turn may be found in file 2.560. The present crude rule of thumb (prior to model results) is to estimate the snap roll as three times the steady heel.

Values of snap roll in excess of  $35^\circ$  are undesirable.

#### Hydrodynamic Design

##### Practice:

###### Standard Maneuvers (Surface Ships)

Good maneuverability and directional stability are important characteristics of the operation of naval vessels.

Current practice is to compare DTMB free-running model tests of certain standard maneuvers to a similar ship. At this time, we have not established firm criteria, but it is anticipated that this will be accomplished in the near future. (5)

CHANGES

COMMENTS

Insert Page 47

Change #5 Delete paragraphs  
beginning with  
Current practice is...  
and These maneuvers...  
and insert the following:  
Current practice is to  
compare DTMB free-running  
model tests of certain  
standard maneuvers to a  
similar ship. The hand-  
ling criteria used are  
three maneuvers referred  
to as the Standard Maneu-  
vers. The Standard  
Maneuvers is a set of  
trials consisting of a  
turning circle, zig-zag  
and a spiral maneuver.

## RUDDERS AND SUBMARINE CONTROL SURFACES 9220-1 (Code 442)

### A. Rudder Design

#### Practice:

##### Section 1. - General

1.1 The aim of rudder design is to provide tight turning, good ability to initiate and check swings rapidly, and good course-keeping ability. Quantitative measures of these are usually investigated by tactical diameter, zig-zags (Kempf or Z-maneuver) and spiral maneuver (Dieudonne) model tests. For replenishment ships, the approach and alongside positions are sometimes investigated in model form. Of course structural reliabil-

ity, minimum propulsive losses and overall cost must be included to obtain complete balanced design.

1.2 The best sources of general design practice are the 1953 Trans. SNAME article "Some Hydrodynamic Aspects of Appendage Design" by P. Mandel and "Hydrodynamics of Ship Design" by Capt. H. E. Saunders. For merchant ship types, typical practice is best shown in J. P. Comstock's article in "Design and Construction of Steel Merchant Ships" by Arnott. Two publications, the SNAME revised edition of Principles of Naval Architecture and a SNAME Panel H-10 Notes on Ship Controllability are expected to be issued in the near future. The manuscript copies indicate they will be very useful.

1.3 For a specific ship type, usual design practice is to first study the design history of earlier ships of the type and to check with the Type Desk for maintenance problems.

#### Criteria:

##### Section 2. - Rudder Planform and Location

2.1 Current practice in selecting rudder planform and location generally follow the theory in the 1953 Trans. SNAME article by P. Mandel. The tabulation of characteristics on page 482 is for specific ships of the U. S. and British Navy and the identification code is available in Code 421 or 442. Model tests are usually run to verify the prediction. Ship characteristics generally indicate desired maneuvering performance. Model tests tests for tactical diameter are usually reliable to within plus or minus 5 percent. In rare instances there are larger discrepancies, such as on DLG 16 where full scale tactical diameter was 16 percent greater than model data (DTBM Reports C-975 and C-1700). It should be noted that full-scale tactical data are sometimes erratic, so that correlation with model data reflects more than just scale factors. A 10 percent margin on tactical diameter by model test predictions is considered a minimum, with a 15 percent margin desirable if readily attainable.

##### 2.2 Additional items to consider are:

(a) Rudders are generally moved out of a position directly in line with propeller shafting, in order to avoid the propeller tail cone vortex. This is done even for single screw ships (e. g. DE 1052) with high power. AGDE 1 is an exception to this practice, since it is expected that the pumpjet will eliminate the tail cone vortex. Auxiliaries with low power are usually built to merchant standards, with the rudder in line with the tail cone.

(b) Unshipping of propellers and shafting should be investigated and adequate clearance provided without having to unship a rudder. In some cases unshipping the tail shaft may require turning the rudder and removing portable rudder plates. This is avoided wherever possible.

(c) The rudder should be well submerged even with the ship lightly loaded aft and heeling in a turn.

(d) The rudder-rudderstock combination of tapers and location are made such as to permit unshipping the rudder without special high blocking. Where the rudder cannot be dropped enough directly downward, provision should be made for first lifting the stock within the ship. Tilting the rudder on the stock taper is possible, but is avoided except as a last resort.

ice, and landing craft have twisted stocks after beaching and breaching with rudders in the sand. In some cases replaceable shear pins have been installed to protect the steering gear from such damage.

#### Section 5. - Rudderstock Material

5.1 For rudders welded integrally to the stock, we specify the low carbon forged steel MIL-S-20140. (See LSD28 and DE1006 plans for details.) This steel has 30,000 p.s.i. yield and 60,000 p.s.i. ultimate strength.

5.2 Beginning approximately April 1965, steel forgings for rudderstock socketed connections have generally been ordered to Mil. Spec. MIL-S-2328. This will permit easier weld repair capability than Mil. Spec. MIL-S-890, which had been used for many years.

5.3 The use of higher strength steels tends to save weight and permit thinner rudder sections, both of which are desirable. There are, however, the following drawbacks: (a) the deflection of the stock tends to be greater, involving a potential problem with seals and, (b) the natural frequency tends to be lower, which probable involves a little more potential vibration.

5.4 Where rudderstocks are required to have little or no magnetic permeability, aluminum bronze has worked well on AMS60 and MS0421 Class. World War II minesweepers had rudderstocks of Tobin bronze (which is really a brass). These bent and twisted in service, hence the later designs used the high-grade and costly aluminum bronze.

5.5 In selecting rudderstocks, corrosion resistance is desirable (since protective coatings are not yet reliable). Ordinary fatigue is not considered to be a problem since there are generally only a few cycles of high stress a year (ship at full power with full rudder angle). Notch toughness is highly desirable, since corrosion pitting is probable over the course of years.

#### Section 6. - Rudder Plating and Framing

6.1 Present practice is to adjust plating and framing to get panel sizes of span equal to about 40 thicknesses of plating. Earlier designs with greater spans (e.g. DD445 Class, DD692 Class, CVA41 Class) suffered loss of rudder plating from panning, fatigue, corrosion, and erosion.

6.2 For rudders not in a propeller race the plating is usually M.S. (e.g. DL1). For rudders in a propeller race, S.T.S. or HY 80 are generally specified (e.g. DL2 Class) because of superior strength and slightly improved corrosion resistance compared with H.T.S. and M.S.

6.3 At the trailing edge of the rudder, a rabbeted casting or forging, with equal galvanic

#### Section 4. - Rudder and Rudderstock Stress Analysis

4.1 Because of the importance of rudders in controlling a ship, a stress analysis is usually made during design, and the shipbuilder is usually required to make one based on actual scantlings. Stresses are limited so as to provide a minimum factor of safety of 2.0 on yield with loads computed as indicated in Section 3.2. Where loads are estimated by less reliable means (e.g. Joessel's formula) the minimum factor of safety is taken as 2.5 on yield.

4.2 For semi-balanced rudders with horn, the best practice is available in Code 442 files for the BB61 stress analysis by New York Naval Shipyard. For gudgeon strength (designed as elastic arch) a method devised by L. W. Ferris is used and available in the Code 442 files.

4.3 For spade rudders the best practice is shown in Code 442 files for the Gibbs and Cox stress analysis of DD931 Class and DL2 Class rudders.

4.4 A computation for rudder hub strength is shown in the Code 442 files for CVA(N)65. DTMB Report Experimental Stress Analysis of a Socketed Connection in Bending by L. A. Becker has some useful test data.

4.5 There are also problems with non-hydrodynamic loads on rudders. AKA, AGB, and LST types have twisted rudderstocks while operating in

## CHANGES

## COMMENTS

Insert Page 149  
(Starting with Section 4)

Change #6 Section 4.1 - Delete words after ... "safety of 2.0..." and insert "on yield for spade rudders and 2.5 on yield for horn rudders."

Change #7 Section 4.2 - Delete existing paragraph and add the following: For semi-balanced rudders with a horn, the best documentation is in MR&S Report 2566-3 and the BB61 stress analysis diagram which is available in Code 6136 files.

Change #8 Section 4.3 - Delete paragraph and add:  
For spade rudders the procedure is documented in MR&S Report 2566-3 and the DD931 and DL2 stress analysis diagrams which are available in Code 6136 files.

Change #9 Change the words  
Code 442 to Code 6136.

Change #10 Add Section 4.6: For non-tapered gudgeons, the gudgeon strength is determined with the aid of the report titled "method of Calculating Stress in a Gudgeon - Envelope 010809. For determining the strength of tapered gudgeons use the report titled "Experimental Stress Analysis of a Socketed Connection in Bending" by L. A. Becker.

property as the side plating, provides the strongest construction (e.g. DL2). Where economy is important, the side plates can be welded to one another (e.g. DE1006).

**6.4 Valuable information on this subject is available in TMB Rept. R-354 "Notes on Casualties to the Twin Rudder of United States Destroyers" by Captain H. E. Saunders.**

#### Section 7. - Bearings

7.1 Bearings are to be designed to take the rudderstock radial and thrust loads and the rudderstock flexural deflection. These are computed using:

- (a) Hydrodynamic loads on rudder
- (b) Weight of rudder plus stock
- (c) For design which includes shock resistance as a requirement, (a factor from General Specifications 9400-1) times the weight produces radial and thrust loads which are not combined with (a) and (b) above.

7.2 Bearings are of two basic types:

- (1) Rolling friction or anti-friction (such as roller or ball bearings) and
- (2) Sliding friction or sleeve (such as floating collars for thrust, bronze sleeve and phenolic bearing type for radial). Recent examples of these types are shown, respectively, on plans DD927-S2202-760457 and DD931-S2200-1426955.

7.3 We have been using friction coefficients of 0.01 for anti-friction types, and from 0.15 to 0.20 for sleeve types. These values are based on commercial practice and some brief tests at Portsmouth Naval Shipyard. In connection with torque estimates, there may be some margin in the 0.2 coefficient for sleeve bearings. There is no significant margin in the 0.1 coefficient for anti-friction bearings.

7.4 Sleeve bearings have low initial cost, are relatively easy to maintain, and in most cases would be relatively easy to repair in emergencies. We usually specify staves of laminated phenolic, with laminations such as to produce edgewise compression. Staff details and clearances are shown in BUSHIPS Standard Plans S2200-921759 and S2200-921760. Clearances are also shown in BUSHIPS Technical Manual Chapter 44. Allowable compressive stress is taken as 3000 p.s.i. This material has a Young's modulus of about 420,000 p.s.i., and can run in water, grease, or oil. Commercial forms are sold such as Westinghouse Marine Micarta, Ryetex, and Tufnol. In special cases where laminated phenolic bearings could be so long as to cause binding from flexure of the rudderstock, other materials are in order, such as gun metal or cobalt-base alloy. These permit higher bearing stresses, so they can be shorter. Typical installations are shown in BUSHIPS

Plans SS564-S1108-935524 and SSN585-518-1713907. A calculation for clearance in the bearing with the stock in its deflected shape is shown in plan SSN585-845-1716223.

7.5 Anti-friction bearings are fairly expensive and require some precision machining to install. They have the compensatory advantages of permitting significant reduction of steering gear torque (in the order of 40%) and can be self-aligning (so that rudderstock deflections and hull movement do not cause binding). There are several manufacturers of roller bearings (spherical and non-spherical), which tends to keep the price reasonable. We usually require that the roller bearing vendor indicate his approval of the shipyard's installation details by signing on the working plan.

7.6 It is understood that roller bearings were installed on a collier at about the time of World War I, and that they had to be replaced by sleeve bearings. No records are available. USS TIMPERMAN (EDD 828) had a roller bearing installation which gave no trouble during the ship's brief career at sea. USS NORFOLK (DL1) and the USS MITCHELL (DL 2) Class have spherical roller bearings which have been operating since about 1950. There had been some concern as to possible dislodging of one or two rollers, due to pounding of a propeller race on a rudder which is generally operating near zero degrees. This has apparently not happened.

7.7 Two unsettled questions on anti-friction bearings are: (a) is it worthwhile requiring an installation with inner race expanded to take up clearances? and, (b) should designs call for an adapter so as to try to standardize on the bearing size? Past practice has permitted builders to use their judgment on these matters, and the actual practices vary. As service experience accumulates, the Ship Specifications can become more specific.

#### Section 8. - Bearing Seals

8.1 Sleeve bearings at the hull can operate with sea water as the lubricant. Usual practice, however, is to call for pressure grease lubrication and a seal. The seal is usually a gland, made in halves to facilitate replacement, with a few rows of packing. It is adjustable only in drydock. It more-or-less retains the grease and excludes sea water and sand or mud particles.

8.2 Sleeve and roller bearings within the hull are usually pressure grease lubricated, and occasionally oil lubricated. Adjustable seals are provided, and made in halves to facilitate unshipping.

CHANGES

COMMENTS

Insert Page 150

Change #11 Delete the last sentence of paragraph 7.3 and insert this sentence: There is no significant margin in the 0.01 coefficient for anti-friction bearings.

Proper value for friction coefficient is 0.01

Change #12 Delete the words gun metal or.

Change #13 Delete paragraphs 8.1 and 8.2 and insert the following:  
8.1 Current practice with sleeve bearings is to use elastomeric seals, (spring-loaded lip seals) at both ends of bearing. These seals should be chosen to be flexible enough to maintain an effective seal for all rudder stock deflections and to accommodate allowable bearing wear. Lubrication is by grease with suitable distribution grooves in the bearing. A vent is required near the grease fitting to determine when bearing is full.

8.2 Use of adjustable seals (compression packing) is generally being discouraged since they lack the flexibility and resilience to accomodate rudderstock motion.

Changes made according to NAVSEC memo SER 29-6148D

8.3 Roller bearing seals at the hull require special attention because sea water will ruin the bearings. The DL1 and the DL2 Class have Syntron seals, adjustable only in drydock. These seals have an internal oil pressure which exceeds the sea pressure, so that if there is any leakage it will be oil going out. There was some difficulty in the building yards, due primarily to the attempt to wrap a straight extruded seal around a stock. When molded circular seals were used there were no problems. These Syntron seals have been operating satisfactorily on DL1 and DL2 for about 15 years. A more conservative solution has been used on recent destroyers, whereby the hull seal is a gland with packing, adjustable from inside the ship. This means moving the hull roller bearing upwards a little, with a slight increase in rudderstock bending moment. This type of seal has the advantage of being capable of repair almost anywhere. (14)

#### Section 9. - Rudder Streamline Sections

9.1 Present practice is to specify the NACA 4-digit symmetrical series. Offsets are available in General Specifications 9220-1. The first two digits in this series are zero, and the last two digits represent the thickness/chord ratio (e.g. an 0024 section has thickness equal to 24% of the chord). (15)

9.2 At the after edge, the offsets show a definite half-breadth. The trailing edge is specified to be left sharp, since this slightly improves lift, does not add to the cost, and provides a little extra strength (particularly for astern operation) compared with a knife edge.

9.3 Usual practice is to specify sections at the root and tip chord, with straight lines connecting like-numbered stations. Unless the thickness-chord ratios tip and root are identical, this results in a slightly warped surface. None of the shipyards have ever complained of this, and apparently the warp can be taken up, even with STS or HY80, without difficulty.

9.4 Some previous designs (e.g. MS0421 Class) had streamlined shapes to DTMB's EPH (ellipse-parabola-hyperbola) section. This practice was discontinued when it was learned that the EPH section had high negative pressure peaks at large angles of attack, and would thus be more likely to cavitate than the NACA section.

#### Section 10. - Rudder Initial Zero Setting

10.1 The rudder indicator zero in the pilothouse is sometimes set with the rudder not parallel to the center-line plane of the ship.

10.2 For twin-screw twin-rudder ships, model tests are ordered to determine SHP to make some high speed in the region of full power. These tests are run over a range of rudder settings (both rudders with trailing edges inboard 4° to both with trailing edge outboard 4°.) The selection is made on the basis of lowest SHP to make desired speed but vibration sometimes is involved. On DD931 Class it was found that optimum rudder settings for propulsion involved unacceptable vibration. The rudder initial settings were modified to ease vibration, at the expense of propulsion. On DLG14 a similar condition was specifically investigated during builder's trials, and a similar compromise made. (See Code 442 rudder files for these ships).

10.3 For ships with single right hand screw, there is a basic tendency to turn to port. For such designs, model maneuvering tests are sometimes ordered to find the rudder angle for straightaway motion. The rudder is then set that way with indicators at zero.

10.4 For twin-rudder twin-screw ships, TMB model tests show that the best setting for minimum SHP is not the same as the best setting for minimum rudder drag. Presumably there is an interaction between propeller and rudder.

#### Section 11. - Astern Operation

11.1 Astern operation is usually investigated only for ships having a military requirement for going astern (e.g. LCU types which retract astern). Model tests are then used for determining controllability, since there is no reliable theory.

11.2 Ship speed for astern operation is usually estimated at 80% of the ahead speed for the same SHP. This is based on model tests of IFSI. If a more refined estimate is needed, propulsion tests should be ordered.

11.3 Astern operation generally does not control scantlings, and generally does control steering gear capacity. Recent practice has been to design the steering gear for ahead operation and limit sustained astern RPM so as not to exceed the steering gear capacity. "Sustained" astern RPM is specified so as to still permit the ship to use full astern RPM for crashback. It should be noted that for astern operation the hydrodynamic forces tend to move the rudder to larger angles, since the center of pressure is well aft of the stock. Accordingly, in going astern with a hydraulic system, when the relief valve opens, the rudder would go to hard over. To avoid this, usual practice is to specify that

CHANGES

COMMENTS

Insert Page 151

Change #14 In paragraph 8.3 after  
the sentence ending  
with "...rudderstock bending  
moment". Add the sentence:  
The hull seal must be separate  
and independent from the bearing  
seal with provision for  
leak off between the two.

Change made according  
to NAVSEC memo  
SER 29-6148D

Change #15 Add in paragraph 9.1 after  
"...of the chord, the  
sentence: The maximum thickness/  
chord ratio equals 0.23.

the safe sustained astern RPM be determined from sea trials, and that suitable warning plates be installed.

11.4 Astern force and center of pressure coefficient for certain rudder shapes are available in Appendix C of DATMOBAS Report 933. (16)

## B. Submarine Control Surfaces

### Practice:

#### Section 1 - General

1.1 Information in "Technical Practices - Rudder Design" is applicable also for submarines. Additional special items, pertinent only to submarines, are included here.

### Criteria:

#### Section 2 - Stability and Control

2.1 The basis intent of submarine control surface design is to obtain positive directional stability, good depth and course keeping ability, and good ability to initiate and check trajectory changes. The preliminary design estimates of required control surfaces are generally tested by DTMB, and adjustments made as necessary. After minimum requirements are met, there is the problem of how much better to make performance. There is no fixed practice on this matter of degree of controllability. Design decision involves judgment, experience, and compromise related to the specific case.

2.2 Stability and control are design requirements for ahead operation, surfaced and submerged. Astern operation is generally quite unstable, and we accept whatever comes out of the design that has been based on ahead operation.

2.3 Basic theory for submarine stability and control is available in the Taylor Model Basin lecture notes "The Dynamical Stability of Submarines" by M. A. Abkowitz, June 1949. Another very good source of stability and control practice is in TMB reports on model tests and full scale evaluation of specific designs. These reports generally include considerable discussion of design suitability in addition to test data.

2.4 Performance requirements for automatic or semi-automatic control systems are specified in terms of "percentage of time within  $\pm 5$  foot band" at particular speed (e.g. 6 knots) and keel depth (periscope depth) in a particular sea state. Computer studies using model data are run at DTMB to determine the practicality of the specification.

## Section 3 - Fairwater Planes and Bow Planes

3.1 Fairwater planes (also called sail planes) or bow planes are provided primarily for assisting the stern planes in low speed fine control of depth (e.g., 4 knots and periscope depth). In cases of stern plane jamming at small angles, the forward planes could overpower the after ones and control depth and pitch angle. In usual design practice, however, the forward planes are not made large enough to be effective in such emergencies. Some submarine operators use bow planes for depth-changing at high speed, but this is not general practice. ALBACORE (AGSS 569) evaluated performance with and without bow planes, and, for her operations, finally concluded they should be omitted. AGSS 555 is being built without bow or fairwater planes, since the ship characteristics do not require fine depth control and the omission reduces weight, cost, and mechanical complexity.

3.2 Bow planes, situated as far forward as possible, have greater pitching leverage than fairwater planes. In such forward locations bow planes have had to be stowed by folding or rotating, since their outreach would make handling at docks and resting quite difficult and also to avoid pounding when surfaced in a seaway. Recent designs (SSB(N) 585, SSB(N) 593 and 608) call for fairwater planes primarily to release the valuable space forward for sonar and torpedoes. Fairwater planes outreach is usually kept within maximum hull dimensions, and rolling alongside a dock is also considered (e.g., see Code 442 file for SSB(N) 597). Fairwater planes are incidentally used as a gangway for access. Sockets for portable stanchions are fitted with faired plugs for operation at sea.

3.3 The leading edge is usually raked so as to deflect mine cables. There is no fixed practice on whether tips should be square (cheaper and more lift) or rounded (costlier, less lift, somewhat quieter). (17)

3.4 In computing forces and centers of pressure, the angle of attack is taken as the plane angle. (Unlike Rudder Design Practice, Section 3.3, the diving planes can be operating with no drift angle reduction.) The usual plane angle is limited to 20° or 25°; based on estimated stall.

3.5 Fairwater or bow plane tilting rate is usually taken equal to that for the stern planes.

3.6 The height of fairwater planes is of considerable importance. SSB(N) 608 and 616 Class planes are about four feet higher (relative to optics and electronics masts) than SSB(N) 598 Class. This has led to greater difficulties in periscope-depth

CHANGES

COMMENTS

Insert Page 152  
(For section 3.4 of this page,  
see NAVSEC Report "Establish-  
ment of Design Practice for  
Rudders and Diving Planes"  
(MR&S Report 2499-2)).

Change #16 Delete paragraph 11.4  
and insert the following:  
11.4 Astern force and center of  
pressure coefficient for certain  
rudder shapes are available in  
Appendix C of DTMB Report 933.  
This data may be used to obtain  
a preliminary estimate for  
maximum permissible astern  
speed. In sea trials the  
maximum permissible shaft RPM  
will be determined and this will  
establish in turn the maximum  
astern speed.

Change #17 Delete sentence beginning  
with: There is no fixed..  
and add Tips should be rounded  
to reduce noise.

control is a seaway than for 598 Class. The separation between periscope and fairwater planes on SS(N) 585 Class appears satisfactory. As an experiment, bow planes have been installed on SSB(N) 626. Evaluation thus far is not conclusive since there are some subjective factors and the seaway involves a variable test environment.

#### Section 4 - Stern Planes and Stabilizers

4.1 The area needed at the stern for stability in the vertical plane is determined by theory (Code 421 has the best information on prediction methods) and model test. The area is usually too large to be made all-movable, so part of it is installed as a fixed stabilizer. At times fixed area is inserted on shaft lines of twin screw subs (e.g., SS(N)571).

4.2 As with bow planes, the angle of attack is taken equal to the plane angle, without any drift corrections. The force and center of pressure determination for the stern plane plus stabilizer combination is lengthy and complex. The best sources of force and torque information are the Code 442 file, "Rudders and Diving Planes SSB(N)608" (which includes reference material), and recent research reports by Georgia Institute of Technology on "Wind Tunnel Investigation of the Effect of a Simulated Submarine Hull on the Aerodynamic Characteristics of All-Movable Control Surfaces Having NACA 0015 Airfoil Sections" dated August 1959, and by U. of Maryland on "Wind Tunnel Investigation of the Characteristics of a Flapped Control Surface Mounted on a Simulated Submarine Hull" dated June 1959. These reports are available in Code 442 file "Fluid Mechanics - Control surfaces".

4.3 The planform and location of stern plane and stabilizer are selected with the following considerations in addition to conventional hydrodynamic efficiency:

(a) The leading edge rake should be such as to deflect mine cables, or else the shape should permit attaching cable guards.

(b) Ample fore-and-aft clearance from the propeller should be maintained, to minimize noise and vibration. Clearance is measured from the centerline of propeller blade at the 0.7 radius to the leading edge of the control surface, and is non-dimensionalized in the form of percent of propeller diameter.

(c) Span should be limited so as to facilitate nesting, coming alongside a dock, and for larger subs to increase the number of drydocks and building ways that can be used. The SSB(N)608 stern planes and stabilizer have an over-all span of 40'-4", which is about

the limit on Electric Boat Division's building ways. This span extends beyond the maximum beam (pressure hull diameter - 33'-0"), but is necessary for stability and control. Portable out-board sections of stabilizers are permissible where necessary for building ways clearance.

4.4 Stern plane tilting rate is generally specified as 5°/sec. minimum, to provide adequate controllability, and 10°/sec. maximum, to minimize the required capacity of the hydraulic system. A more refined specification is shown in the Preliminary Design section on technical practices for hydrodynamics. The most reliable method of specifying stern plane rate is from a computer study of its effect on trajectories or depth control in a seaway.

4.5 Since the stern planes are vital for depth control, particular emphasis is placed on minimizing corrosion of the stocks. We require protective coatings on exposed portions, and there is a routine requirement for periodic inspection. At present this problem is not satisfactorily solved. New coatings are being tried, and we keep up with the latest service experience obtainable from the Submarine Ship Type Branch.

#### Section 5 - Rudders

5.1 The design of submarine rudders is generally the same as covered in "Technical Practices - A. Rudder Design". The significant differences are discussed below.

5.2 A top-side rudder is in a flow which has been disturbed by the sail and superstructure. This was first demonstrated by a wake survey on a model of SSB(N)608. Accordingly, the top-side rudder is not very effective for stability, where small angles are involved, even though quite effective for turning. A large fixed stool support for the upper rudder was used on SSB(N)608, to get the upper rudder into a cleaner flow region.

5.3 A dorsal rudder (see plan AGSS569-800-1934050) is a flap on the after end of the sail, designed to reduce snap roll in submerged turns. As a submarine goes into a turn, the angle of attack on the sail would produce lift causing large inward heel. The dorsal rudder introduces a camber which reduces the undesirable lift on the sail. Timing the movement of the dorsal and conventional rudders is important in achieving this. Dorsal rudders are still considered experimental, and USS ALBACORE (AGSS569) represents the only application at present.

5.4 For AGSS 555, rudder plating and stiffeners are of fiberglass reinforced plastic. Rudders were fabricated by Republic Aviation Corp. for

Portsmouth Naval Shipyard, and are filled with syntactic foam. In this application fairly thick rudders, NACA 0020, are specified in order to provide buoyancy. Service experience is desirable before further applications.

## Section 6 - Initial Zero Settings

6.1 The diving plane initial settings involve indicator zero even though planes may be tilted relative to baseline. Settings are selected on the basis of model tests so as to produce steady flight at constant depth at significant speeds. A small hull angle is generally accepted rather than take the higher plane drag needed for zero boat angle. For example, on USS Triton (SSR(N)586), the bow planes are set parallel to base line, the stabilizers and stern planes are set one-half degree rise, and the estimated hull angle is one degree down (at higher speeds).

6.2 On single screw subs the stern planes and rudders are also set at an angle so as to counteract the propeller torque. Theoretically the setting is independent of ship speed, since control surface lift and also propeller torque are both proportional to square of speed. (Some anomalous results, reported by Portsmouth from Builders Trials of USS BARBEL (SS580) are not considered in setting controls for single screw boats). These settings for counteracting propeller torque are in the right direction for acting as guide vanes to the propellers aft of them. The stern plane angles for countering propeller torque are combined algebraically with those for flight at constant depth. On SSR(N) 598 class, with a single right-hand propeller, the net result was to require the port stern plane to be set at 2° 30' dive, the starboard stern plane at 0° 30' dive, the upper rudder 1° trailing edge to port, and the lower rudder 1° trailing edge to starboard.

## Section 7 - Sea Slap

7.1 The practice is to assume that waves acting on exposed control surfaces are equivalent to a static uniform load of 1000 pounds per square foot. Under this loading the Ship Specifications usually indicate that

(a) Structure may be stressed up to the yield point (this particularly involves torque keys and keyways).

(b) The control surface torque may exceed hydraulic gear capacity (because of the long lever arm to sea slap center of pressure).

In that case, popping the relief valve is acceptable. On SS(N)597 the Electric Boat Division made a computer analysis of the response of the hydraulic system to such transient loading. For that purpose we arbitrarily indicated that the loading could be taken as

$$1000 \sin \frac{2 \pi T}{0.2} \text{ lbs/sq. ft. where}$$

T varies from 0 to 0.2 seconds

7.2 The 1000 p.s.f. comes from a 1924 Portsmouth analysis of casualties to bow and stern planes of the S-48 to S-1 and T-1 to 3 classes, due to pounding in a seaway. Although it is recognized that sea slap can be several times greater than 1000 p.s.f. it is implicitly assumed that in very rough weather the submarine will submerge.

## Section 8 - Bearings

8.1 Departures from practice listed in "Technical Practices - Rudder Design" are as follows:

(a) Laminated phenolic bearings are not commonly used on submarines.

(b) Anti-friction (roller) bearings are not used for radial loads. Gun metal and cobalt base alloy (such as made by the Stoddy Co.) are the usual materials for radial loading.

(c) Rudder carrier bearings take thrust in a free-flooding space. They are made of nickel-copper silicon alloy (S-metal or else of nickel copper aluminum alloy K-Monel). A typical installation is shown in plan SSR(N)595-519-1717598. Less costly materials have been tried in the past but did not give satisfactory service.

## Section 9 - Filling Material

9.1 Until about 1957 the only filling material for submarine control surfaces was wood, plus hot vegetable pitch to fill interstices.

9.2 Present practice also permits use of foamed-in place plastics, which are expected to be cheaper. In order to get high crushing strength as needed for deep submergence, the density and the water absorption of the plastic must be carefully selected.

## Section 10 - X-Stern

10.1 The x-stern of ALBACORE has been tested, and results are available in formal DTMB classified reports. In brief, the x-stern:

(a) solves the problem of getting adequate rudder effectiveness without exceeding hull block dimensions,

(b) provides increased safety in case one ram jams hard over (per DTMB letter noted in 11.1),

(c) adds some complexity to the controls,

(d) provided more diving plane effectiveness than desirable at high speeds.

## Section 11 - Dive Brakes

11.1 Dive brakes were tested at sea as part of the ALBACORE Phase 3 conversion trials. DTMB Confidential Letter Report 09080/ALBACORE (546:

CHANGES

COMMENTS

Insert Page 154

Change #18 Delete sentences in  
paragraph 8.1 after  
"...are as follows."

Add the following:

(a) Anti-friction bearings  
are no longer used for any  
submarine control surface  
stocks.

(b) All bearings whether  
thrust or radial on rudders  
and diving planes stocks are  
cobalt base alloy (MIL-C-15345)  
or Stoddy Co., Whittier,  
Calif. alloys 1 and 6.

Change made accord-  
ing to NAVSEC memo  
SER 29-6148D

PCC:jw) Ser. 0516 of 8 May 1962 to BUSHIPS Code 525 gives results. In brief, the brakes make an appreciable contribution to deceleration. In future designs, it will be desirable to obtain a computer prediction of emergency recovery trajectories for various dive brake configurations before ordering installation.

APPENDIX A

Derivation of Minimum Cost and Minimum Weight Equations

## DESIGN CALCULATION SHEET

Sheet of

Subject DERIVATION OF MINIMUM COST &amp; MINIMUM WEIGHT EQ.

Ship or Project

Section

Prepared by RCS

Date 4/18/77 Checked

Reviewed

THE FOLLOWING EXAMPLE OF RUDDER COST AND WEIGHT WAS USED TO OBTAIN INFORMATION NECESSARY FOR THE DERIVATIONS OF MINIMUM COST AND MINIMUM WEIGHT EQUATIONS FOR RUDDERS.

EXAMPLE FROM NAVSEC'S CODE 406 FILE

CHARACTERISTICS OF ACTUAL SHIP RUDDER:

TOTAL COST = \$29,000  
TOTAL WEIGHT = 25,000 LB.

## COST BREAKDOWN

HOURS	MATERIAL	LABOR
MAN HOURS 3000 HRS TOTAL	\$15,000	
IRON WORK & TESTING 2000 HRS		\$5,000 RUDDER
RUDDER 1,000 HRS		\$9,000 IRON WORKS
	\$15,000	\$14,000

THE MATERIAL COST INCLUDES RUDDER STOCK & BEARING MATERIAL.

THERE IS NO WAY TO SEPERATE STOCK & BEARING MATERIAL COST.

STEEL COST = \$15,000  
IRON WORKER LABOR COST = \$9,000  
WELDER LABOR COST = \$5,000

TOTAL LENGTH OF  $\frac{1}{8}$ " FILLET WELD = 2000 FT.  
 $PW = \frac{\$5000}{2000 \text{ FT.}} = \$2.5/\text{FT.}$

M. Rosenblatt & Son, Inc.  
DESIGN CALCULATION SHEET

No. 2566

Sheet of

Subject

Ship or Project

Section

Prepared by

RCS

Date

4/18/74

Checked

Reviewed

USING  $\frac{1}{8}$ " FILLET WELD AS A BASIS THE STANDARD COST IS  $\$1.18/\text{FT.}$  WHICH INCLUDES LABOR, MATERIAL COST AND WORKER EFFICIENCY. SINCE THE ACTUAL COST =  $\$2.5/\text{FT.}$  A K FACTOR IS USED TO CORRECT THE STANDARD CALCULATION.

$$K = \frac{\$2.5/\text{FT.}}{\$1.18/\text{FT.}} = 13.9$$

THE RUDDER IS ASSUMED TO BE RECTANGULAR IN SHAPE.

USING THE ASSUMPTIONS AND SPECIFIC COST DATA ABOVE THE EQUATIONS FOR MINIMUM RUDDER

Subject

Ship or Project

Section

Prepared by

Date

Checked

Reviewed

1. DETERMINATION OF RUDDER PLATE THICKNESS  
BASED ON MINIMUM RUDDER WEIGHT.

$$W = \frac{2 \times 490}{12} A t + \left[ \left( \frac{12b}{mt} + 1 \right) (c) + \left( \frac{12c}{mt} + 1 \right) b \right] \frac{t'}{12} \times D \times 490$$

$$+ \left( \frac{12c}{mt} + 1 \right) \times b \times \frac{t'}{12} \times \frac{6t}{12} \times 490 + \left( \frac{12b}{mt} + 1 \right) \frac{c \times t'}{12} \times \frac{6t}{12} \times 490$$

ASSUME A RECTANGULAR SHAPE & 50"

W = WT OF RUDDER, LBS

A = RUDDER AREA = 50 - FT

t = MINIMUM PLATE THICKNESS OR ADJUSTED THICKNESS, INCH.

t' = STIFFERS & FLAT BARS THICKNESS, INCHES

b = RUDDER SPAN = FT

c = MEAN CHORD = FT

D = AVERAGE RUDDER THICKNESS = 0.634 X MEAN THICKNESS = FT

m = STIFFENER PANEL CONSTANT = 50

MEAN THICKNESS = MAX. THICKNESS AT MEAN CHORD c, FT

✓ NO. OF HORIZONTAL WEB SPACES =  $12b/mt$

✓ NO. OF VERTICAL WEB SPACES =  $12c/mt$

✓ WIDTH OF FLAT BAR, FEET, =  $6t/12$

$$\text{OR } W = \frac{490}{6} A t + \frac{2bc \cdot D \times 490}{mt} + \frac{(b \cdot c) t' \cdot D \times 490}{12}$$

$$+ \frac{bct \times 490}{12} + \frac{(b \cdot c) t' \cdot t \times 490}{24}$$

$$W = 490 \left\{ \frac{A}{6} + \frac{(b \cdot c) t'}{24} \right\} t + \frac{2bc \cdot D}{mt} + \frac{(b \cdot c) \cdot D \cdot (t \cdot t')}{12}$$

Subject

Ship or Project

Section

Prepared by

Date

Checked

Reviewed

$$\text{EQUATE } \frac{\partial W}{\partial t} = 0$$

$t$  FOR MINIMUM WEIGHT OF CONTROL SURFACE

$$= \left[ \frac{D t'}{m \left( \frac{1}{12} + \left( \frac{b+c}{6c} \right) \frac{t'}{48} \right)} \right]^{1/2}$$

$$\text{OR } t = \left[ \frac{a_1 t'}{m (a_2 + a_3 t')} \right]^{1/2}$$

WHERE  $a_1 = b \times c \times D$

$$a_2 = A \div 12$$

$$a_3 = (b+c) \div 48$$

Subject \_\_\_\_\_

Ship or Project \_\_\_\_\_

Section \_\_\_\_\_

Prepared by \_\_\_\_\_

Date \_\_\_\_\_

Checked \_\_\_\_\_

Reviewed \_\_\_\_\_

# DETERMINATION OF RUDDER PLATE THICKNESS

BASED ON MINIMUM COST OF CONTROL SURFACE

$$COST = W(P_S + P_L) + LK P_W$$

$$W = 490 \left\{ \left[ \frac{A}{6} + \frac{(b+c)t'}{24} \right] t + \frac{25ct'D}{11t} + \frac{(b+c)t'D}{12} + \frac{6ct'}{11} \right\}$$

WHERE  $P_S$  = MATERIAL \$/LB.

$P_L$  = IRON WORK LABOR \$/LB.

$P_W$  = WELDER LABOR \$/FT.

$K$  = 13.9

$L$  = LINEAR LENGTH OF WELDING

$$L = \left( \frac{12c}{11t} \right) \left( \frac{12b}{11t} + 1 \right) \left( 2D + \frac{2mt}{12} \right) + \left( \frac{12c}{11t} + 1 \right) (2D + 2b)$$

$$L = \left( \frac{144cb}{11t^2} + \frac{12c}{11t} \right) \left( 2D + \frac{2mt}{12} \right) + \frac{24cD}{11t} + 2D +$$

$$\frac{24cb}{11t} + 2b$$

$$= \frac{288cbD}{11t^2} + \frac{24cD}{11t} + \frac{24cb}{11t} + 2D + 2b$$

$$L = \frac{288cbD}{11t^2} + \frac{48cD}{11t} + \frac{48cb}{11t} + 2(b+c+D)$$

$$COST = W(P_S + P_L) + K \left[ \frac{288cbD}{11t^2} + \frac{48cD}{11t} + \frac{48cb}{11t} + 2(b+c+D) \right] P_W$$

$$COST = W + \frac{K(P_W)}{P_S + P_L} \left[ \frac{288cbD}{11t^2} + \frac{48}{11t} (cD + cb) + 2(b+c+D) \right]$$

M. Rosenblatt & Son, Inc.

DESIGN CALCULATION SHEET

No.

Sheet 2 of

Subject

Ship or Project

Section

Prepared by

Date

Checked

Reviewed

$$\begin{aligned} \frac{\partial \text{COST}}{\partial t} = 0 &= (P_3 + P_2) \times 490 \left[ \frac{A}{6} + \frac{(b+c)t'}{2} - \frac{256CDt'}{m^2} \right] \\ &+ KP_w \left[ -\frac{5766CD}{m^2 t^3} - \frac{48CD}{m^2} - \frac{48c6}{m^2} \right] \\ &= (81.7)A + 20.92(b+c)t' - \frac{9806CDt'}{m^2} - \frac{KP_w}{P_3 + P_2} \left( + \frac{5766CD}{m^2 t^3} \right) \\ &- \frac{KP_w}{P_3 + P_2} \left( \frac{48(CD + bC)}{m^2} \right) \end{aligned}$$

THE ABOVE EQUATION IS NON-LINEAR SO  
THE MINIMUM  $t$  IS FOUND BY ITERATION.

M. Rosenblatt & Son, Inc.  
DESIGN CALCULATION SHEET

No. 2566

Sheet of

Subject EXAMPLE CALCULATION FOR MINIMUM COST & WEIGHT

Ship or Project

Section

Prepared by

RCS

Date

Checked

Reviewed

EXAMPLE CALCULATION FOR MINIMUM COST AND  
WEIGHT OF A TYPICAL RUDDER

EXAMPLE RUDDER CHARACTERISTICS

STIFFENER AND FLAT BAR THICKNESS  $t' = 0.375$  IN.

STIFFENER PANEL CONSTANT  $m = 50$

RUDDER SPAN  $b = 20$  FT.

MEAN CHORD  $c = 14.5$  FT.

RUDDER AREA  $A = 290$  FT.<sup>2</sup>

AVERAGE RUDDER THICKNESS = 1.537 FT.

CONSTANT  $K = 13.9$

$$\frac{K P_W}{P_S + P_L} = 6$$

#### 2.4.1 Calculation of Rudder Plate Thickness for Minimum Weight

W = Wt. of Rudder, Lbs.

A = Rudder area = 290 Ft.<sup>2</sup>

t = Min. Rudder Plate Thickness or Adjusted Thickness, inches

t' = Stiffeners and Flat Bars Thickness, inches = 0.375

b = Rudder Span = 20 Ft.

c = Mean Chord = 14.5 Ft.

D = Average Rudder Thickness = 0.684 x Mean Thickness = 1.577

m = Stiffener Panel Constant = 50 (For the Example in Appendix A)

Mean Thickness = Maximum Thickness at Mean Chord c., Ft.  
= 1.0513 Ft.

a<sub>1</sub> = b x c x D = 445.7

a<sub>2</sub> = A ÷ 12 = 24.166

a<sub>3</sub> = (b + c) ÷ 48 = 34.5 ÷ 48 = 0.7187

$$t = \left[ \frac{a_1 \times t'}{m(a_2 + a_3 \times t')} \right]^{\frac{1}{2}}$$

①	②	③	④	⑤	t
t'	a <sub>3</sub> x t'	② + a <sub>2</sub>	t' ÷ ③	$\frac{a_1 \times ④}{m}$	⑤ <sup>1/2</sup> For Min Wt
0.375	0.2695	24.727	0.015	0.1337	0.367

## 2.4.2 Calculation of Minimum Thickness

To determine minimum thickness based on cost the equation below must be iterated using an assumed thickness  $t$  until the result equals zero. It will be useful to plot the result of each iteration versus  $t$  to speed convergence to the value of zero. Since the equation is a cubical equation, at least three points should be plotted. Note that one of these points should have an opposite sign compared with the other points.

$$a_4 = 81.7 (A) = 23,693$$

$$a_5 = 20.42 (b + c) = 704.49$$

$$a_6 = a_1 \left( \frac{980}{m} \right) = 8735.7$$

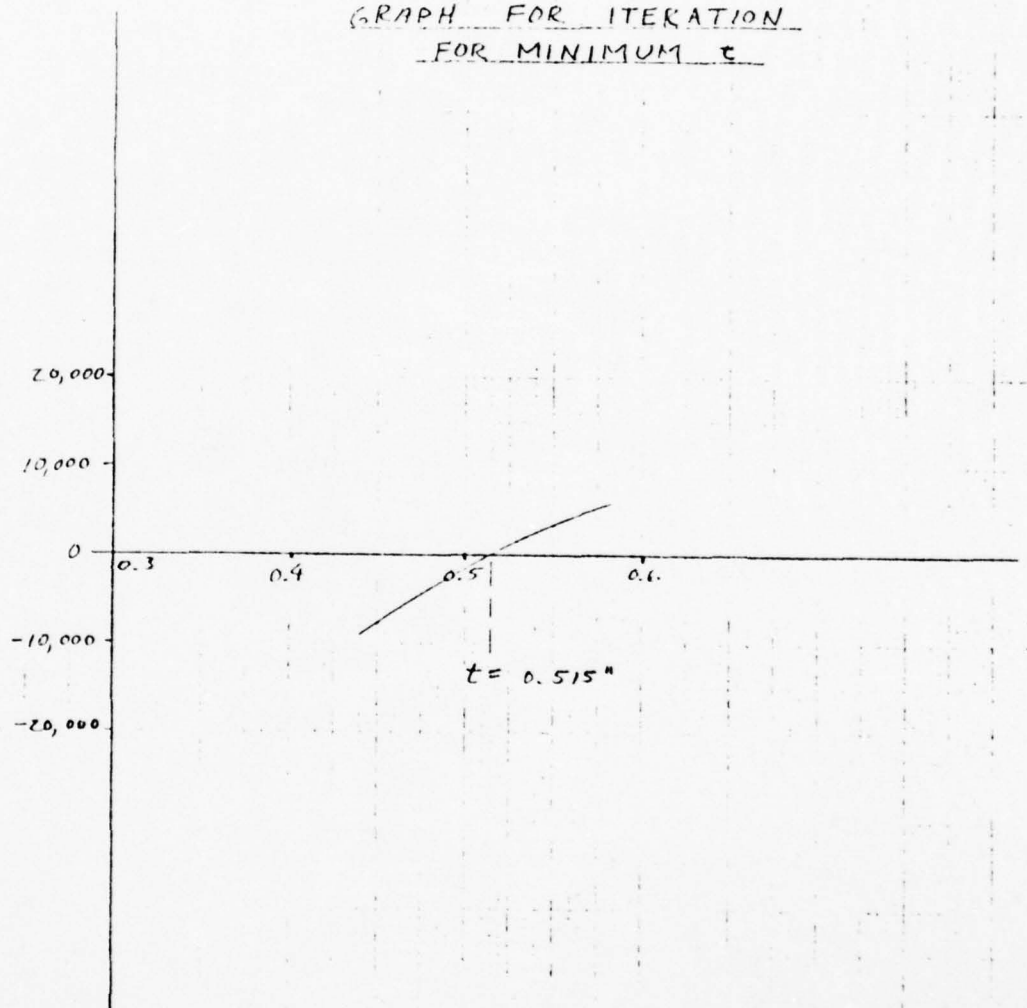
$$N = \frac{KP_w}{P_s + P_L} = 6 \text{ (or an actual number derived from a cost study)}$$

$$a_7 = N (a_1) \left( \frac{576}{m^2} \right) = 616.136$$

$$a_8 = \frac{N (48) (cD + bc)}{m} = 1793.77$$

①	②	③	④	⑤	⑥	ITERATION CHECK
Assumed $t$	$a_5 x t$	$\frac{a_6 x t^2}{t^2}$	$\frac{a_7}{t^3}$	$\frac{a_8}{t^2}$	$\text{②} - \text{③} - \text{④} - \text{⑤} + a_4$	1) If ⑥=0 then assumed $t$ = for minimum cost 2) if ⑥≠0 assume a new $t$ and iterate again
0.25	264.18	10829	3703.2	5946.4	3478.5	TRY $t = 0.45$
0.45	264.18	10177	2761.4	8882.8	-7864	TRY $t = 0.51$
0.51	264.18	12594	4246.5	6915.6	-193.92	CLOSE TO ZERO POINT REACHED END OF FOR ZERO POINT

GRAPH FOR ITERATION  
FOR MINIMUM  $\epsilon$



### 2.4.3 Calculation of Rudder Weight

$$a_{10} = A \div 6 = 290 \div 6 = 48.33$$

$$a_{11} = (b + c) \div 24 = 2 \times a_3 = 2 \times 0.718 = 1.437$$

$$a_{12} = 2bcd \div m = 2a_1 \div m = 2 \times 445.7 \div = 17.838$$

$$a_{13} = (b + c) \times D \div 12 = 7.418$$

$$a_{14} = b \times c \div m = \frac{5.6}{10.22}$$

$$a_{15} = (a_{13} + a_{14}) = + = 10.22$$

$$W = 490 \left[ (a_{10} + a_{11} t')t + a_{12} \left( \frac{t'}{t} \right) + (a_{13} + a_{14}) t' \right]$$

①	②	③	④	⑤	⑥	⑦	W
t	$a_{11}xt'$	② + $a_{10}$	③ x t	$a_{12}xt'/t$	$a_{15} \times t'$	④ + ⑤ + ⑥	490 x
0.367	0.539	48.87	17.93	18.22	3.53	39.46	17592

#### 2.4.4 Calculation of Rudder Cost

$$a_{16} = \frac{288 (a_1)}{m^2} = 51.34$$

$$a_{17} = b + c + D = 36.04$$

$$\text{Cost} = W + N \left[ \frac{a_{16}}{t^2} + \frac{a_8}{Nxt} + 2 \times a_{17} \right]$$

1	2	3	4	5	Cost \$
t	$\frac{a_{16}}{t^2}$	$\frac{a_8}{Nxt}$	② × a <sub>17</sub>	N × [② + ③ + ④]	W + ⑤
0.515	193.6	582.1	72.08	5086.6	24,678

APPENDIX B

Report Titled Experimental Stress Analysis  
of a Socketed Connection in Bending

**EXPERIMENTAL STRESS ANALYSIS OF A  
SOCKETED CONNECTION IN BENDING**

**by**

**Louis A. Becker**

**April 1962**

**Report 1592  
S-F013 03 01**

## TABLE OF CONTENTS

	Page
ABSTRACT .....	1
INTRODUCTION .....	1
DESCRIPTION OF MODELS .....	2
INSTRUMENTATION AND TEST PROCEDURE .....	7
TEST RESULTS .....	10
DISCUSSION OF RESULTS .....	21
SUMMARY AND CONCLUSIONS .....	22
RECOMMENDATIONS .....	23
ACKNOWLEDGMENTS .....	23
REFERENCES .....	23

## LIST OF FIGURES

	Page
Figure 1 – Model Used for a Depth of Penetration of Three Diameters .....	3
Figure 2 – Model Components .....	4
Figure 3 – Model Used to Compare Rudder Nut and Tapered Key .....	5
Figure 4 – Strain Gage Locations for Socketed Joint Connections .....	7
Figure 5 – Test Setup .....	8
Figure 6 – Bending Stress Distribution for Three-Diameter Penetration, Thick-Wall Yoke, 75,000 In-Lb .....	11
Figure 7 – Bending Stress Distribution for Three-Diameter Penetration, Thin-Wall Yoke, 75,000 In-Lb .....	11
Figure 8 – Bending Stress Distribution for 1 1/4-Diameter Penetration, Thick-Wall Yoke, 75,000 In-Lb .....	12
Figure 9 – Bending Stress Distribution for One-Diameter Penetration, Thick-Wall Yoke, 75,000 In-Lb .....	12
Figure 10 – Bending Stress Distribution for One-Diameter Penetration, Thin-Wall Yoke, 75,000 In-Lb .....	13
Figure 11 – Bending Stress Distribution for 1/2-Diameter Penetration, Thick-Wall Yoke, 75,000 In-Lb .....	13
Figure 12 – Bending Stress Distribution for 1/2-Diameter Penetration, Thin-Wall Yoke, 75,000 In-Lb .....	14
Figure 13 – Bending Stress Distribution for 1 1/4-Diameter Penetration, Thick-Wall Yoke, 75,000 In-Lb .....	14
Figure 14 – "K" Factor versus Penetration .....	15
Figure 15 – Effects of Vibration on Top Fiber Strains of the Yoke .....	17
Figure 16 – Model after Maximum Applied Load .....	18
Figure 17 – Sketch of Damage to Model .....	18
Figure 18 – Closeup of Damage to Tapered Key .....	19
Figure 19 – Bending Strain Distribution for 1 1/4-Diameter Penetration, Thick-Wall Yoke, at a Moment of 900,000 In-Lb .....	19

	Page
Figure 20 – Deflection of Head of Testing Machine versus Applied Load .....	20
Figure 21 – Bending Stresses in 1 1/4-Diameter Penetration, Thick-Wall Yoke, at a Moment of 540,000 In-Lb .....	20

#### LIST OF TABLES

Table 1 – Material Properties .....	2
Table 2 – Principal Test Dimensions .....	6
Table 3 – Test Schedule .....	9
Table 4 – Bending Stresses .....	15
Table 5 – Face Stresses at a Moment of 75,000 In-Lb .....	16
Table 6 – Face Stresses Measured during Maximum Loading Test .....	17

## ABSTRACT

This report presents a semiempirical curve for use in designing socketed connections subjected to pure bending. This type of connection is frequently used in rudder and control surface connections on surface ships and submarines. The curve is for use only within a limited range of parameters considered of immediate interest to the Bureau of Ships. These include the depth of penetration of the shaft into the socket, the thickness of the socket wall, the presence of relief in the socket wall, and the type of attachment of the stock to the socket. The design curve was obtained by measuring strains at discrete locations on the socketed connection loaded in pure bending. The tests were repeated as the various parameters were changed. The resulting design curve enables the user to predict the maximum flexural stress in the socketed connection with a stock penetration of one stock diameter or more.

## INTRODUCTION

One of the problems facing the ship designer is the socketed connection, a type used in ship construction. Two examples of its use are in the connection of rudders to their stocks and in the connection of diving planes to their stocks. Most of these designs require the insertion of a tapered shaft into a matching socket. The shaft is secured either by a nut on the end of the shaft or by a tapered key driven through the assembly.

At the present time, most designs call for a penetration of 2 or 2 1/2 stock diameters. In order to develop the surface friction of the joint, the two pieces must be fitted so that they have a metal-to-metal contact of at least 80 percent. This necessitates machining both the tapered end of the stock and the inside of the socket to a very smooth finish (16 rms or better) and usually requires hand finishing during assembly. Considering the sizes involved on some of the newer ships, it is obvious that such an assembly is both large and very costly. The problem was aggravated by the hull shape and the use of large single propellers with shafts of large diameter developed for USS ALBACORE and subsequent submarines. These hulls, which narrow toward a point at the stern, do not have sufficient space for the penetrations desired. Thus, considerable interest has been shown in improving the socketed connection design, particularly along the lines of making the assembly smaller and lighter.

Because of the need for a design procedure for this type of structure, the David Taylor Model Basin was requested<sup>1</sup> to determine the governing design criteria for this type of joint under pure bending. Specifically, the investigation was to determine:

- a. If the entire joint assembly should be treated as two interacting beams or as a single monolithic structure.

---

<sup>1</sup>References are listed on page 23.

- b. If there is any appreciable difference in the strength of the joint when the middle third of the tapered fit is relieved.
- c. The variation in the strength of the joint as the length of the taper engagement is varied from 1/2 to 3 stock diameters.
- d. The difference in cost between a rudder nut and a taper key connection.

Accordingly, tests were conducted at the Model Basin in 1960 and 1961 to investigate the above requirements. This report presents the results of an investigation conducted on model scale and includes the effects of stock penetration, yoke\* wall thickness, relief, and type of stock attachment (rudder nut or tapered key). Within the limits of the investigation, some basic conclusions about the design methods are drawn.

### DESCRIPTION OF MODELS

The experimental program employed scaled models of typical socketed connections. The models were designed so that it would be possible to investigate the effects of different stock penetrations, types of connections, yoke wall thicknesses, and relief. Since the proposed new stern arrangement of USS ALBACORE<sup>2</sup> (AGSS 569) was of particular interest, it was used as the basic structure for scaling the models.

All the models had the same general configuration and consisted of two shafts or stocks made of 4140 steel. Material properties are given in Table 1. In general, the models

TABLE 1

Material Properties

Piece	Tensile		Compressive Yield psi
	Yield psi	Ultimate psi	
Yoke 1	42,500	93,100	43,100
Yoke 2	41,900	93,500	45,400
Yoke 3	42,900	94,000	44,200
Yoke 4	—	—	48,500
Stock 1	82,900	111,200	95,500
Stock 2	80,600	108,800	90,600

were scaled to one-fourth the size proposed for ALBACORE. The model stock diameters were 4 1/2 in. Each stock had a 2 in/ft of diameter taper on one end, and the two stocks were joined by a yoke as shown in Figures 1 and 2. The tapered surfaces were ground to provide at least 80 percent contact of the yoke with the stocks. The stocks were attached to the yokes either by a tapered key or by a rudder nut, as shown in Figure 3. One of the yoke wall thicknesses was scaled from that proposed for ALBACORE and a second yoke scaled to 0.6 the thickness was made to determine the effects of reduced yoke wall thickness. Duplicate models were made to determine the effect of adding a relief to the middle third of the yoke except at 1 1/4-diameter penetration.

\* Throughout this report, the piece with the internal tapered sockets will be referred to as the yoke.

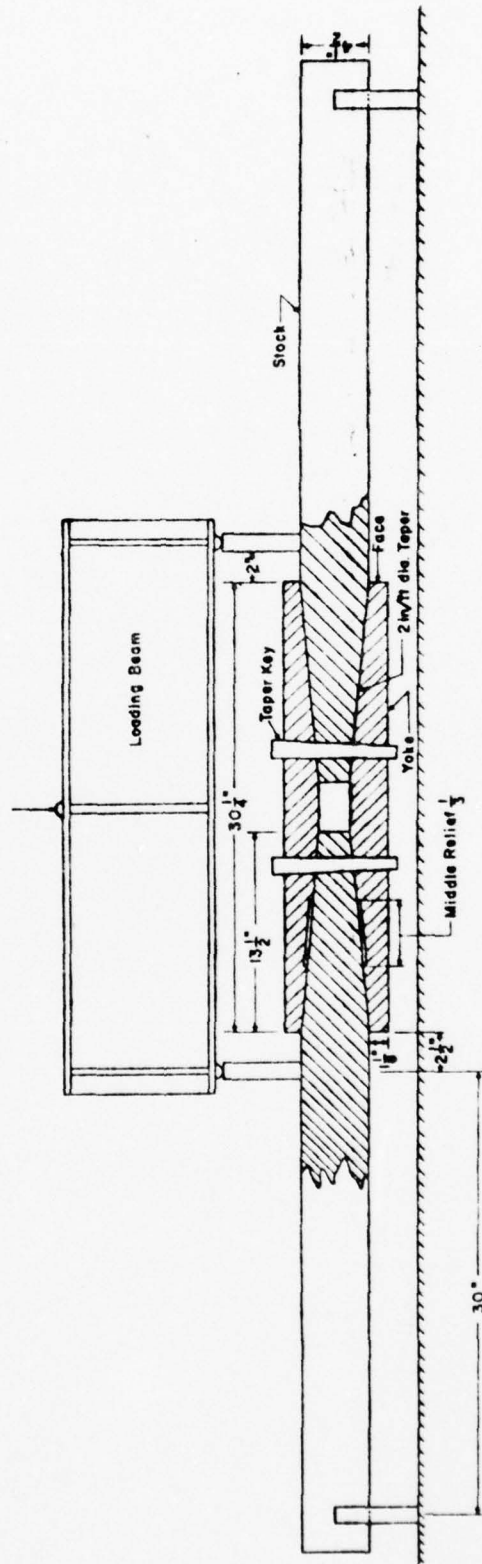


Figure 1 - Model Used for a Depth of Penetration of Three Diameters

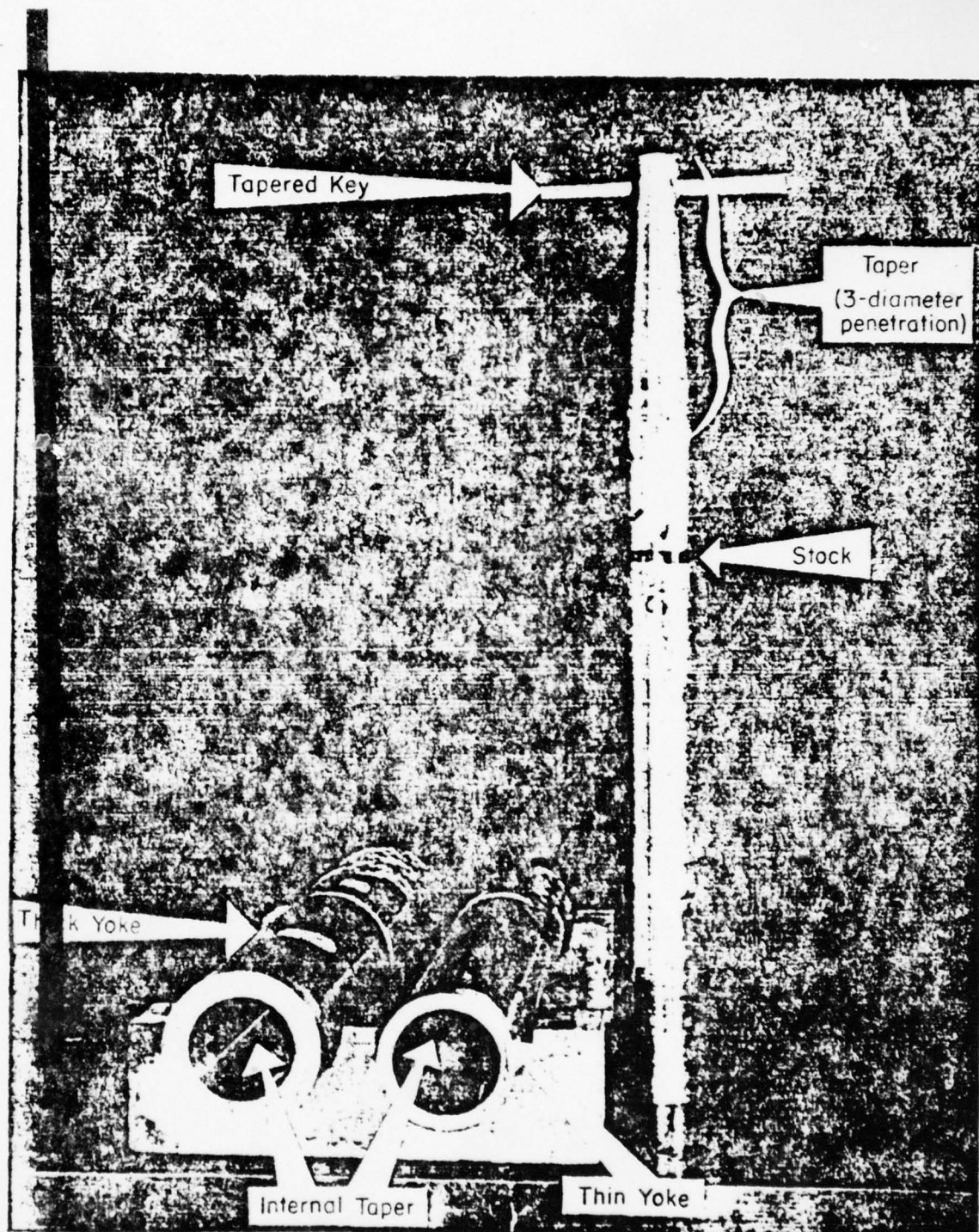


Figure 2 - Model Components

AD-A071 783

ROSENBLATT (M) AND SON INC NEW YORK

F/G 13/10

DEVELOPMENT OF A TECHNICAL PRACTICE FOR RUDDERS AND DIVING PLAN--ETC(U)

AUG 74 R SHEFFIELD

N00024-73-C-5189

UNCLASSIFIED

MR/S-2566-3

NAVSEC-6136-74-271

NL

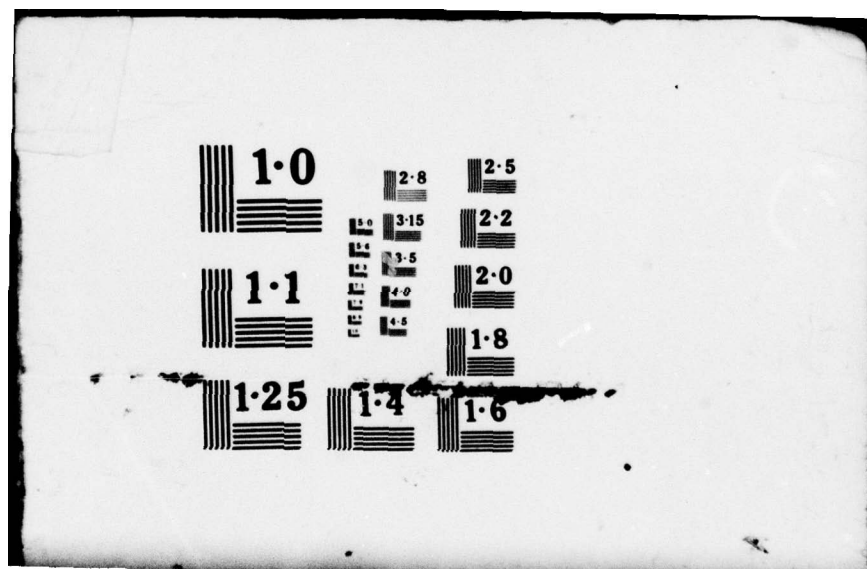
2 OF 2  
AD  
A071783

AD  
A071783



END  
DATE  
FILMED

8-79  
DDC



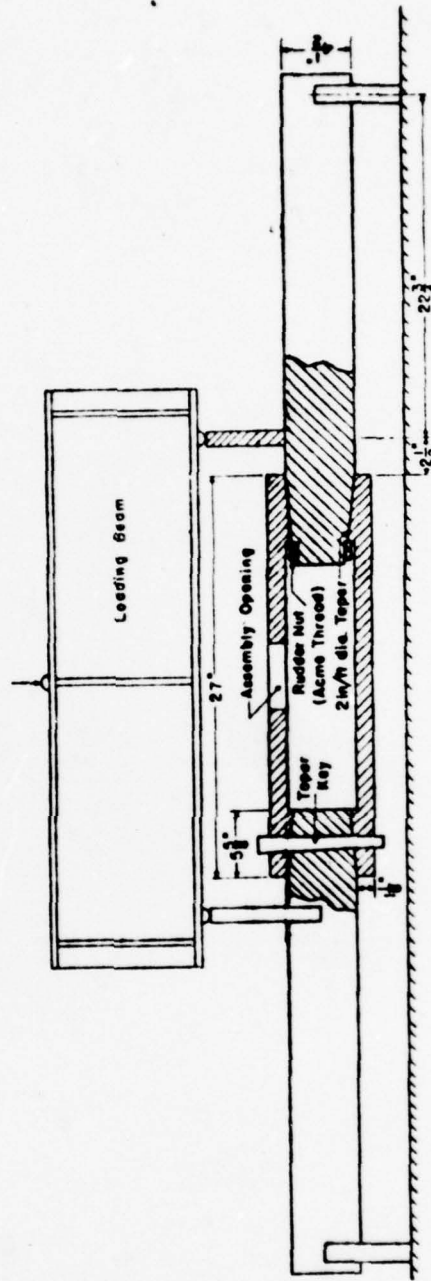
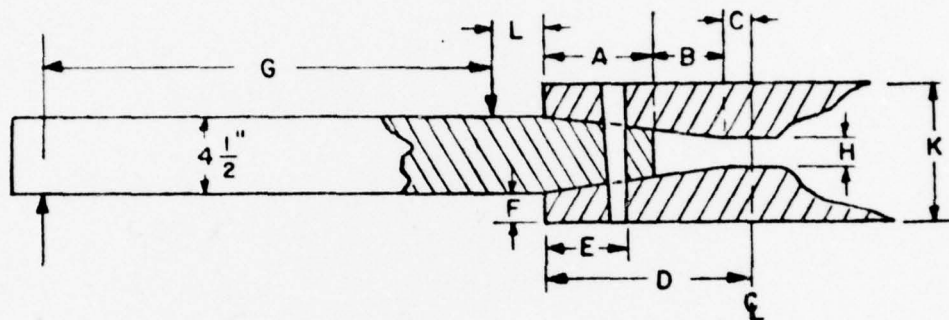


Figure 3 - Model Used to Compare Rudder Nut and Tapered Key

Pertinent dimensions for all models are given in Table 2. To economize on model construction costs, two basic stocks and four yokes were systematically modified during the course of testing to provide the required variations in parameters for the 18 models listed in Table 2.

TABLE 2  
Principal Test Dimensions



Model Number	A in.	B in.	C in.	D in.	E in.	F in.	G in.	H in.	K in.	L in.
1	13 1/2 or									
2	3 Dia	1/2	1 1/4	15 1/4	12 1/2	1 1/8	30	2 1/8	6 3/4	2 1/2
3	13 1/2 or									
4	3 Dia	1/2	1 1/4	15 1/4	12 1/2	11/16	30	2 1/8	5 7/8	2 1/2
5	4 1/2 or	9 1/2	1 1/4	15 1/4				2 1/8		
6	1 Dia	3/4	1	6 1/4	3 1/2	1 1/8	30	3 5/8	6 3/4	2 1/2
7	4 1/2 or	9 1/2	1 1/4	15 1/4				2 1/8		
8	1 Dia	3/4	1	6 1/4	3 1/2	11/16	30	3 5/8	5 7/8	2 1/2
9	2 1/4 or									
10	1/2 Dia	11 3/4	1 1/4	15 1/4	1 5/8	1 1/8	30	2 1/8	6 3/4	2 1/2
11	2 1/4 or									
12	1/2 Dia	11 3/4	1 1/4	15 1/4	1 5/8	11/16	30	2 1/8	5 7/8	2 1/2
13	5 5/8 or									
14	1 1/4 Dia	0	7 7/8	13 1/2	2 3/4	1 1/8	22 3/4	4 1/2	6 3/4	2 1/2
15	5 5/8 or									
16	1 1/4 Dia	0	7 7/8	13 1/2	-	1 1/8	22 3/4	4 1/2	6 3/4	2 1/2
17	5 5/8 or				2 3/4					
18	1 1/4 Dia	0	7 7/8	13 1/2	-	1 1/8	22 3/4	4 1/2	5 3/4	2 1/2

## INSTRUMENTATION AND TEST PROCEDURE

Prior to testing, each model was instrumented with strain gages as shown in Figure 4. Two basic groups of gages were used. The first group was used to compare longitudinal bending strains in the stock and yoke with theory and to check the symmetry of loading. The second group was used to measure the face strains in order to determine bearing stresses.

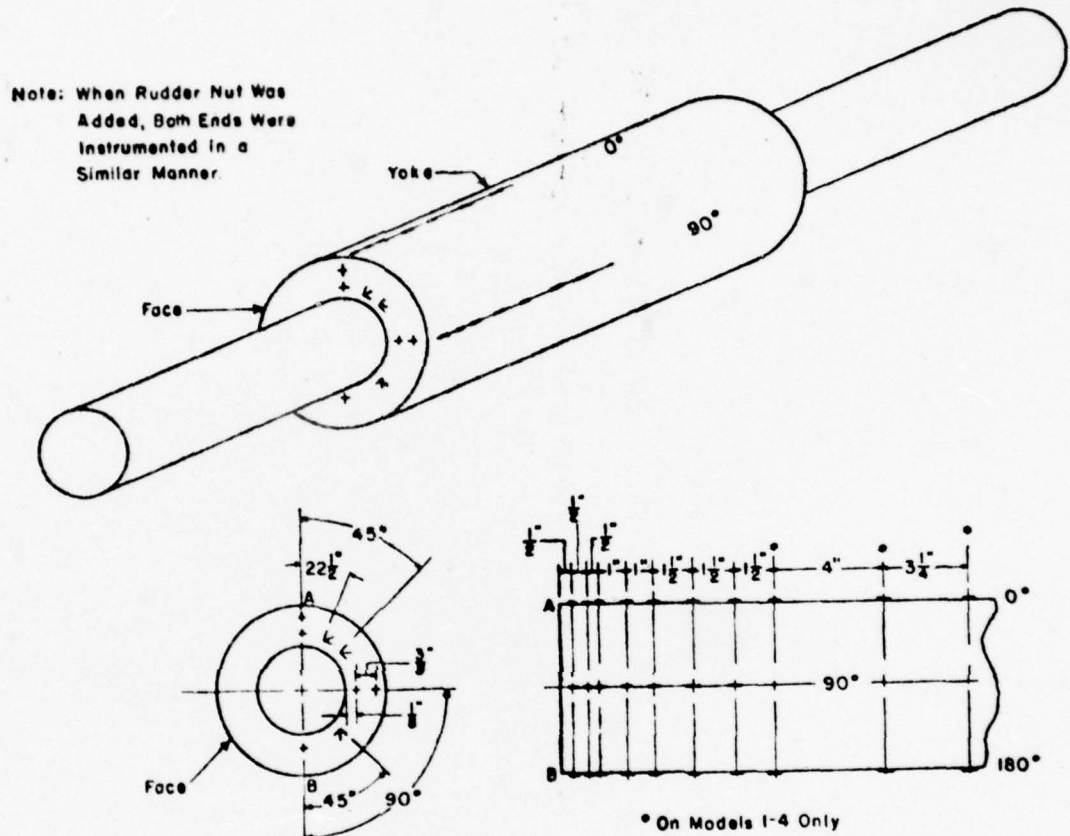


Figure 4 - Strain Gage Locations for Socketed Joint Connections

Each model was tested in the 600,000-lb testing machine. The basic test setup is shown in Figure 5. The extreme ends of the model were supported on knife edges. The model was subjected to pure bending across the test section by applying the load through the loading beam. The loading beam was used to keep the load symmetric. No torque or shear was applied at the yoke.

The test of each model consisted of loading the model in increments of 1000 or 2000 lb. All strain gages were read at each increment of load. This procedure was continued until a maximum strain of 1000  $\mu\text{in./in.}$  was observed. The tests were stopped at this point since no yielding could be permitted because the various pieces were to be used again.

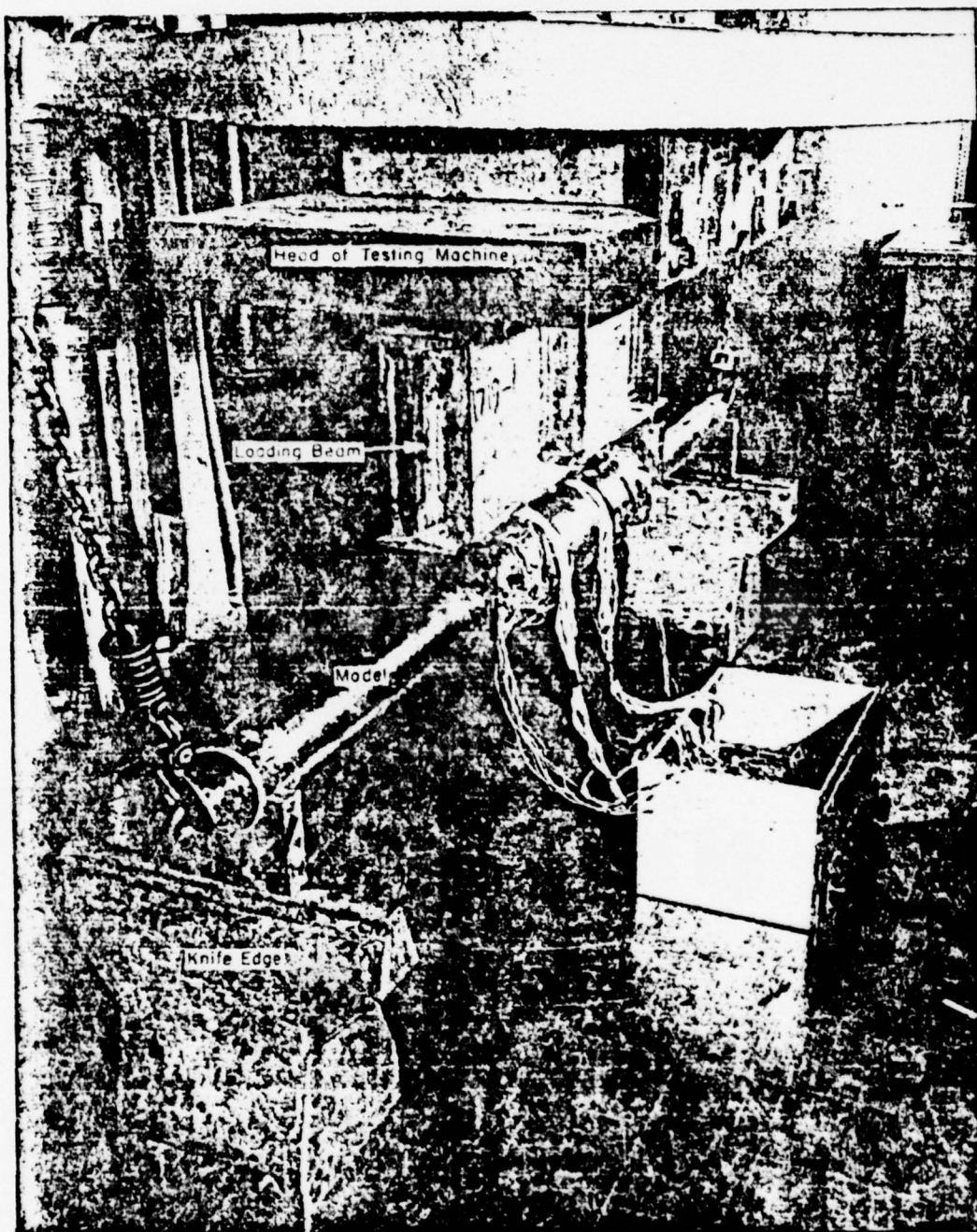


Figure 5 - Test Setup

This procedure was followed on all tests listed in Table 3.

Up to this point all testing was static. However, there is considerable vibration of the stocks in a ship due to hull frequency, blade frequency, shaft speed, etc. The amplitude and frequency of this vibration varies considerably from ship to ship, and no given vibratory

TABLE 3

## Test Schedule

Test Number*	Model Number	Penetration in stock diameters	Yoke	Relief	Attachment
3LTR	2	3	Number 1 thick	yes	Taper Key
3STR	4	3	Number 1 thin	yes	Taper Key
3LT	1	3	Number 2 thick	no	Taper Key
3ST	3	3	Number 3 thin	no	Taper Key
1.25LT	13	1 1/4	Number 2 thick	no	Taper Key
1.25LN	15	1 1/4	Number 2 thick	no	Rudder Nut
1.25(90)LT	17	1 1/4	Number 2 thick	no	Taper Key
1.25(90)LN	18	1 1/4	Number 2 thick	no	Rudder Nut
1.25(A)LT	14	1 1/4	Number 2 thick	no	Taper Key
1.25(A)LN	16	1 1/4	Number 2 thick	no	Rudder Nut
1LTR	6	1	Number 4 thick	yes	Taper Key
1STR	8	1	Number 4 thin	yes	Taper Key
1LT	5	1	Number 2 thick	no	Taper Key
1ST	7	1	Number 3 thin	no	Taper Key
0.5LT	9	1/2	Number 2 thick	no	Taper Key
0.5ST	11	1/2	Number 2 thin	no	Taper Key
0.5LTR	10	1/2	Number 2 thick	yes	Taper Key
0.5STR	12	1/2	Number 2 thin	yes	Taper Key

\*The meaning of the test number is as follows

1.25 - Number of stock diameters of penetration of stocks into yoke.  
 (90) - Special consideration - (A) indicates tests run after vibration of assembly, (90) indicates taper key turned vertical instead of on neutral axis.  
 L - Thickness of yoke - L is thick, S is thin.  
 T - Type of attachment - T is taper key, N is rudder nut.  
 R - Relief.

loading can be considered as representative for all ships. However, it was felt that vibration should not be neglected. Accordingly, a random sinusoidal vibration with a maximum alternating force of  $\pm 1000$  lb and a maximum frequency of 25 cps was applied to the center of the model by means of a Lazan<sup>3</sup> oscillator. This vibratory load was applied for 8 hr to a thick yoke model having a depth of penetration of 1 1/4 diameters. The model used had a tapered key in one stock and a rudder nut in the other stock. Bending loads were applied to the model before and after vibration and the strains were compared.

## TEST RESULTS

The bending strains measured on the extreme fiber of the yoke during these tests are converted to stresses directly from the following equation:

$$\sigma = E \epsilon \quad [1]$$

where  $\sigma$  is stress in psi,

$E$  is modulus of elasticity in psi, and

$\epsilon$  is strain in in/in.

The resulting stresses for the models with tapered key are plotted in Figures 6 through 12. Figure 13 compares the stresses resulting from a tapered key connection with those resulting from a rudder nut connection. All these strains were taken at an applied moment of 75,000 in-lb. This was the highest moment that could be safely applied to all models without causing yielding. In each of these figures the theoretical stresses, computed by assuming the structure to be monolithic, were also plotted. These were computed from the equation:

$$\sigma = \frac{Mc}{I} \quad [2]$$

where  $\sigma$  is the stress in psi,

$M$  is applied moment in in-lb,

$I$  is moment of inertia in<sup>4</sup>, and

$c$  is the distance from the neutral axis to the extreme fiber in inches

An examination of Figures 6 through 13 indicates differences between the theoretical and experimental bending stresses. The differences become quite large as the length of penetration is reduced. The results shown in these figures are summarized in Table 4 which indicates the maximum experimentally determined stress, the corresponding theoretical stress computed by Equation [2], and the correction factor  $K$ , which is the ratio of these two stresses. The variation of  $K$  with penetration is plotted in Figure 14. It must be noted that all the results are based on Equation [1]. This is not strictly correct when the depth of penetration is very small or when the yoke is very thin. Under these conditions there may also be some high circumferential stresses. This is evident by the sign reversal in the bottom fiber of the small depth of penetration models. No allowance was made for this since it was felt that the stresses were small compared to the maximum bending and that their effects were accounted for in the correction factor. This is one reason for limiting the use of Figure 14 to one-diameter penetration or more.

Other types of data also collected during the tests included face stresses (Tables 5 and 6) and bending results before and after vibration (Figure 15). One result of the vibration tests was that the rudder nut was loose at the end of the 8 hr of vibration.

(Text continued on page 18.)

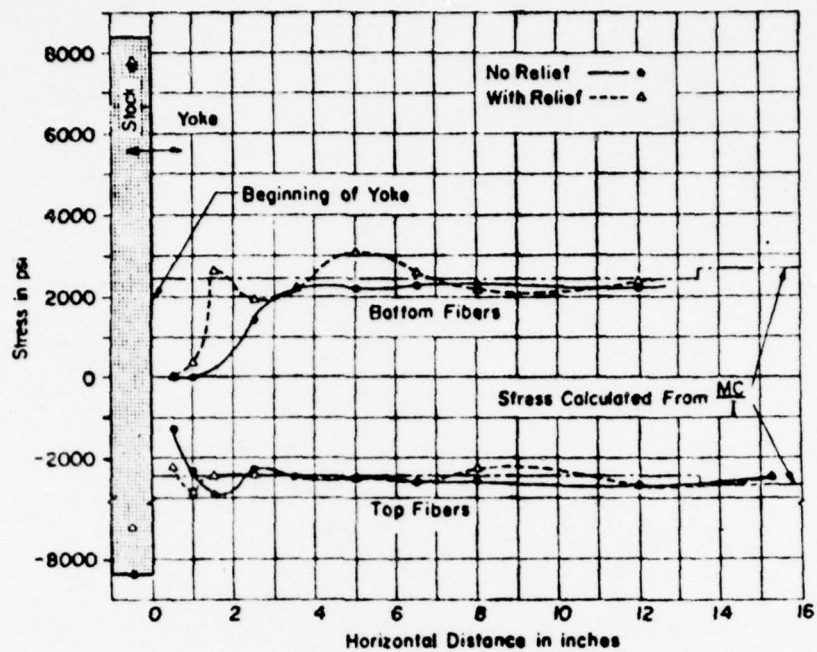


Figure 6 - Bending Stress Distribution for Three-Diameter Penetration, Thick-Wall Yoke, 75,000 In-Lb

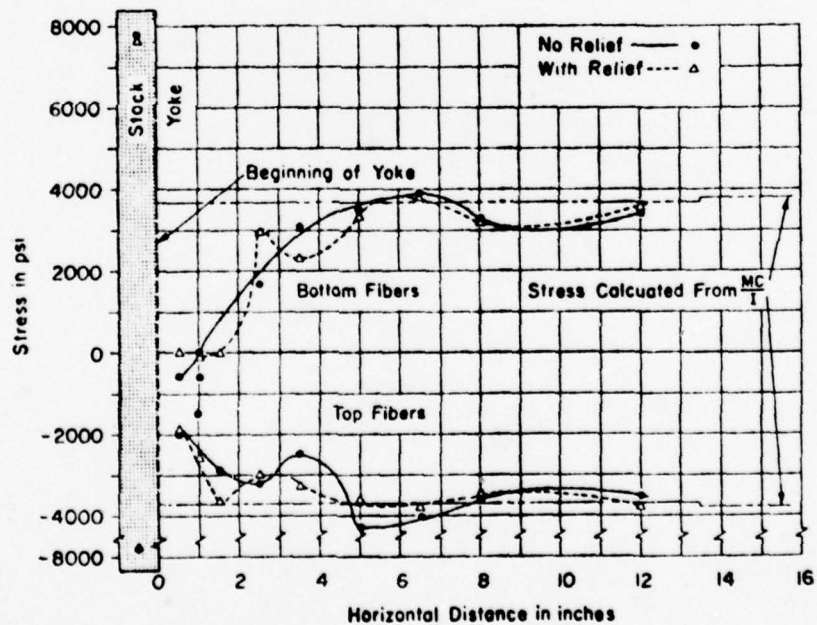


Figure 7 - Bending Stress Distribution for Three-Diameter Penetration, Thin-Wall Yoke, 75,000 In-Lb

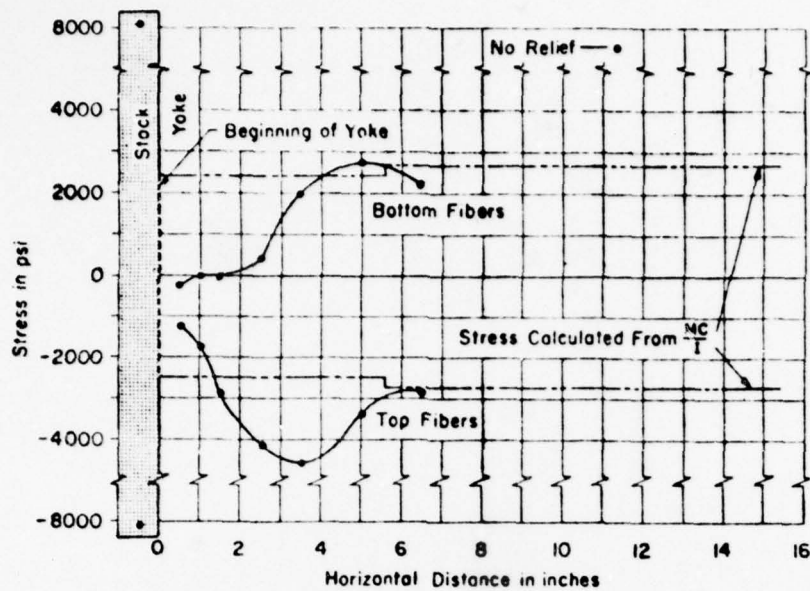


Figure 8 - Bending Stress Distribution for 1 1/4-Diameter Penetration, Thick-Wall Yoke, 75,000 In-Lb

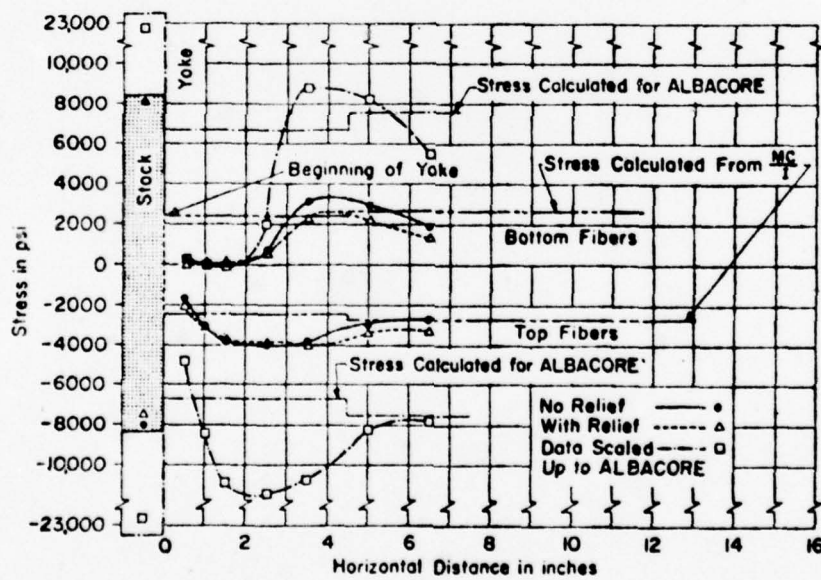


Figure 9 - Bending Stress Distribution for One-Diameter Penetration, Thick-Wall Yoke, 75,000 In-Lb

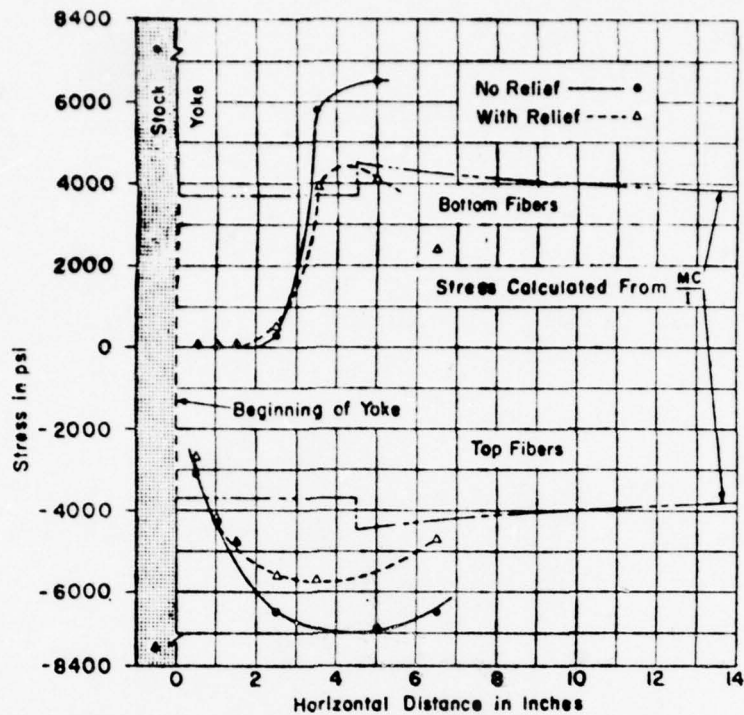


Figure 10 -- Bending Stress Distribution for One-Diameter Penetration, Thin-Wall Yoke, 75,000 In-Lb

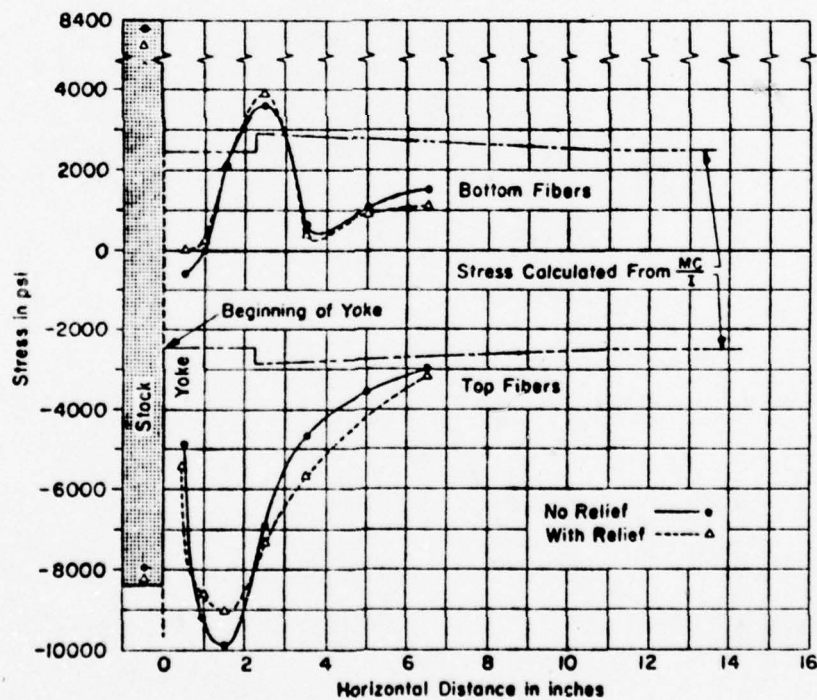


Figure 11 -- Bending Stress Distribution for 1/2-Diameter Penetration, Thick-Wall Yoke, 75,000 In-Lb

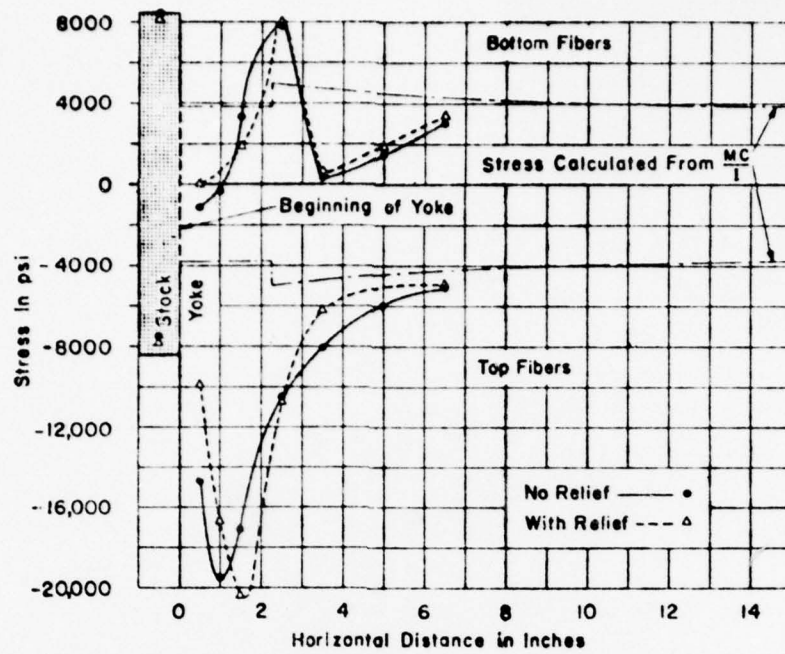


Figure 12 - Bending Stress Distribution for 1/2-Diameter Penetration, Thin-Wall Yoke, 75,000 In-Lb

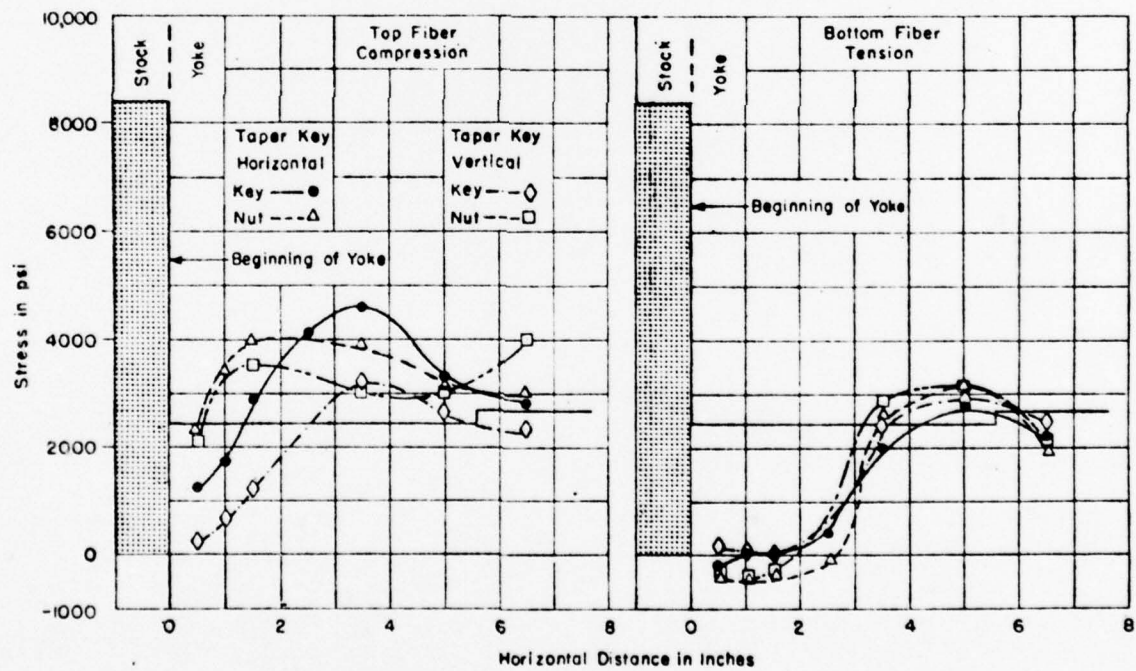


Figure 13 - Bending Stress Distribution for 1 1/4-Diameter Penetration, Thick-Wall Yoke, 75,000 In-Lb

TABLE 4

Test Number	Maximum Experimental Stress $\sigma_e$ psi	Corresponding Theoretical Stress $\sigma_t$ psi	$K = \frac{\sigma_e}{\sigma_t}$
3LTR	3100	2400	1.29
3LTN	2900	2400	1.21
3STR	3900	3700	1.03
3STN	4400	3700	1.19
1LTR	4000	2400	1.66
1LTN	4100	2400	1.71
1STR	5700	3700	1.54
1STN	7200	3700	1.95
0.5LTR	9000	2400	3.74
0.5LTN	9900	2400	4.11
0.5STR	20400	3700	5.51
0.5STN	19550	3700	5.28
1.25LNN	4000	2400	1.67
1.25LTN	4600	2400	1.92
1.25(90)LNN	3500	2400	1.46
1.25(90)LTN	3200	2400	1.33
1.25(A)LNN	4130	2400	1.72
1.25(A)LTN	4800	2400	2.00

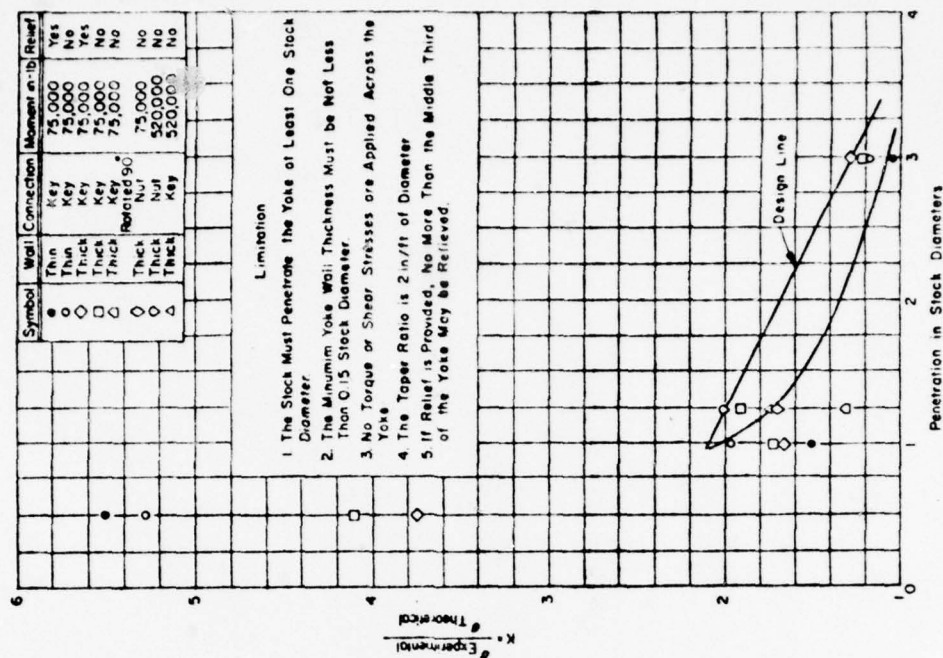


Figure 14 - "K" Factor versus Penetration

TABLE 5

Face Stresses at a Moment of 75,000 In-Lb

All stresses in psi; all angles in deg.

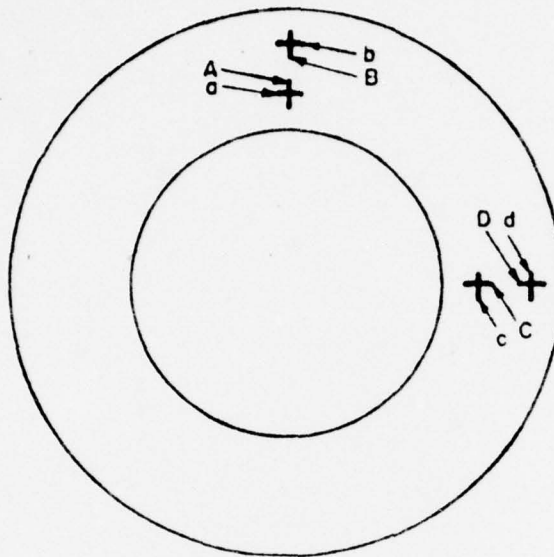
Location	Test								
	3LTR	3LT	1LTR	1LT	0.5LTR	0.5LT	1.25L T or N	1.25(90) LT or LN	1.25(A) LT + LN
A	- 500	- 500	-	0	- 2,000	- 1,000	-	-	-
a	+5000	+4000	-	+5000	+12,000	+12,000	-	-	-
B	-2000	-3000	-3000	-4000	- 9,000	- 7,000	+ 250 -19,300	+1250	+ 6,300 + 900
b	+4000	+5000	+2000	+3000	+12,000	+13,000	+ 1,900 + 1,500	+2300	+24,700 +14,000
C	-3000	-6000	-6000	-7000	-17,000	-26,000	- 4,500 -22,300	+1300 +1200	+ 3,350 + 1,650
c	+5000	+4000	+7000	+6000	+13,000	+11,000	+ 2,000 +17,500	+4300 +6550	+11,700 +15,500
D	-2500	-4500	-	-4000	-11,000	- 2,000	-	-	-
d	+5000	+4000	-	+6000	+ 9,000	+10,000	-	-	-
E	-	-3000	-5000	-3500	-12,000	-14,000	-	-	-
e	-	+4000	+4000	+4500	+ 9,000	+10,000	-	-	-
F	0	0	-1000	-	-	+ 500	-	-	-
f	+1000	+1000	-1000	-	-	+ 6,000	-	-	-
G	0	0	-1000	+1000	0	0	+ 250 +7200	-1900 +2200	+ 1,900
g	+2000	+2000	+3000	+4000	+ 7,000	+ 7,000	+ 3,900 + 660	+4500 + 660	+ 7,000
H	0	0	-4000	- 500	+ 1,000	+ 1,000	+ 1,200 + 800	+5700 +5700	+ 700 + 2,650
h	+4000	+4000	+5000	+6000	+14,000	+15,000	+ 4,750 + 5,650	+1050 + 600	+16,500 + 800
I	0	- 500	-	-	-	-	-	-	-
i	+ 500	+ 500	-	-	-	-	-	-	-
J	-	-	0	0	0	0	-	-	-
j	-	-	-1000	-1000	- 1,000	- 1,000	-	-	-
K	0	0	- 500	0	- 1,000	- 1,000	-	-	-
k	-1500	-1500	-3500	-2000	- 3,000	- 4,000	-	-	-
α	0	7	-	7	7	8	-	-	-
γ	-	8	18	2	10	10	-	-	-
δ	58	45	-	-	-	-	-	-	-

Location	Test					
	3STR	3ST	1STR	1ST	0.5STR	0.5ST
L	-1000	- 200	-	-	- 5,000	- 5,000
l	+7000	+7000	-	-	+22,000	+28,000
M	-2000	-3000	- 3,000	- 2,000	- 6,000	- 9,000
m	+4000	+6000	+12,000	+11,000	+15,000	+27,000
N	0	-2000	-	- 2,000	- 8,000	-21,000
n	+7000	+6000	-	+ 7,000	+16,000	+17,000
O	-1000	-3000	0	- 2,000	- 7,000	-18,000
o	+6000	+5000	+10,000	+ 7,000	+13,000	+19,000
P	-1000	-1000	- 3,000	- 1,000	-	- 3,000
p	+4000	+3000	+ 5,000	+ 5,000	-	+ 1,800
Q	0	-	-	+ 1,000	-	+ 1,000
q	- 100	-	-	- 500	-	- 1,000
R	- 200	0	0	0	+ 1,000	- 500
r	-2000	-2000	- 3,000	- 2,000	- 6,000	- 9,000
φ	3	4	-	- 17	1	5
θ	- 8	-12	-11	- 3	- 5	+ 1
λ	23	-	-	41	-	55

TABLE 6

## Face Stresses Measured during Maximum Loading Test

The stresses shown in this table are determined elastically from measured strains. Therefore stresses above 50,000 psi are not valid.



Moment in lb-in.	Key End		Nut End	
	Gage*	Stresses, psi	Gage*	Stresses, psi
900,000	A	- 68,000	A	- 7,000
	a	+152,000	a	+157,000
	B	- 82,000	B	+ 70,000
	b	+136,000	b	+219,000
	C	- 40,000	C	- 3,000
	c	- 12,000	c	+ 71,000
	D	+ 3,000	D	-
	d	+ 34,000	d	-
540,000	A	0	A	+ 10,000
	a	+ 49,000	a	+ 47,500
	B	- 6,500	B	+ 17,000
	b	+ 38,000	b	+ 38,000
	C	- 6,600	C	+ 1,000
	c	- 2,000	c	+ 34,500
	D	+ 4,000	D	-
	d	+ 17,000	d	-

\*Indicates gage location in diagram.

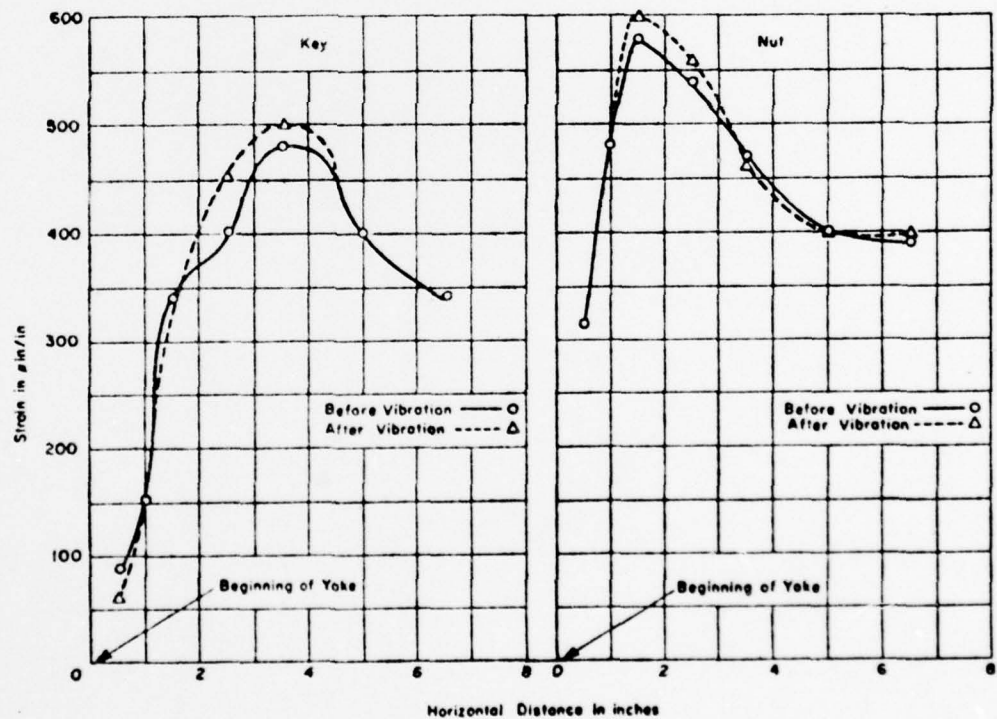


Figure 15 - Effects of Vibration on Top Fiber Strains of the Yoke

The final test was taken to failure. The results of this test are shown in Figures 16 through 21.

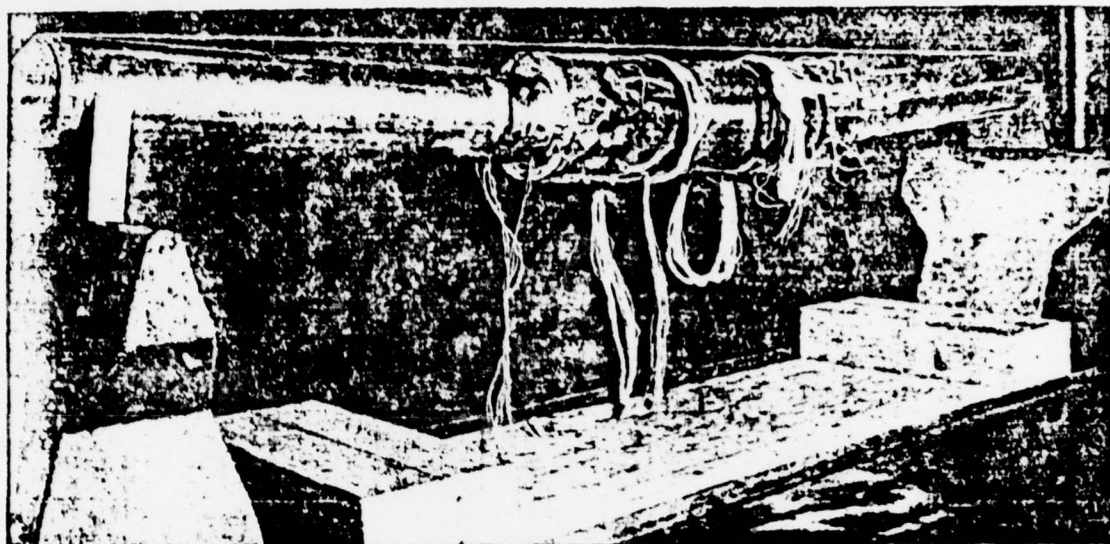


Figure 16 - Model after Maximum Applied Load

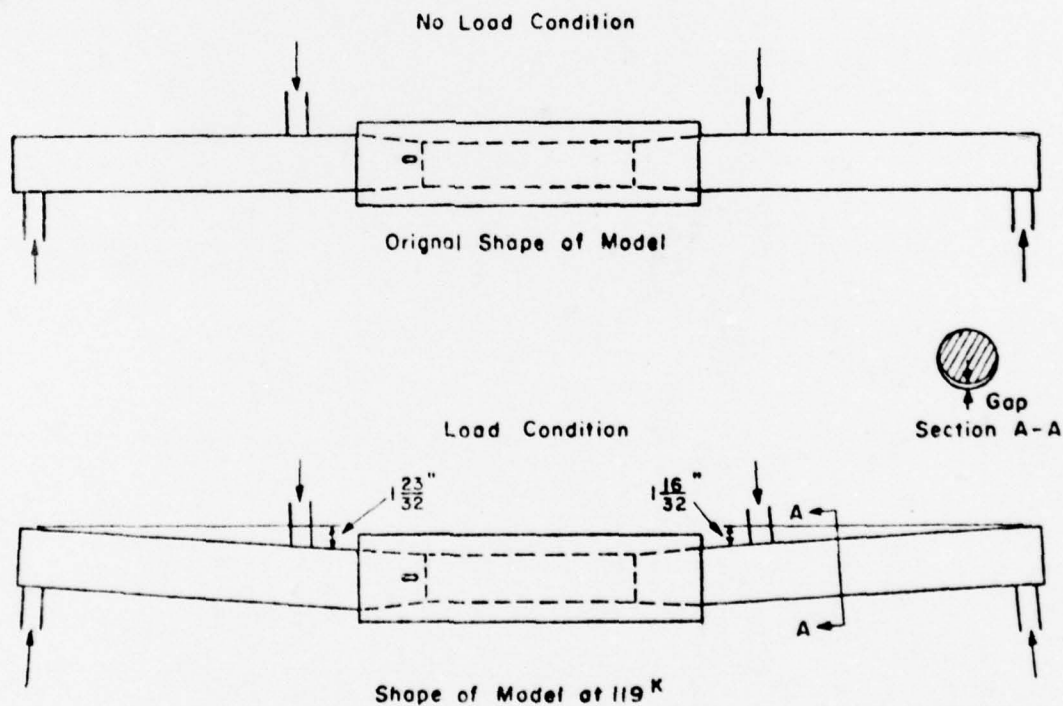


Figure 17 - Sketch of Damage to Model

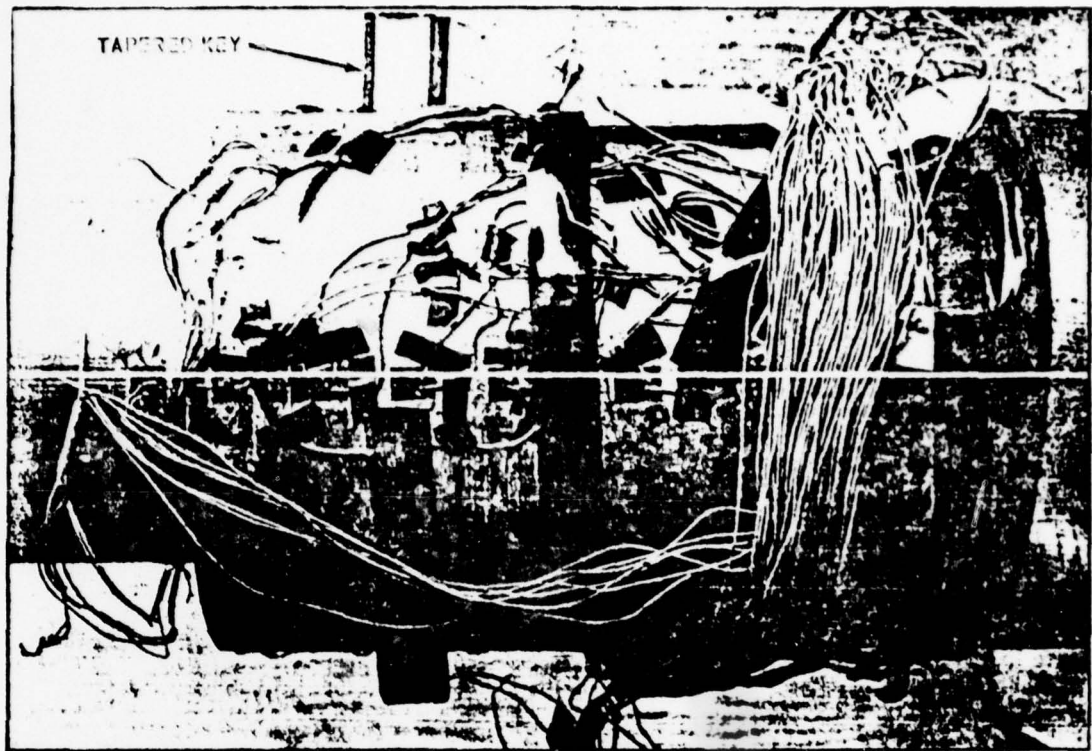


Figure 18 - Closeup of Damage to Tapered Key

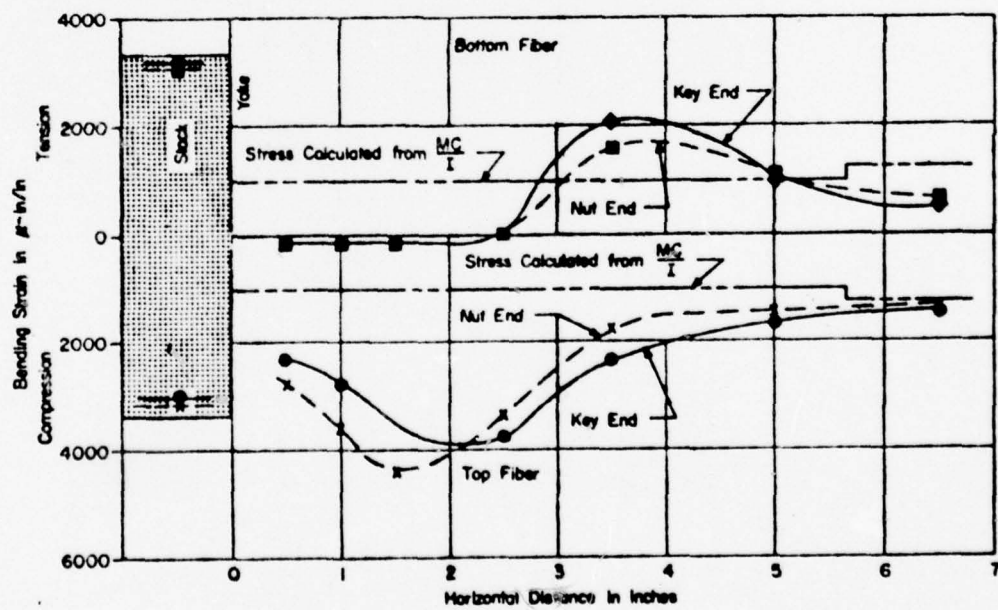


Figure 19 - Bending Strain Distribution for 1 1/4-Diameter Penetration, Thick-Wall Yoke, at a Moment of 900,000 In-Lb

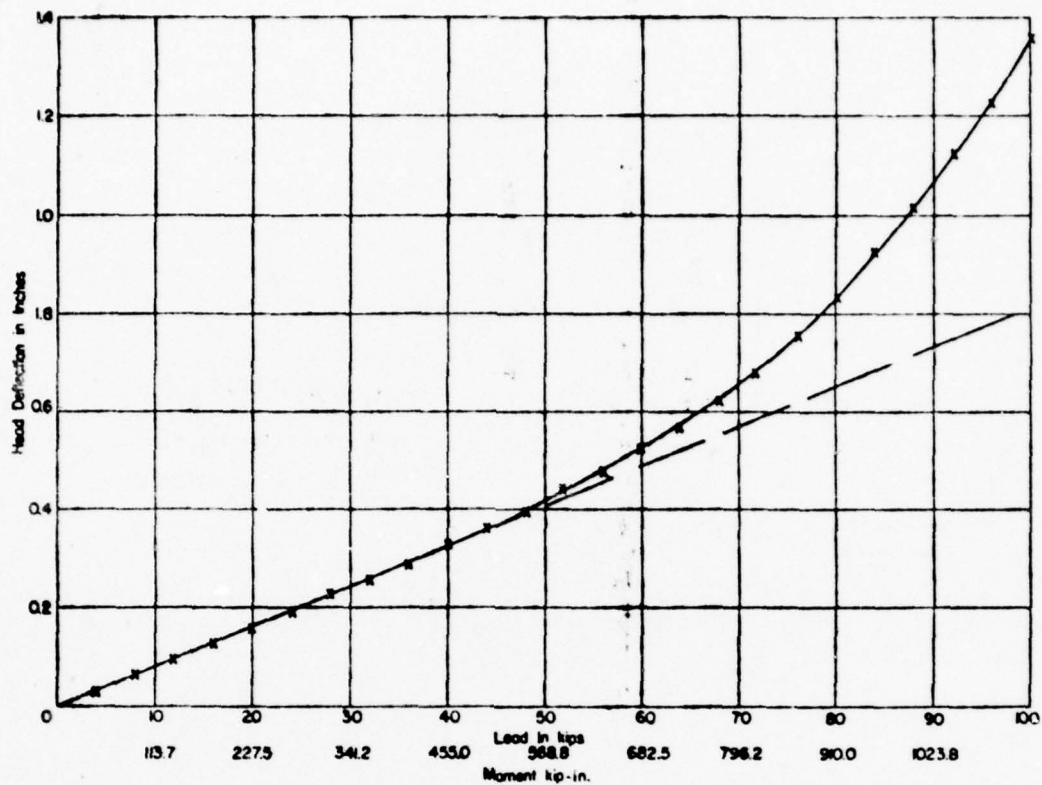


Figure 20 - Deflection of Head of Testing Machine versus Applied Load

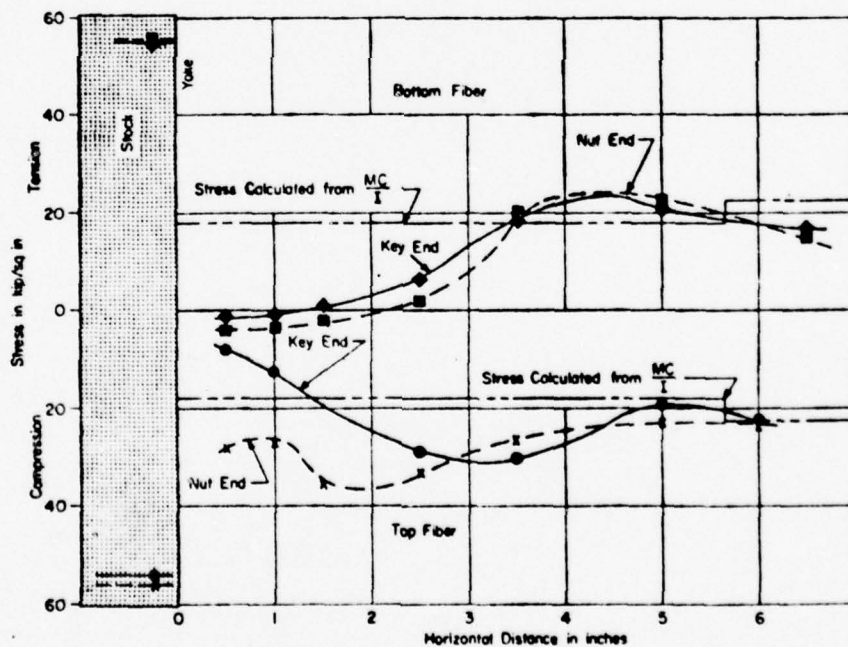


Figure 21 - Bending Stresses in 1 1/4-Diameter Penetration, Thick-Wall Yoke, at a Moment of 540,000 In-Lb

The models were disassembled after each test. To get some idea of the joint friction developed, one stock was removed from the assembly by loading the model in tension in the testing machine. The loads required to remove the stock from the yoke are tabulated below:

Penetration stock diameter	Load pounds
3	15,000 ± 1,000
1 1/4	not removed
1	7,500 ± 500
1/2	5,000 ± 500

### DISCUSSION OF RESULTS

The pertinent results obtained from this program are summarized in Figure 14. Within the limits imposed by the experimental program, this curve can be used to predict the maximum bending stresses in a socketed connection. These limits are as follows:

1. The stock must penetrate the yoke no less than 1 stock diameter.
2. The minimum yoke wall thickness must be no less than 0.15 stock diameter.
3. No torques or shear stresses are applied across the yoke.
4. The taper ratio is 2 in/ft of diameter.
5. If relief is provided, no more than the middle third of the yoke may be relieved.

Although these limitations do not necessarily preclude the successful design of other connections, they do indicate that any great departure from them would require additional experimental verification.

Within these limitations, the bending stresses can be computed from the equations

$$\sigma = \left(2.5 - \frac{\psi}{2.5}\right) \frac{Mc}{I} \quad \text{when } 1 < \psi < 3.7 \quad [3a]$$

or

$$\sigma = \frac{Mc}{I} \quad \text{when } \psi > 3.7 \quad [3b]$$

where  $\psi$  is the stock penetration in stock diameters and  $\sigma$ ,  $M$ ,  $c$ , and  $I$  are defined in Equation [2]. Equations [3] are valid only in the elastic range.

As expected, the 1/2-diameter thin-wall yoke reached the 1000  $\mu$  in/in. limit at a lower load than any of the other models. This load was equivalent to an applied moment of 75,000 in-lb (35 percent of the design load for USS ALBACORE). Since this is the highest moment that could be applied to one model, it is the moment that should be used for comparison purposes. Therefore, the strains observed in each model at 75,000 in-lb are presented. Since the

model with the thick-wall yoke having a 1-diameter depth of penetration was scaled from the proposed ALBACORE design, it was also subjected to the proposed design moment, 210,000 in-lb, and the resulting strains were measured.

Several attempts were made to calculate the face stresses listed in Tables 5 and 6. However, this was abandoned as impractical because of the large number of variables present. Within the test limits, none of the bearing stresses are high enough to cause concern but they should be considered in any extreme design.

During the majority of these tests, the tapered key was on the neutral axis so that the extreme fiber strains would not be influenced locally by this key. Since this is not the normal orientation, one test was run with a model rotated 90 deg to determine any adverse effects from testing at the unusual orientation. Figure 13 indicates that there are no adverse effects provided there is enough area to prevent a shear failure at the keyway.

No difference in cost figures between the rudder nut and the tapered key types of assemblies can be presented except on the model scale. It took about twice as long to fabricate and assemble the key end as it did the nut end although the material costs are about the same for the two assemblies.

When the final test was run, it was decided to investigate the effects of gross overload and test to failure. It was hoped to learn something about the failure mechanism of a joint of this nature. As the test progressed, however, it became apparent that the model was ductile enough that it would just bend excessively. At a load of 119,000 lb, which corresponds to a moment of 1,300,000 in-lb, the deflection was so great that the joint was considered operationally useless. Examination of the model after the load was removed showed the model to be badly deformed (Figures 16 and 17). The disassembled model revealed that the machined fit was badly distorted (Figure 16) and the tapered key was bent (Figure 18). No apparent thread damage was observed at the nut end.

The flexural stresses obtained during these tests are shown in Figure 19 for a moment of 900,000 in-lb. Although this moment was only two-thirds of the maximum applied moment, it was chosen since it was about the highest load at which most gages were still operative. It is noted that the data of Figure 19 do not fit the curve of Figure 14 due to yielding. However, by using a plot of head deflection versus load (Figure 20), it is possible to get some idea of the onset of yielding in the model. If the flexural stresses are plotted for a moment of 520,000 in-lb, the onset of yield as shown by the head deflection (Figure 20), the results are compatible with those of Figure 14. To provide additional data, the results obtained in this way are plotted in Figure 14. The slight discrepancy is attributed to experimental scatter and nonsymmetry of loading.

## SUMMARY AND CONCLUSIONS

Based on the data from these tests the following conclusions are drawn:

1. It is possible to predict the flexural stresses, within design accuracy, for a socketed connection loaded in pure bending if the stock penetrates the yoke at least one stock diameter.
2. It is impractical to predict the stresses on the face of the yoke. However, within the range of parameters considered in these tests, the face stresses are not large enough to cause concern.
3. Relief does not significantly affect the bending stresses in the yoke.
4. The bending stresses are about the same whether the rudder nut or the tapered key is used.
5. The 1 1/4-diameter model began to yield at a moment of 520,000 in-lb, but it was able to sustain a moment of 1,300,000 in lb without breaking. However, the bearing surfaces were badly deformed and a permanent deflection of approximately 1/2 in. was observed.
6. On the model scale, the cost of fabricating the nut was about half that of the key. However, this may be entirely different for full scale.

### RECOMMENDATIONS

If a considerable amount of design work outside the scope of this program is planned, it is recommended that additional experimental work be done. This should be designed to extend the curves of Figure 14 particularly in terms of yoke thickness and taper ratio.

### ACKNOWLEDGMENTS

The author wishes to express his thanks to all the members of the Model Basin staff who assisted with the tests. In particular, the author wishes to thank Mr. John Frazier, Industrial Department, for his assistance and helpful suggestions made during the model construction phase and to Mr. Robert Abrams who ran a number of the tests and reduced a great deal of the data.

### REFERENCES

1. Bureau of Ships ltr A11/NS731-037(442) Serial 442-132 of 30 Dec 1959.
2. Bureau of Ships Hull Contract Guidance Plan AGSS 589-800-1934052.
3. Robinson, Q.R., "Vibration Machines at the David Taylor Model Basin," David Taylor Model Basin Report 821 (Jul 1952).

# INITIAL DISTRIBUTION

## Copies

- 13 CHBUSHIPS
  - 2 Sci & Res Sec (Code 442)
  - 1 Lab Mgt (Code 320)
  - 3 Tech Info Br (Code 335)
  - 1 Ships Res Br (Code 341)
  - 1 Stru Mech, Hull Matl & Fabri (Code 341A)
  - 1 Prelim Des Br (Code 420)
  - 1 Prelim Des Sec (Code 421)
  - 1 Hull Des Br (Code 440)
  - 1 Prop, Shaft, & Bearing Br (Code 644)
  - 1 Hull Arrgt, Struc, & Preserv (Code 633)

## 10 CUR, ASTIA

- 1 CHONR, Stru Mech Br (Code 439)
- 1 NAVSHIPYD BSN
- 1 NAVSHIPYD PUG
- 1 NAVSHIPYD NYK
- 1 NAVSHIPYD CHASN
- 1 NAVSHIPYD LBEACH
- 1 NAVSHIPYD PEARL
- 1 NAVSHIPYD PHILA
- 1 NAVSHIPYD NORVA
- 1 NAVSHIPYD SFRAN
- 1 NAVSHIPYD MARE
- 1 CO, USNROTC & NAVADMINU, MIT
- 1 O in C, PGSCOL, Webb
- 1 SUPSHIP, Camden
- 1 NYSB Corp, Camden
- 1 SUPSHIP, New York
- 1 SUPSHIP, Newport News
- 1 NNS & DD Co, Newport News
- 1 SUPSHIP, Quincy
- 1 SUPSHIP, Groton

## Copies

- 1 EB Div, Gen Dyn Corp
- 1 Gibbs and Cox, Inc., New York
- 1 Bethlehem Steel Co, Quincy
- 1 Todd Shipyard, New Orleans
- 1 Md SB & DD Co, Baltimore
- 1 Avondale Marine Ways, Inc, New Orleans
- 1 National Steel Co, San Diego

APPENDIX C

Report Titled Method of Calculating  
Stress in a Gudgeon - Envelope 010809

Nov. 24, 1936

Method of Calculating Stress in a Gudgeon

The estimated force acting on a gudgeon is derived from the maximum rudder pressure, which exists when the vessel is moving full speed ahead with rudder hard over. This condition should not be confused with that of maximum torque, which is usually full speed astern for naval vessels.

Suppose in a given case, (Fig. No. 1) the maximum water pressure  $P$  acts with center of pressure below center of gudgeon. A pivoting point  $O$  is assumed and the thrust  $T$  on the gudgeon is determined by taking moments about  $O$ . Thus in Fig. No. 1  $T = \frac{b}{a} P$ .

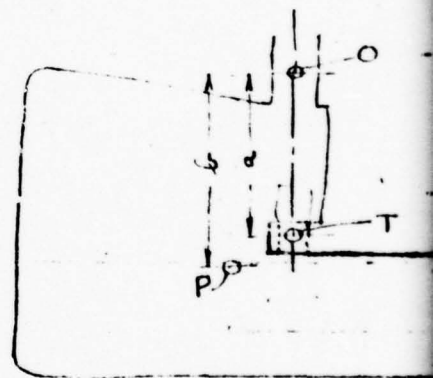


FIG. NO. 1

The line of action of  $T$  is taken normal to the plane of the rudder, so when the rudder is put over  $35^\circ$ ,  $T$  makes an angle of  $55^\circ$  with centerline of the ship.

The thrust  $T$  is transmitted to the gudgeon by means of a pintle or an extension of the

rudder stock. The distribution of pressure between pintle and gudgeon is the next matter to be decided upon and this has an important influence on the stresses.

Suppose a rigid pin were fit in a bearing with perfect fit and no clearance. Then force the pin sidewise a very small distance,  $dx$ , causing distortion in the bearing.

The maximum radial distortion will be  $dx$ ; at other points it will be  $dx \cos \alpha$ . If the intensity of radial pressure  $p$  is taken as proportional to the radial deformation —

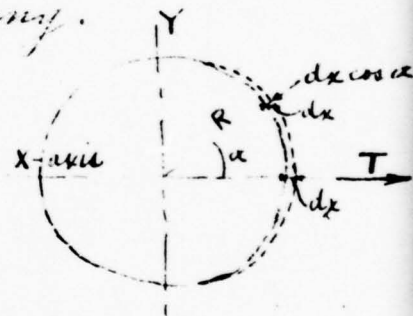


FIG. NO 2

—  $\frac{p}{p_0} = \frac{dx \cos \alpha}{dx}$  or  $p = p_0 \cos \alpha$ ,  $p_0$  being the maximum intensity of pressure.

In Fig. no. 2 the applied thrust  $T$  is shown in the direction of the  $x$ -axis. For equilibrium the sum of the  $x$ -components,  $p \cos \alpha$ , of radial pressure must equal the total thrust  $T$ . Considering just the quadrant above the  $x$ -axis —

$$\frac{1}{2} T = l \int_0^{\frac{\pi}{2}} p \cos \alpha d\alpha = l p_0 \int_0^{\frac{\pi}{2}} \cos^2 \alpha d\alpha$$

wherein  $l$  = axial length of the gudgeon.

Integrating the equation gives

$$p_0 = \frac{L T}{R \pi \lambda}$$

It is believed that the above distribution of pressure provides a good assumption for the gudgeon investigation.

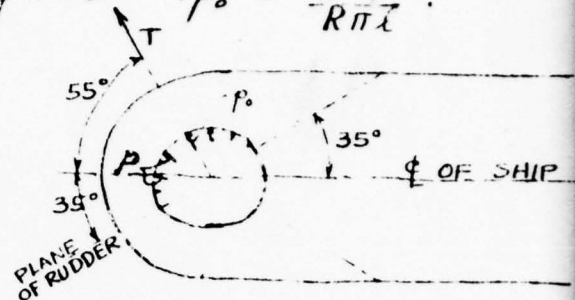


FIG. NO 3

While there is actually a little clearance between the two circles, it would take only a slight bending to make contact for nearly 180°. Fig. No. 4 illustrates this method of loading. The radial forces are shown acting on the inner circle of the gudgeon, but their points of application may be taken on any circle so long as the proper value of radius  $R$  is used in the formula for  $p_0$ .

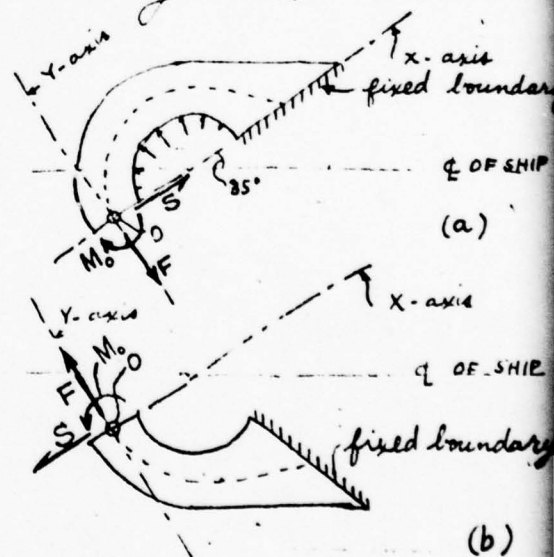


FIG. NO 4

Assume an X-axis at an inclination of 35° with CL of the ship, with origin at the mid-depth of the metal. Then consider the portion above the X-axis (Fig. 4a) and that below-

(Fig. 4b) as independent bodies fixed at their right boundaries. The upper body (a) may be thought of as a cantilever acted upon by the radial loads, by reactions  $F$  and  $S$  and by moment  $M_0$ ; the lower body is acted upon by  $F$ ,  $S$  and  $M_0$ . Assumed directions of the forces and moments are shown by arrows. The three unknowns  $F$ ,  $S$  and  $M_0$  may be determined by calculating, for point  $O$ , the  $X$ -displacement, the  $Y$ -displacement and the change of slope and imposing the conditions for continuity at this point just as in an ordinary arch calculation.

Since the thickness of metal is quite large in comparison with the radius of curvature it is advisable to use the curved beam theory, where the neutral axis is shifted toward the center of curvature and the stress varies directly with distance from the neutral axis and inversely with distance from the center of curvature. Reference to the curved beam theory: "Applied Elasticity" by Timoshenko and Tessels, p. 216-220.

In order to get results which will be general

applicable, calculations are carried out for four ratios of outside to inside diameter: 1.40, 1.60, 1.80 and 2.00. For simplicity in calculation the mean radius  $\frac{R_2+R_1}{2}$  is taken = 10 units in each case (for the true circular portion) and the radial loads,  $P$ , are considered as applied at <sup>a circle of 10 units</sup> ~~the mean~~ radius. Stations are taken 10° apart for numerical integration.

The shift of neutral axis of a rectangular section due to curvature is given by the formula

$$Y = \frac{R_2+R_1}{2} - \frac{R_2-R_1}{\log_e \frac{R_2}{R_1}}$$

The following table gives values of  $R_1$ ,  $R_2$  and  $Y$  for each 10° station.

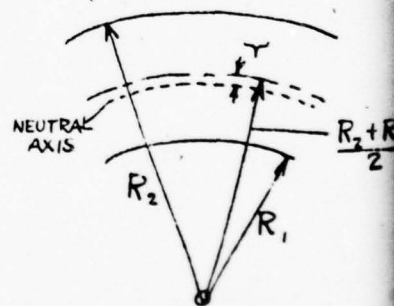


FIG. N25

Station in upper body	1.40 ratio				1.60 ratio				1.80 ratio				2.00 ratio			
	$R_2$	$R_1$	$\frac{R_2+R_1}{2}$	$Y$	$R_2$	$R_1$	$\frac{R_2+R_1}{2}$	$Y$	$R_2$	$R_1$	$\frac{R_2+R_1}{2}$	$Y$	$R_2$	$R_1$	$\frac{R_2+R_1}{2}$	$Y$
10°	11.667	8.333	10.000	.091	12.308	7.692	10.000	.179	12.957	7.143	10.000	.279	13.333	6.667	10.000	.383
20°	11.667		10.000	.091	12.308		10.000	.179	12.857		10.000	.279	13.333		10.000	.383
30°	11.712		10.022	.095	12.355		10.024	.184	12.906		10.024	.282	13.384		10.026	.387
40°	12.079		10.206	.115	12.742		10.217	.211	13.311		10.227	.318	13.803		10.235	.429
50°	12.873		10.603	.164	13.580		10.636	.278	14.186		10.664	.399	14.711		10.689	.525
60°	14.235		11.284	.262	15.017		11.354	.405	15.686		11.414	.554	16.267		11.467	.704
70°	16.500		12.416	.460	17.406		12.549	.654	18.182		12.662	.847	18.856		12.762	1.038
80°	20.341	8.333	14.337	.881	21.458	7.692	14.575	1.151	22.416	7.143	14.780	1.425	23.245	6.667	14.956	1.682

The intensity of radial pressure  $p$  at a point  $\alpha$  degrees from the direction of the resultant is given by the formula  $p = p_0 \cos \alpha$  as explained on page (2). Tabulated values are as follows:-

$\alpha$	$p$	portion acted upon	
5°	.996 $p_0$	sta. 80° to 90°	& 90° to 100°
15°	.966	" 70 " 80	" 100 " 110
25°	.906	" 60 " 70	" 110 " 120
35°	.819	" 50 " 60	" 120 " 130
45°	.707	" 40 " 50	" 130 " 140
55°	.574	" 30 " 40	" 140 " 150
65°	.423	" 20 " 30	" 150 " 160
75°	.254	" 10 " 20	" 160 " 170
85°	.087 $p_0$	" 0 " 10	" 170 " 180

In making the calculations it is most convenient to deal with a layer of the gudgeon just one unit thick in the axial direction. With a pressure intensity =  $p$  pounds per sq. unit at 10 units radius, the total load on a 10° sector is  $p \times 10 \text{ arc } 10^\circ = 1.7453 p = 10(\text{rad } 10^\circ) p$

The general method of making the calculations for bending moment, slope and displacement will now be illustrated for a typical section, say station 30°. Refer to Fig. No. 6

Bending moment at Sta. 30°  
 due to radial load =  $M_r =$   
 $10 \times 1.745 \text{ p.} [0.81 \sin 5^\circ + 25 \sin 15^\circ + 4.23 \sin 5^\circ]$

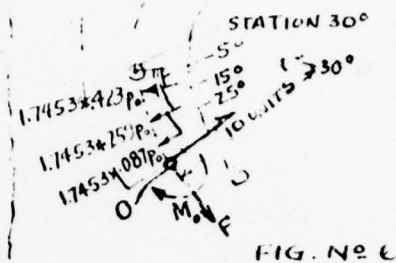
Change in slope of the 10°  
 sector of unit circle at Sta. 30° is the  
 center is given by the

formula  $\Delta d\phi = \frac{M_r d\phi}{EA r}$ , wherein  $d\phi = 10^\circ$  in circular  
 measure,  $A$  = sectional area for a layer 1 unit thick,  
 $r$  = shift of the neutral axis. The  $y$ -displacement  
 of the origin  $O$  due to bending at Sta. 30° is found  
 by multiplying the change in slope,  $\Delta d\phi$ , by the  
 abscissa,  $10 - 10 \cos 30^\circ$ . The  $x$ -displacement of the origin  
 is found by multiplying the change in slope,  $\Delta d\phi$ , by  
 the ordinate,  $10 \sin 30^\circ$ .

The bending moment at Sta. 30° due to  $S = M_s =$   
 $S \times 10 \sin 30^\circ$ . The change in slope and the  
 displacements set up by  $M_s$  are calculated as  
 explained in the last paragraph.

Force  $F$  causes a bending moment,  $M_F$ , at Sta.  
 $= F \times [10 - 10 \cos 30^\circ]$ . The same method is used for  
 calculating slope and displacements.

The bending moment at Sta. 30° caused



by  $M_0$  is equal to  $M_0$ . The same method is used for calculating slope and displacements.

At the stations which are forward of the  $\phi$  of the pintle, some inaccuracy is involved by using the curved beam theory when the two boundaries of the beam are no longer concentric. Thus in Fig. 7 the sector  $a b c d$  is figured as though it were  $a b' c' d$ . It does not appear that this involves any important error and no better method seems available.

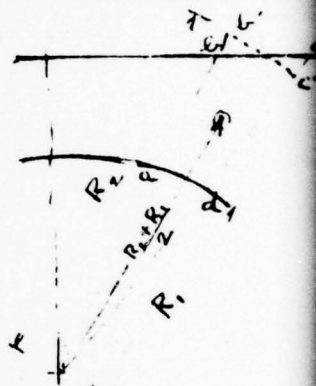


FIG. NO 7

For all sections such as shown in Fig. 7 the radial loads are considered as applied at 10 units radius from the center. The leverages for moments and displacements are figured to the mid-width of the metal,  $\frac{R_2 + R_1}{2}$ .

The complete calculations of bending moments, slopes and displacements are kept for future reference.

Note: It is believed that the calculations would have been a little easier had the two bodies been assumed separated at the  $\phi$  of the pintle even though some of the radial load would then be applied to the lower body.



Summary of elastic effects on upper body at point O due to radial load,  $M_0$ ,  $S$  and  $F$ .

	Ratio	Slope	y - displ.	x - displ.
radial load	1.40	+ 2303.2 $\frac{F d \phi}{E}$	+ 32934. $\frac{F d \phi}{E}$	- 13130. $\frac{F d \phi}{E}$
	1.60	+ 909.0 "	+ 12373. "	- 6937. "
	1.80	+ 494.6 "	+ 7417. "	- 3696. "
	2.00	+ 322.6 "	+ 4941. "	- 2345. "
$M_0$	1.40	+ 47.29 $\frac{M_0 d \phi}{E}$	+ 395.80 $\frac{M_0 d \phi}{E}$	- 346.14 $\frac{M_0 d \phi}{E}$
	1.60	+ 17.761 "	+ 153.28 "	- 128.99 "
	1.80	+ 9.351 "	+ 82.35 "	- 67.54 "
	2.00	+ 5.814 "	+ 52.57 "	- 42.40 "
$S$	1.40	- 346.14 $\frac{S d \phi}{E}$	- 3203.6 $\frac{S d \phi}{E}$	+ 2837.9 $\frac{S d \phi}{E}$
	1.60	- 128.99 "	- 1212.7 "	+ 1052.3 "
	1.80	- 67.54 "	- 641.5 "	+ 549.2 "
	2.00	- 42.40 "	- 405.2 "	+ 344.0 "
$F$	1.40	- 395.80 $\frac{F d \phi}{E}$	- 5143.0 $\frac{F d \phi}{E}$	+ 3203.6 $\frac{F d \phi}{E}$
	1.60	- 153.28 "	- 2048.6 "	+ 1212.7 "
	1.80	- 82.35 "	- 1121.0 "	+ 641.5 "
	2.00	- 52.57 "	- 724.46 "	+ 405.2 "

Summary of elastic effects on lower body.

	Ratio	Slope	y - displ.	x - displ.
$M_0$	1.40	- 24.22 $\frac{M_0 d \phi}{E}$	- 78.35 $\frac{M_0 d \phi}{E}$	- 154.41 $\frac{M_0 d \phi}{E}$
	1.60	- 9.291 "	- 32.35 "	- 61.08 "
	1.80	- 4.960 "	- 18.07 "	- 33.26 "
	2.00	- 3.152 "	- 11.82 "	- 21.41 "
$S$	1.40	- 154.41 $\frac{S d \phi}{E}$	- 685.3 $\frac{S d \phi}{E}$	- 1185.7 $\frac{S d \phi}{E}$
	1.60	- 61.08 "	- 292.0 "	- 484.0 "
	1.80	- 33.26 "	- 166.41 "	- 269.0 "
	2.00	- 21.41 "	- 110.42 "	- 175.7 "
$F$	1.40	+ 78.35 $\frac{F d \phi}{E}$	+ 446.7 $\frac{F d \phi}{E}$	+ 685.3 $\frac{F d \phi}{E}$
	1.60	+ 32.35 "	+ 198.24 "	+ 292.0 "
	1.80	+ 18.07 "	+ 115.57 "	+ 166.41 "
	2.00	+ 11.82 "	+ 77.77 "	+ 110.42 "

For each ratio three simultaneous equations are set up, which, when solved, give values of  $M_o$ ,  $S$  and  $\frac{d\phi}{E}$  cancels out in each case.

Ratio 1.40.

$$\left\{ \begin{array}{l} +2303.2 p_o + 47.29 M_o - 346.14 S - 395.80 F = -24.22 M_o - 154.41 S + 78.35 \\ +32934 p_o + 395.80 M_o - 3203.6 S - 5143.0 F = -78.35 M_o - 685.3 S + 446.7 \\ -18130 p_o - 346.14 M_o + 2837.9 S + 3203.6 F = -154.41 M_o - 1185.7 S + 685.3 \\ +71.51 M_o - 191.73 S - 474.15 F = -2303.2 p_o \quad \text{slope equation} \\ +474.15 M_o - 2518.3 S - 5589.7 F = -32934 p_o \quad \text{y-displacement eq} \\ -191.73 M_o + 4023.6 S + 2518.3 F = +18130 p_o \quad \text{x- " " "} \end{array} \right.$$

Solving —  $M_o = 14.96 p_o$ .  $S = 1.026 p_o$ .  $F = 6.698 p_o$ .

Ratio 1.60

$$\left\{ \begin{array}{l} +909.0 p_o + 17.761 M_o - 128.99 S - 153.28 F = -9.291 M_o - 61.08 S + 32.35 F \\ +13378 p_o + 153.28 M_o - 1212.7 S - 2048.6 F = -32.35 M_o - 292.0 S + 198.24 F \\ -6937 p_o - 128.99 M_o + 1052.3 S + 1212.7 F = -61.08 M_o - 484.0 S + 292.0 F \\ +27.052 M_o - 67.91 S - 185.63 F = -909.0 p_o \quad \text{slope equation} \\ +185.63 M_o - 920.7 S - 2246.8 F = -13378 p_o \quad \text{y-displacement eq} \\ -67.91 M_o + 1536.3 S + 920.7 F = +6937 p_o \quad \text{x- " " "} \end{array} \right.$$

Solving —  $M_o = 15.958 p_o$ .  $S = 1.143 p_o$ .  $F = 6.804 p_o$ .

Ratio 1.80

$$\begin{cases} +494.6 p_o + 9.351 M_o - 67.54 S - 82.35 F = -4.960 M_o - 33.26 S + 18.07 F \\ +7417. p_o + 82.35 M_o - 641.5 S - 1121.0 F = -18.07 M_o - 166.41 S + 115.57 F \\ -3696. p_o - 67.54 M_o + 549.2 S + 641.5 F = -33.26 M_o - 269.0 S + 166.41 F \\ +14.311 M_o - 34.28 S - 100.42 F = -494.6 p_o \quad \text{slope equation} \\ +100.42 M_o - 475.1 S - 1236.6 F = -7417. p_o \quad \text{y-displacement eq} \\ -34.28 M_o + 818.2 S + 475.1 F = +3696 p_o \quad \text{x-} \end{cases}$$

Solving:  $M_o = 16.64 p_o$ ,  $S = 1.216 p_o$ ,  $F = 6.881 p_o$ .

Ratio 2.00

$$\begin{cases} +332.6 p_o + 5.894 M_o - 42.40 S - 52.57 F = -3.152 M_o - 21.41 S + 11.82 F \\ +4941. p_o + 52.57 M_o - 405.2 S - 724.46 F = -11.82 M_o - 110.42 S + 77.77 F \\ -2345. p_o - 42.40 M_o + 344.0 S + 405.2 F = -21.41 M_o - 175.7 S + 110.42 F \\ +9.046 M_o - 20.99 S - 64.39 F = -332.6 p_o \quad \text{slope equation} \\ +64.39 M_o - 294.78 S - 802.2 F = -4941. p_o \quad \text{y-displacement eq} \\ -20.99 M_o + 519.7 S + 294.78 F = +2345. p_o \quad \text{x-} \end{cases}$$

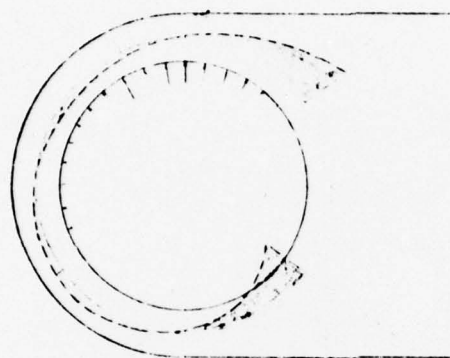
Solving:  $M_o = 15.69 p_o$ ,  $S = 1.185 p_o$ ,  $F = 6.983 p_o$ .

From the values of  $M_o$ ,  $S$  and  $F$  the following bending moments are calculated.

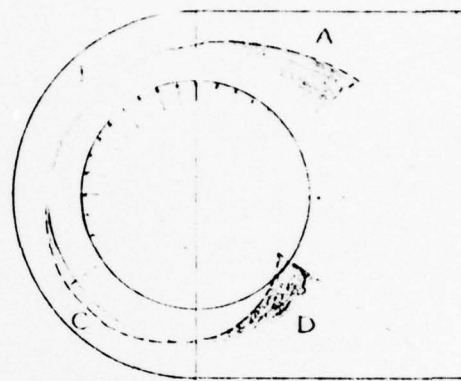
		Bending Moment			
Station		1.40 ratio	1.60 ratio	1.80 ratio	2.00 ratio
Upper Body	0°	+14.46 p.	+15.96 p.	+16.64 p.	+15.69 p.
	10°	+12.32	+13.10	+13.64	+12.72
	20°	+ 8.22	+ 8.76	+ 9.14	+ 8.24
	30°	+ 3.31	+ 3.58	+ 3.80	+ 2.87
	40°	- 1.74	- 1.74	- 1.71	- 2.70
	50°	- 6.36	- 6.64	- 6.79	- 7.87
	60°	-10.07	-10.61	-10.94	-12.14
	70°	-12.40	-13.20	-13.72	-15.05
	80°	-13.09	-14.13	-14.81	-16.29
	90°	-12.02	-13.25	-14.07	-15.73
	100°	- 9.11	-10.52	-11.46	-13.30
	110°	- 4.51	- 6.03	- 7.07	- 9.10
	120°	+ 1.49	- 0.11	- 1.22	- 3.42
	130°	+ 8.62	+ 7.02	+ 5.88	+ 3.51
	140°	+17.34	+15.74	+14.71	+12.15
	150°	+27.88	+26.47	+25.44	+22.89
	160°	+40.46	+39.35	+38.61	+36.08
	170°	+56.06	+55.60	+55.36	+53.03
180°	+77.11 p.	+77.63 p.	+78.27 p.	+76.31 p.	
Lower Body	0°	+14.96 p.	+15.96 p.	+16.64 p.	+15.69 p.
	-10°	+15.74	+16.92	+17.72	+16.70
	-20°	+14.45	+15.79	+16.67	+15.55
	-30°	+11.11	+12.56	+13.50	+12.25
	-40°	+ 5.89	+ 7.39	+ 8.36	+ 6.97
	-50°	- 1.09	+ 0.43	+ 1.38	- 0.16
	-60°	- 9.50	- 8.07	- 7.14	- 8.87
	-70°	-18.80	-17.36	-16.40	-18.30
	-80°	-28.99	-27.52	-26.67	-28.68
	-90°	-40.44	-39.10	-38.29	-40.55
	-100°	-53.95	-52.78	-52.15	-54.75
	-110°	-71.02 p.	-70.31 p.	-70.10 p.	-73.17 p.

Positive moments tend to increase radius of curvature.  
negative " " decrease " " "

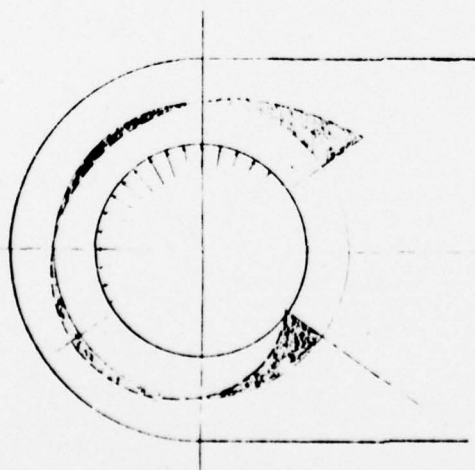
The calculations leading to the above results are kept for reference.



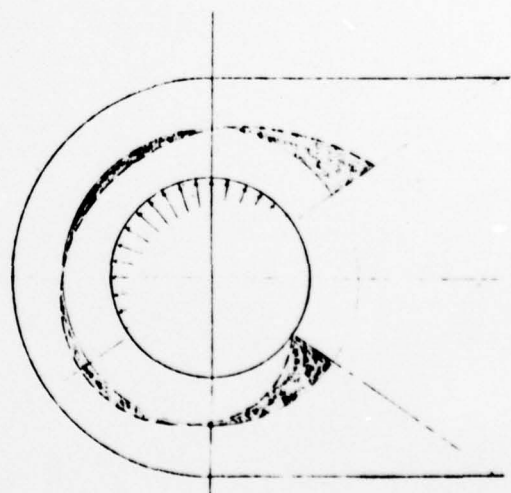
RATIO 1.40



RATIO 1.60



RATIO 1.80



RATIO 2.00

FIGURE No 8  
DISTRIBUTION OF LOAD & BENDING MOMENT

It will be observed that, within practical limits diameter ratio has very little influence on the location of maximum bending moments. There are four regions, A, B, C and D in Figure No. 8, in which a maximum stress appears possible.

Suppose in a given case the thrust on a layer 1 unit thick is 10000\* and the ratio  $\frac{R_2}{R_1} = 1.60$ .

Try station  $-10^\circ$  (in region C). At 10 units radius

$$p_o = \frac{2T}{10 \pi r} = \frac{2 \times 10000}{10 \times 3.1416 \times 1} = 636.6 \text{ * per sq. unit.}$$

$$\text{Bending moment at sta. } -10^\circ = +16.92 p_o = 10771 \text{ * x units}$$

$$\text{Bending stress at inside curve} = \frac{M \left[ \frac{R_2 + R_1}{2} - r - R_1 \right]}{A r R_1}$$

$$= \frac{10771 [10.000 - .179 - 7.692]}{4.616 \times .179 \times 7.692} = 3608 \text{ */sq. unit tension.}$$

$$\text{Direct stress due to } S = \frac{S \sin 10^\circ}{A} = 27 \text{ */sq. unit tension.}$$

$$\text{" " " " } F = \frac{F \cos 10^\circ}{A} = 924 \text{ */sq. unit tension.}$$

$$\text{Combined stress} = 3608 + 27 + 924 = 4559 \text{ */sq. unit tension}$$

Making similar calculations and including the direct stress due to radial load in the upper body the following stresses are found. At sta.  $150^\circ$  the greatest stress in region A is found to be 4365 \*/sq. unit tension. In region B the greatest stress comes at sta.  $80^\circ$  and is 2490 \*/sq. unit compress

In region D the greatest stress comes at sta. -8 and is  $3460 \text{ #/sq. unit}$  compression.

From the foregoing it is concluded that in all cases the circumferential tension at inner surface at sta.  $-10^\circ$  ( $45^\circ$  from  $\phi$ ) may be taken as the maximum stress.

It should be noted that the bending moment in region A is greater than in region C but the stress is slightly less due to greater thickness of metal.

If the sides were curved in as in Fig. 9(b) instead of carried along straight (Fig. 9(a)), the stress at A might be considerably higher than at C. Shape shown in Fig. 9(b) is not recommended.

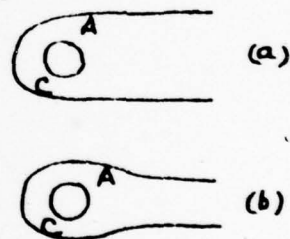


FIG. NO 9

Suppose  $\frac{R_2}{R_1} = 1.40$  and  $T = 10000 \text{ #}$  on a unit layer  
 As before  $p_0 = 636.6 \text{ #/sq. unit.} + 15.74 \times 636.6 = 10020 \text{ #/sq. unit.}$   
 Bending stress  $= \frac{10020 [10.000 - .091 - 8.333]}{3.334 \times .091 \times 8.333} = 6246 \text{ #/sq. unit tension.}$   
 Direct stress due to  $S = \frac{S \sin 10^\circ}{A} = 34 \text{ #/sq. unit tension.}$   
 " " " "  $F = \frac{F \cos 10^\circ}{A} = 1259 \text{ #/sq. unit tension.}$   
 Combined stress at sta.  $-10^\circ = 6246 + 34 + 1259 = \underline{7539 \text{ #/sq. unit tension.}}$

By similar calculations it is found that 10000 # thrust on a unit layer will produce a combined tensile stress of 3333 #/sq unit for 1.80 ratio and 2408 #/sq unit for 2.00 ratio.

These results are used in plotting the curve on sheet (17). The foregoing data gives four points on the curve and another point (at ratio 1.4375) is available from a previous independent calculation.

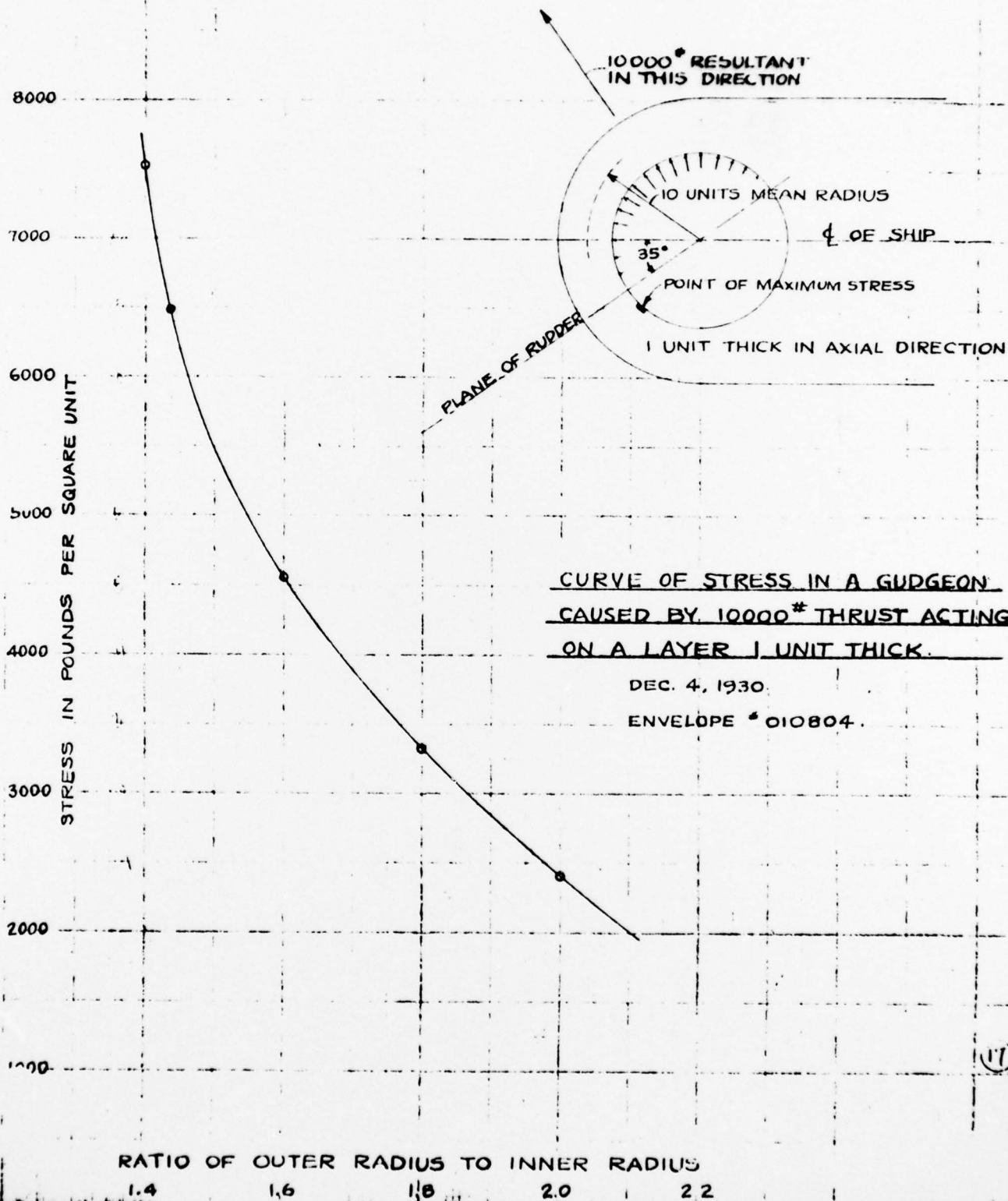


Illustration of use of stress curve.

For cruiser C.L. 25 the thrust on the gudgeon  
 $T = 630600^\#$ . Depth of gudgeon = 19". Outside radius

$R_2 = 13\frac{3}{8}"$ , inside radius  $R_1 = 8"$ .

$$\frac{R_2}{R_1} = 1.67.$$

$$\frac{R_2 + R_1}{2} = 10.688".$$

Let 1 unit = 1.0688".

1 sq. unit = 1.1423 sq. in.

$$\frac{630600}{19} = 33189^\# \text{ thrust acts on a 1 inch layer.}$$

From the curve, for ratio 1.67 —

$10000^\#$	load on 1 unit layer causes stress of	$4070^\#/\text{sq. unit}$
$\div 1.0688$		$\div 1.1423$
$9356^\#$	" " 1 inch " " "	$3563^\#/\text{sq. inch}$
$\times 3.54735$		$\times 3.54735$
$33189^\#$	" " 1 " " " "	$12639^\#/\text{sq. inch}$

Class F cast steel used. Factor of safety =  $\frac{85000}{12639} = \underline{6.7}$ .

Results for other vessels, figured in a similar manner are tabulated on the following sheet. In all cases the dimensions  $R_1$  and  $R_2$  are taken to the steel section, bronze liners being excluded.

Maximum Stress in Gudgeon due to Water Pressure on Rudder

Ship	Speed in knots	Stress in #/sq in	Material. Cast Steel	Factor of Safety	Remarks
Destroyer #251	35.	10386.	<sup>ult stress</sup> B 60000	5.8	
Omaha, C.L. 4	35.	13980.	B 60000	4.3	
Marblehead, C.L. 12	35.	14540.	B 60000	4.1	not sure about material
Salt Lake City, C.L. 25	32.5	12639.	<sup>ult</sup> F 85000	6.7	
C.L. 26 to 31	32.5	14073	F 85000	6.0	
C.L. 33 & 35	32.7	9820	F 85000	8.7	
C.L. 32, 34 & 36	32.7	15330	F 85000	5.5	
Saratoga, C.V. 3	35.	14297	<sup>ult</sup> D 70000	4.9	lower gudgeon
C.V. 4	29.25	16810	D 70000	4.2	not final
V-1 to 3	21.	8680	B 60000	6.9	
V-4	15.	7620	B 60000	7.9	
V-7	17.	3519	B 60000	17.1	not sure about material
CB 1					
CVB 41					
BB 57		9550			Calc. 12/19/49
DD 692					
102 SQ. FT.	39	21530		279	
DD 445, 155 SQ. FT.	34.	27440	68000	228	
DD 828		26500	55000		

Ferris.